Effects of Psychosocial Stress on Retinal Neurodegeneration

Dissertation

DISSERTATION ZUR ERLANGUNG DES DOKTORGRADES
DER NATURWISSENSCHAFTEN (DR. RER. NAT.)
DER FAKULTÄT FÜR BIOLOGIE UND VORKLINISCHE MEDIZIN
DER UNIVERSITÄT REGENSBURG

vorgelegt von

Forkwa Kieran Tembei

Aus
ANGIE-KAMERUN

2012

Das Promotionsgesuch wurde eingereicht am: 09.10.2012

Die Arbeit wurde angeleitet von: Prof. Dr. med. Ernst R. Tamm

Prüfungsausschuss:
Vorsitzender: PD Dr. Stefan Reber

1. Gutachter: Prof. Dr. Ernst Tamm
2. Gutachter: Prof. Dr. Inga Neumann
3. Prüfer: Prof. Dr. Stephan Schneuwly

MY FAMILY

Table of Content

1 INTRODUCTION

1.1. Loss of vision due to retinal degeneration

Loss of vision or complete blindness is a serious disabling condition that is caused for the most part by a damaged or dysfunctional eye. One of the prominent disease factors that damage the eye and render it dysfunctional is a degeneration of the retina. An intact and functional retina is one of the very important prerequisites for vision as it is in charge of the initial capture and processing of visual signals for onward transmission to the brain via the optic nerve. The retina possesses a unique structural and functional organisation with an outer monolayer of cells forming the retinal pigment epithelium layer (RPE), an inner neural retina composed of different types of neurons, glia cells and vessels.

The various types of neurons of the neural retina are closely interdependent alongside the RPE and the choroid that nourishes them [2]. The repercussion of such interdependence is that, in many instances a primary dysfunction in one retinal component causes a secondary dysfunction in others [3, 4], thus rendering the retina extremely vulnerable to dysfunction and degeneration hence a wide range of retinal degenerative diseases.

Retinal degenerative diseases affect people of all ages ranging from Leber congenital amaurosis in babies through retinitis pigmentosa (RP) in youths and age related macular degeneration (AMD) in the old. They show several phenotypic features amongst which are; impaired vision, night blindness and tunnel vision which may culminate with increasing severity to a total loss of vision. So far, there is no completely successful treatment for retinal degenerative diseases, thereby necessitating immense medical attention and research.

1.2. Anatomy and physiology of the retina

1.2.1. Retinal structure

The retina is the innermost layer of the eye and is composed of several layers of neurons interconnected by synapses. The vertebrate retina has ten distinct layers which are from the innermost to the outermost; an inner limiting membrane, nerve fibre layer, ganglion cell layer, inner plexiform layer, inner nuclear layer, outer plexiform layer, outer nuclear layer, external limiting membrane, photoreceptor outer segments and the RPE. At the posterior end, ganglion cell axons converge at the blind spot to form the optic nerve.

Amongst the neurons of the retina, photoreceptors are specialized to convert the light energy of a photon into electrical energy in a process termed phototransduction. Two main photoreceptors are known; the rods and cones. Both have the same basic structure. Closest in front, there is an axon terminal which releases the neurotransmitter glutamate onto bipolar cells, followed by the cell body which contains the cell's organelles. Farther back is the inner segment, a specialized part of the cell containing mitochondria that provide ATP for the sodium-potassium pump. Finally, there is an innermost photoreceptor outer segment which contains light absorbing visual pigment opsins packaged in membrane bound discs and serves as the site for visual phototransduction.

A third photoreceptor type known as photosensitive ganglion cells has also been discovered [5] and is thought to regulate circadian rhythms. The proportion of rods and cones varies between species and depends on whether they are nocturnal or diurnal. In humans there are three different types of cones which are distinguished by their response to different wavelengths of light.

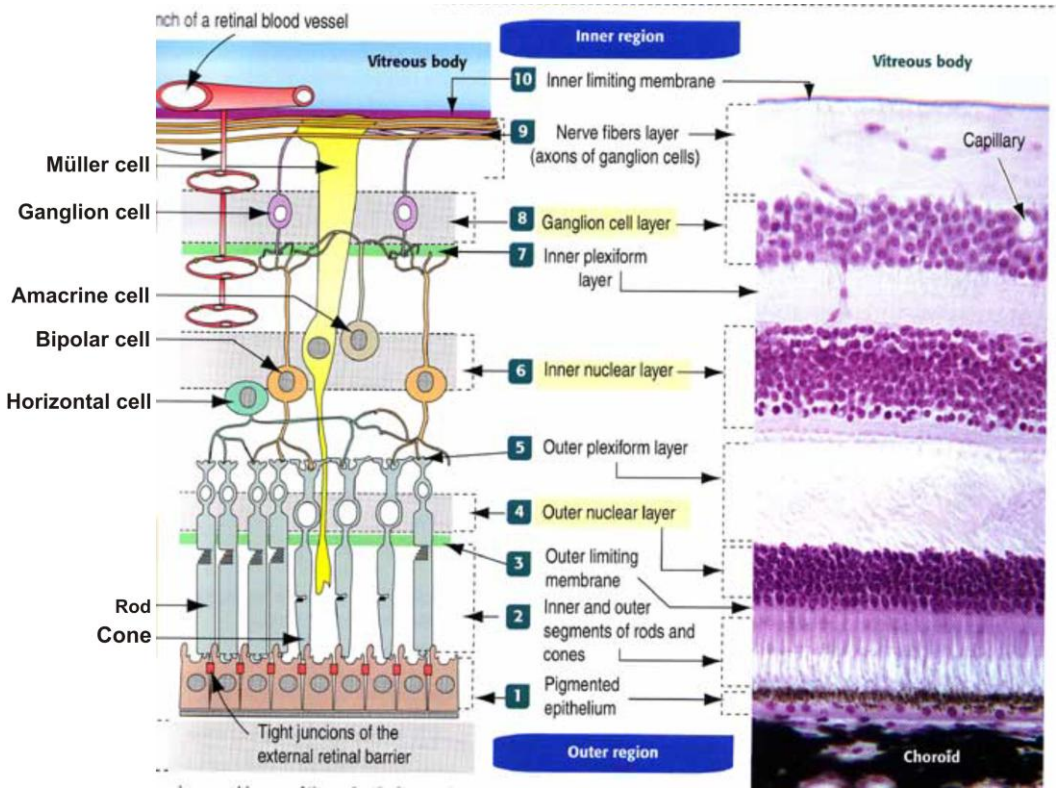

Figure 1: Overview of the construction of the mammalian retina. Shown are a schematic drawing of various cell types and their connections on the left and a histological section on the right. Adapted from www.bio.miami.edu.

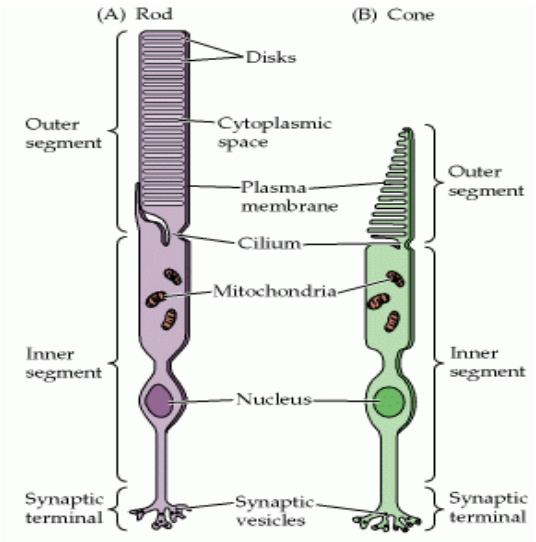

Figure 2: Structure and structural differences between rods and cones. Although they are generally similar in structure, rods (A) and cones (B) differ in their size and shape, as well as in the arrangement of the membranous disks in their outer segments. Adapted from, Purves Neuroscience 2nd edition.

1.2.2. Visual phototransduction

Vision is possible because light activates visual phototransduction in the retina, thereby generating an electrical signal that is conveyed by an ensemble of neurons to the brain. In the dark cGMP gated sodium channels in photoreceptor outer segments are open because cGMP is bound to them. Hence, positively charged ions like sodium enter the photoreceptor cell thereby depolarizing it to potential of about −40 mV called the dark current. Phototransduction begins with a photo bleaching event where the rhodopsin or iodopsin in the outer segment absorbs a photon that causes retinal to change shape from Cis to Trans. This isomerisation of retinal generates a series of unstable rhodopsin intermediates, the last of which binds to transducin G protein in the membrane hence activating transducin. Each photoactivated rhodopsin can activate about 100 transducins that in turn activate the enzyme cGMP-specific phosphodiesterase (PDE). Finally, activated PDE catalyzes the hydrolysis of about 1000 cGMP molecules thereby reducing the intracellular concentration of cGMP. This results to the closing of cGMP-gated Na^+ channels in the photoreceptor membrane and subsequent photoreceptor hyperpolarisation. This hyperpolarisation event causes voltage-gated calcium channels to close, leading to a decrease in the influx of calcium ions into the cell thus the intracellular calcium ion concentration falls. The lack of calcium means that less glutamate is released to the bipolar cell than before as calcium is required for the glutamate-containing vesicles to fuse with the cell membrane. The result is a depolarisation of one population of bipolar cells and hyperpolarisation in the other depending on the nature of receptors (ionotropic or metabotropic) in the postsynaptic terminal. The generated signal is then conveyed to the optic nerve via ganglion cells for onward transmission to the brain.

1.2.3. Retinal degenerative diseases

Retinal degenerative diseases are a significant cause of vision loss or complete blindness around the globe [6]. The most occurring of these diseases include glaucoma, AMD, diabetic retinopathy and retinitis pigmentosa (RP).

1.2.3.1. Age related macular degeneration

It is a late onset disease that causes permanent damage to photoreceptor cells in the macula, leading to a loss of central vision. Early signs of vision loss from AMD include shadowy areas in central vision and unusually fuzzy or distorted vision. It develops as dry (non-neovascular) or wet (neovascular, exudative). In the dry (nonexudative) form, cellular debris called drusen accumulates between the retina and the choroid and by so doing impair photoreceptor function. In the wet (exudative) form, blood vessels grow up from the choroid into the sub retinal space leading to a detachment of the retina. The dry form is more common than the wet form with about 85 to 90 % of patients diagnosed with dry AMD. However, the wet form is more severe. AMD usually occurs in people over the age of 50 years and accounts for approximately 50 % of registered blindness in Western Europe and North America [7].

1.2.3.2. Retinitis Pigmentosa (RP)

RP is a group of genetic eye conditions that cause progressive retinal dystrophy and lead to incurable blindness. Affected individuals first experience defective dark adaptation or nyctalopia (night blindness), followed by reduction of the peripheral visual field (known as tunnel vision) and loss of central vision late in the course of the disease. RP can be inherited in an autosomal dominant, autosomal recessive or X-linked manner. It affects approximately 1 in 3000 individuals and about 100 genes have been associated with the RP phenotype (Hartong et al., 2006). Most of these

mutations affect photoreceptors directly and hereby induce apoptotic processes that lead to a progressive retinal dystrophy and subsequently incurable blindness.

1.2.3.3. Glaucoma

Glaucoma is characterized by progressive retinal ganglion cell death which leads to visual field loss that may progress to blindness in the long run. Glaucoma can roughly be divided into two main categories being "open angle" and "closed angle" (or angle closure) glaucoma. The angle refers to the area between the iris and cornea through which aqueous humor must flow to exit the eye via the trabecular meshwork. Closed angle glaucoma can appear suddenly and is often painful, visual loss progresses quickly but the discomfort often leads patients to seek medical attention before permanent damage occurs. Open angle glaucoma tends to progress at a slower rate and patients may not notice they have lost vision until the disease has progressed significantly. Glaucoma is a leading cause of irreversible vision loss worldwide second only to cataracts.

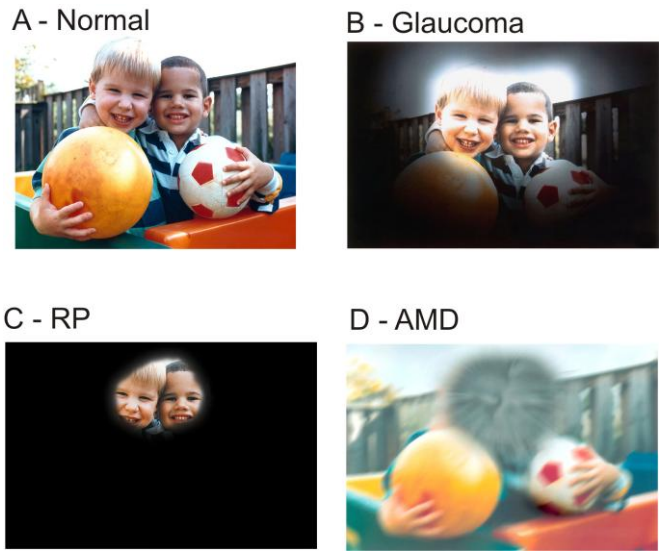

Figure 3: Simulation of retinal degeneration phenotypes. Showing normal vision (A),Loss of peripheral vision in Glaucoma (B), Tunnel vision in RP (C) and loss of central vision in AMD (D). Photo modified from wikimedia.org/wiki/File:Eye_disease_simulation.

1.3. Causes and pathways leading to photoreceptor degeneration

Besides being indispensable, photoreceptors are the most vulnerable neurons in the retina. As such, dysfunction and degeneration of photoreceptors is responsible for the overwhelming majority of retinal degenerative diseases. Once photoreceptors begin to degenerate and independent of the cause, they loose their functional state, their outer segments become disorganized and the retina outer nuclear layer (ONL) thins down as photoreceptor nuclei disappear, a process that is accompanied by visual complications.

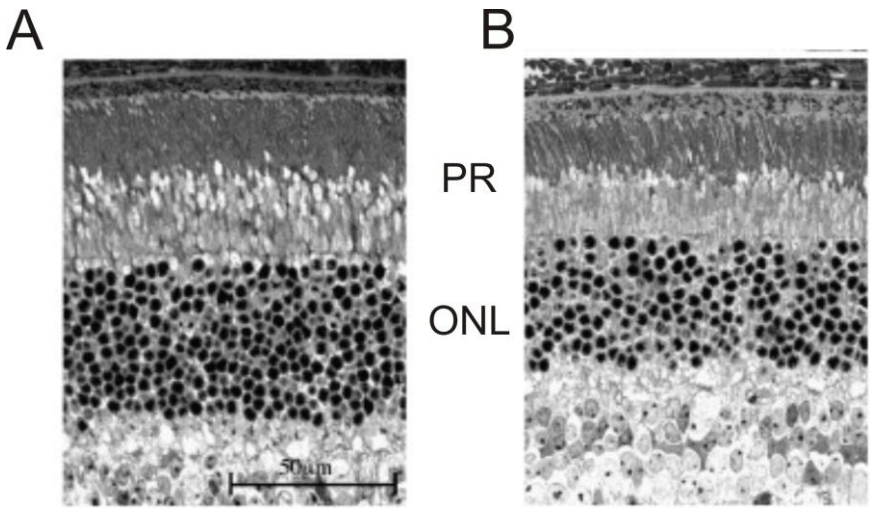

Figure 4: Photoreceptor degeneration in the retina. Normal retina morphology (A) and a degenerating retina (B), showing less dense photoreceptors and a thinner ONL in a degenerating retina. Photo modified from [8].

1.3.1. Causes of photoreceptor degeneration

Neurodegeneration in the retina could result from a diverse range of causes, these include genetic diseases [9], environmental insults such as light damage [10] and as a result of normal aging [11, 12].

1.3.1.1. Genetic causes of photoreceptor degeneration

In terms of disease aetiology, genetically linked retinal degenerative diseases can be divided into inheritable and multifactorial forms. Amongst inheritable degenerations are RP, macular, cone and cone-rod degenerations which are inherited predominantly in a monogenic manner through autosomal dominant, autosomal recessive or X-linked genes [13, 14].

More than a hundred genes have been implicated in inherited photoreceptor degenerations [15], with each of them contributing only to a small fraction of cases as they are of a minor allele frequency. The most common single genes that cause retinits pigmentosa include the RP GTPase regulator RPGR [16], Rhodopsin RHO [17] and Usherin USH [18]. The ATP binding cassette subfamily A member 4 (ABCA4) gene is the most commonly mutated macular degeneration gene which causes Stargarts disease, con-rod degeneration or RP depending on mutational severity [19].

AMD represents a multifactorial form of photoreceptor degeneration with an overwhelming impact. Contrary to RP, fewer genes have been implicated in AMD. Amongst those identified of significant effect are the Complement Factor H [20, 21] and the age related maculopathy susceptibility 2 (ARMS2) genes [22]. Other AMD associated genes include the complement component 3 and 2 (C3 & C2), complement factors B and I (CFB & CFI) and apoplipoprotein E [23].

1.3.1.2. Environmental influence on photoreceptor degeneration

Apart from genes, a few other factors have been implicated in photoreceptor degeneration, the most prominent of which is the environment, notably light exposure [24-26]. Exposure to high amounts or prolonged durations of light is known to exacerbate the course of both inherited and acquired retinal degenerations in mice and

rats [26-28]. The process of light damage of photoreceptors depends on the multi step regeneration of rhodopsin in the RPE during phototransduction. It relies on a functional visual cycle where photobleaching of rhodopsin produces 11-cis retinal with the release of opsin. Following isomerisation and release from opsins, 11-trans retinal is reduced to all trans retinol which travels back to the RPE where it is first converted to all 11-cis retinol and then oxidised to 11-cis retinal. Once produced, 11-cis retinal travels back to the rod outer segments where it is again conjugated to opsin to form a new functional rhodopsin. Continuous regeneration of rhodopsin permits prolonged photobleaching that leads to a sustained stimulation of the photo transduction cascade which causes stress on photoreceptor cells and eventually leads to their death via apoptosis [29, 30]. This involvement of activated rhodopsin in light damage has been demonstrated in mice that are deficient in rhodopsin kinase and arrestin as both proteins are involved in the termination of rhodopsin regeneration [31]. Furthermore, it has been demonstrated that inhibition of 11-cis retinal regeneration using 13-cis retinoic acid leads to a protection against light damage [32].

1.3.2. Pathways leading to photoreceptor degeneration

Allying with the diverse causes of photoreceptor degeneration is a wide range of pathways through which photoreceptor demise is influenced amongst which are; oxidative stress [33], lipid oxidation [34], complement activation [35], endoplasmic reticulum stress [36], ciliary transport defects and altered bioenergetic function [37].

Disorders involving faulty fatty acid synthesis and metabolism do contribute to photoreceptor apoptosis in several ways. Firstly, they could lead to the accumulation of toxic adducts in the retina which promote photoreceptor demise due to increased accumulation of reactive oxygen and nitrogen species [38], an example here is a mutation in the ELOVL4 gene that is responsible for a Stargart´s like macular

dystrophy [39]. Furthermore, the oxidation of polyunsaturated fatty acids which exist in high amounts in photoreceptor outer segments generates intermediates that initiate destructive free radical chain reactions which have deleterious effects on photoreceptors [40]. A second pathway involved in photoreceptor demise is a defective ciliary transport system. Photoreceptor cells contain a modified cilium that is required for the transportation of substances necessary for viability and phototransduction from inner segments where they are synthesised to the outer segment where they are needed [41]. Disruption of ciliary transportation between the two photoreceptor segments therefore compromises several cellular functions such as ion movements, energy utilization and phototransduction itself with far reaching consequences on photoreceptor apoptosis [42]. Like in other parts of the central nervous system, oxidative stress has ruinous effects on photoreceptors. As such, rhodopsin mutations which cause protein misfolding and their subsequent retention in the endoplasmic recticulum do trigger photoreceptor apoptosis. This is because they increase reactive oxygen and nitrogen species signalling that drives what is termed the unfolded protein response which is an attempt to decrease the amount of unfolded protein. In case the amount of misfolded protein surpasses the unfolded protein response, the resulting cellular stress drives several proapoptotic pathways [36, 43]. Another system implicated in photoreceptor degeneration is complement activation, whereby complement activation products such as; C3a, C5a, oxidised lipids and toxic adducts are known to activate the innate immune system resulting to deposition of cellular debris on the basolateral RPE [34]. There exist a homeostatic balance in rods and cones which when disturbed by the death of rod cells in a condition like RP results to secondary death of cones for diverse reasons which include; the absence of rod-derived survival factors, nutrient deprivation due to an abnormal rod-cone

interface, toxic metabolites released by dying rods and oxidative stress due altered functioning of the retina [44].

1.3.3. Photoreceptor demise in retinal degenerations

Despite high diversity in disease aetiology and pathogenesis for various forms of retinal degenerations, it has been shown in several animal models of retinal degenerative diseases that final cell demise occurs via apoptosis [9, 45-47]. To arrive at this conclusion, scientists have taken advantage of the fact that apoptosis diametrically differs from necrosis hence can readily be distinguished by the occurrence of internucleosomal DNA fragmentation which occurs in apoptosis but is absent in necrosis. DNA fragmentation can be visualized by the presence of a characteristic DNA ladder using agarose gel electrophoresis [48] or in situ labelling with terminal deoxynucleotidyl transferase (TdT)-mediated incorporation of biotinylated nucleotides into the 3' ends of DNA fragments (terminal dUTP nick end labelling [TUNEL]) [49]. Furthermore, substantial evidence is provided by the fact that inhibitors of apoptosis do reduce the severity of induced retinal degeneration [50]. Apart from photoreceptor cell loss, pathologic apoptosis has also been implicated in several neurodegenerative diseases amongst which are; Alzheimer's disease, Huntington's disease [51], Amyotrophic lateral sclerosis [52] and Ischemic brain damage [53].

Apoptosis is a term derived from Greek (apo-from ptosis-falling). This is a form of cell death in which a series of biochemical events lead to characteristic cell morphology and death. It is characterized by nuclear condensation, cell shrinkage, membrane blebbing, DNA fragmentation and a final break-up of the cell into apoptotic bodies that are phagocytocised by neighbouring cells without any inflammation [54]. The principal regulators of apoptosis are a family of cysteine

proteases called caspases [55]. However, other caspase independent pathways are progressively being found [56].

Though apoptosis results in cell death, it has a variety of functions in normal development and survival as it removes several types of cells which include; virally infected cells, transient cells such as glial cells used for guiding neurons during nervous development and cells with inappropriate or no function, etc.

1.4. Research and therapeutic strategies for retinal degeneration

Although the percentage of idiopathic retinal disorders is very low, there is no successful treatment strategy available. Furthermore, the complexity of most retinal degenerative diseases imposes many black boxes in disease mechanisms that need to be elucidated. The information gathered thereof could be exploited to develop molecules that can be used to perform targeted disruptions of the respective pathways involved in disease aetiology and pathogenesis thereby inhibiting disease onset and progression. Furthermore, some retinal diseases are characterised by a sudden onset and rapid progression thereby necessitating the development of molecules that can robustly arrest the progressive loss of neurons that usually characterizes these diseases and by so doing reduce disease severity and improve prognosis for patients.

Pathologic apoptosis is an important feature shared by both animal models and human retinal dystrophies. Therefore, studying the mechanisms by which potential therapeutic interventions can arrest pathologic apoptosis of neurons in the retina will provide salient information about mechanisms of retinal neurodegeneration. Such information is prerequisite for the development of potential rescue strategies that could subsequently be refined and used to provide clinical benefits against retinal degenerative diseases.

1.4.1. Animal and Experimental models

To understand the molecular mechanisms of disease induction and progression or develop potential therapeutic strategies for the preservation of vision in patients, several animal models have been established. The largest category of models consists of mutant mice and even zebra fish. Given that apoptosis is the common pathway in retinal degenerative diseases, several experimental models like light induced damage of photoreceptors have been developed to acutely induce huge amounts of apoptosis in the retina and by so doing, permit a better analysis of the process of apoptosis in the retina. The light induced model of photoreceptor damage was developed following the usage of light to accelerate loss of photoreceptor cells in mice and rats [57-59]. Also, NMDA induced excitotoxicity due to an excessive influx of Ca^{2+} is used to induce huge apoptosis in RGCs [60].

The light induced model for studying photoreceptor loss offers a wide range of advantages over animal models. Firstly, photoreceptor cell loss after light damage occurs by apoptosis as is the case in RP and AMD which is not always the case in other models [9]. Secondly, light itself is a co-factor that enhances many retinal dystrophies in which visual cell apoptosis is occurring [57]. Moreover, the severity of degeneration can easily be manipulated by varying some aspects such as light intensity, wavelength and duration of exposure. A great advantage of the light damage model is the fact that, unlike in animal models where photoreceptor loss occurs progressively with cells at different stages of demise, excessive light exposure causes apoptosis in an acute manner whereby all affected photoreceptor cells pass into apoptosis at more or less the same time thereby making it easier to study the process.

1.4.2. Therapeutic strategies to promote photoreceptor survival

Despite the high occurrence and overwhelming impact of retinal degenerative diseases on the quality of life, there is no available therapy to cure the underlying disease cause. In diseases like AMD and diabetic retinopathy, invasive clearance of accumulated debris and or LASER coagulation is used to arrest choroidal or retinal neovascularisation respectively. However, these treatment strategies have no influence on the underlying apoptotic cell death that causes vision loss. Several drugs under research are designed to develop neuroprotective substances to control apoptotic cell death by influencing diverse causes of primary or secondary photoreceptor degeneration which include; neovascularisation, inflammation and oxidative damage, while others like neurotrophic factors or channel blockers seek to provide trophic support or stabilise cell functioning. At present more intensive research is needed to improve and develop neuroprotective substances that could eventually be authorised and used to arrest photoreceptor demise in neurodegenerative diseases.

1.5. Stress

Stress can be described as a constellation of events which consists of a stimulus (stressor) which elicits a reaction from the nervous system (stress perception) that activates physiologic systems in the body (stress response) (Dhabhar et al. 1999). The stress response is a complex stereotypic reaction of an organism to a real or threatened disturbance of the body's homeostasis and or integrity of the body's control systems aimed at reducing the adverse effects of the stressor and restoring the body's equilibrium. In general, the physiological stress response in vertebrates involves a coordinated activation of the sympathetic nervous system (SNS) and the

Hypothalamus Pituitary Adrenal (HPA) axis, both geared towards a fight or flight response.

Once the body recognises any threat, the neurons of the SNS get activated in a matter of seconds leading to a firing of preganglionic sympathetic neurons that release acetylcholine which binds and activates nicotinic acetylcholine receptors on post ganglionic neurons. In response to this stimulus, SNS nerves start to secrete the catecholamines noradrenaline and adrenaline into the peripheral circulation. These catecholamines bind to adrenergic receptors in the peripheral tissue causing a variety of effects which include; increase in heart rate, widening of bronchial passages, pupillary dilation, perspiration, pilo erection, vasoconstriction and an increase in blood pressure.

Apart from the SNS, a delayed physiological reaction usually after a few minutes involves an activation of the HPA axis, a process that leads to the release of GCs mainly cortisol in humans or corticosterone (CORT) in rodents into the blood stream. GCs belong to a class of steroid hormones (synthesized from cholesterol) [61] characterised by an ability to bind with the GR. Together with mineralocorticoids and androgens, these hormones are synthesised in the adrenal cortex.

1.5.1. Acute vs Chronic stress

A very important aspect of stress is its duration. Stress is termed acute (short-term) when stressor exposure lasts for minutes to hours and chronic when stressor exposure lasts several days to months continuously. Generally, the effects of a stress response could be helpful when the duration is short and limited (acute) but could become deleterious when the duration of stress is protracted (chronic) [62]. Under normal circumstances, a stress response is initiated to ensure survival. However, the effects of

a stress response usually interfere with many other pathways especially through gene regulation where genes regulating many aspects such as metabolism and immune responses are either activated or repressed. Due to these extensive effects of a stress response, chronic stressor exposure may trigger a number of imbalances and diseases [63]. In animals, exposure to chronic stress has been found to cause physiological changes such as enlargement of the adrenals, ulceration of the intestines, thymus/lymph nodes atrophy [64] and immunosuppression [65]. Behaviourally exposure to chronic stress has been found to increase depression [66] and anxiety [67] in rats.

1.5.2. Psychosocial stress

Psychosocial stress is characterised by the fact that the stressor does not trigger somatic and behavioural manifestations directly but rather indirectly through the nervous system [68]. Such an activation of the nervous system without any contact is purely psychological and occurs mainly through cognitive means. Depending on the underlying causative factor, psychosocial stress could be short-termed (acute) for example a job interview or sustained (chronic) such as living in a war zone.

Most often social stress occurs when same species have to live together in colonies in which conspecific threat is of daily occurrence. In such colonies, a hierarchical existence usually exists in which some animals are in a dominant position while others stay in a subordinate position. Subordinated animals show major aspects of stress such as weight loss and alterations in several aspects of life such as; sleep, feeding, sex and aggressive behaviour [69, 70].

1.5.3. Psychosocial stress in mice via chronic subordinate colony (CSC) housing

CSC housing was established and used to induce a chronically stressful situation in male mice by housing four smaller male mice together with a larger dominant male in a polycarbonate observation cage for 19 consecutive days [64]. During this time, the dominant male always dominates all four experimental mice which are considered to be in a subordinate position based on their defensive behaviours which include; flight, retreat and a submissive upright posture.

A very important aspect of this paradigm is that, in order to avoid physical injury, excessively aggressive dominant males which bite experimental mice are not used. As such, once a colony has been established, the experimental mice are more or less only psychosocially stressed with only intermittent and short lasting attacks from the dominant male. Furthermore, to avoid habituation, the dominant male is replaced by a novel dominant male on day 8 and 15. After 19 days of CSC housing, stressed mice suffer from adrenal insufficiency as it has been shown that adrenal cells from these mice do not respond to ACTH *in vitro* [71] and so cannot produce appropriate amounts of GCs. Additionally, CSC mice show increased anxiety, thymus atrophy and adrenal hypertrophy [64].

1.6. Glucocortcoid synthesis, release and their effects

1.6.1. The HPA axis and the release of GCs

The Hypothalamo-Pituitary-Adrenal axis (HPA) consists of the Hypothalamus, the Pituitary and the Adrenals functioning together through direct stimulation [72] and negative feed back inhibition [73]. Once there is an activation of the HPA axis, parvocellular neurons within the paraventricular nucleus (PVN) of the hypothalamus get stimulated leading to the release of corticortrophin releasing hormone (CRH) and

arginine-vasopressin (AVP) which get transported through the hypophyseal portal circulation to the anterior pituitary. Once in the anterior pituitary, these hormones bind to their receptors in the membrane of pituitary corticotroph cells [74] where CRH in a mechanism potentiated by AVP induces the cleavage of the adrenocortico trophic hormone (ACTH) precursor proopiomelanocortin (POMC) into 2 peptides; beta-lipotrophic hormone (B-LPH) and ACTH which are then released into the blood stream [75]. ACTH binds to its receptors in the adrenal cortex where its main action is to stimulate the synthesis and release of GCs. Once in circulation, GCs have a series of effects and are also involved in a negative feed back mechanism that controls their own release through an inhibition of the hypothalamus and the pituitary, thereby decreasing the release of CRH and ACTH respectively [73].

Apart from playing an important role in stress regulation through the secretion of GCs, the HPA axis plays a role in the regulation of other body processes which include; sexual behaviour, arousal, food intake, immune function and circadian events such as the sleep wake cycle.

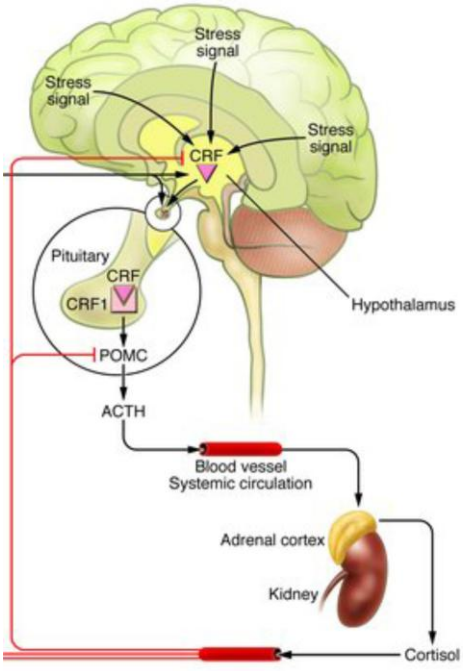

Figure 5: Basic illustration of the HPA axis. Shown are the hypothalamus, pituitary and adrenals functioning together to produce cortisol and the negative feed back loop involved in the regulation of this axis. Adapted from [1].

1.6.1.1. GC synthesis

The main GC in mice is CORT which is synthesized as follows: cholesterol obtained from the diet or synthesized from acetate by a CoA reductase enzyme is actively transferred into the inner mitochondrial surface where the cholesterol side chain cleavage enzyme converts it to pregnenolone which is then transported to the smooth endoplasmic recticulum where it is converted to deoxycort via progesterone. Deoxycort is transported to the mitochondria where it is finally converted into CORT.

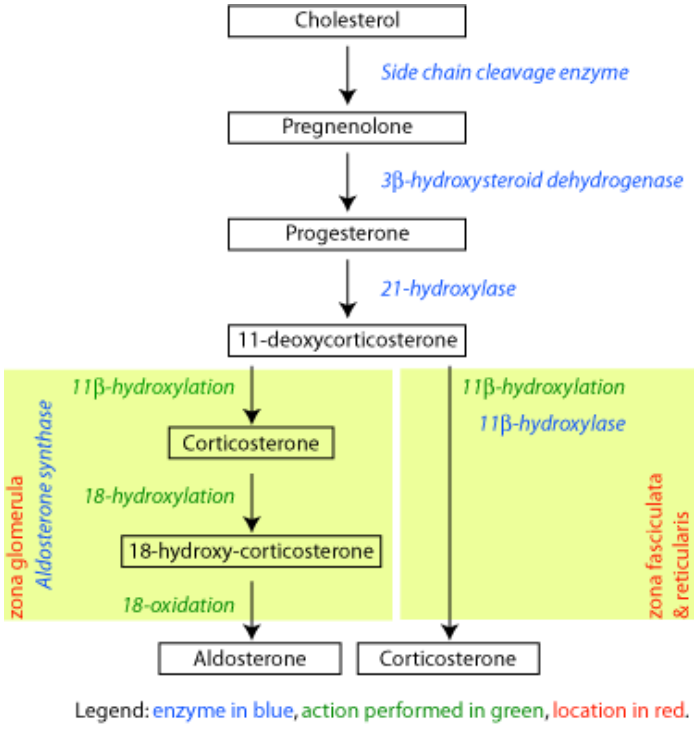

Figure 6: Schematic representation of corticosterone synthesis, Photo Adapted from http://en.wikipedia.org/wiki/18-Hydroxycorticosterone.

1.6.2. Glucocorticoid effects and modes of action.

One of the major functions of GCs is the wide role they play in metabolism especially of glucose from where the name Glucocortiscoids arises. GCs stimulate gluconeogenesis from non hexose substrates such as lactate, amino acids and

pyruvate. Other roles of GCs in metabolism include mobilization of amino acids from extra hepatic tissues and increase lipolysis in adipose tissue [76, 77]. Apart from metabolism, GCs exhibit several other functions, one of which is GC inhibition of the synthesis of prostaglandins and leukotrienes which are the two main products in inflammation [78], hence their anti inflammatory role. Furthermore, GCs play a role in immunosuppression as they suppress cell mediated immunity by inhibiting genes that code for some cytokines especially interleukin 2 (IL-2). They also suppress humoral immunity by causing B cells to express smaller amounts of IL-2 receptors [79].

GCs mediate their effects via the ubiquitously expressed mineralocortiocid receptors (MRs) and GRs. Additionally, GCs may also exert non genomic actions via GR independent membrane receptors [80], providing a mechanism by which CORT exerts non-genomic actions. The GR receptor is intracellularly localised and sequestered in the cytoplasm as an inactive complex with molecules of heat shock proteins (HSP-90) and other cytosolic proteins [81]. Binding of GCs to the GR leads to their release and translocation into the nucleus where it binds to GC response element (GRE) in the promoter region of target genes, thus permitting it to stimulate or inhibit gene transcription of target genes [82-84].

1.6.3. The role of glucocorticoids in apoptosis and neuroprotection

When it comes to the regulation of apoptosis, GCs are most often described as a doubled edge sword. One of the factors that seem to determine the role of GCs on apoptosis is the cell type. GCs are known to inhibit apoptosis in several cell types such as neutrophils, hepatocytes and photoreceptors [85-87]. On other hand, they also enhance apoptosis in a wide variety of cell types amongst which are lymphocytes, myeloma cells and monocytes [88]. The role of GCs on apoptosis is not only cell type

dependent but also context dependent as they are known to general inhibit apoptosis during inflammation but favour apoptosis in situations of oxidative stress [89].

When it comes to neuroprotection, the role GCs play seems to be very much dependent on the duration and concentration following systemic elevation or exogenous application. In the acute situation, elevated CORT levels have been shown to profoundly attenuate NMDA mediated excitotoxicity of neurons and light damage of photoreceptors [86, 90]. Meanwhile, higher concentrations and chronic elevation of CORT were shown to have adverse effects on neurons in several studies [91-93].

Summarily, the role of GCs in apoptosis and neuroprotection is incongruous and depends on several factors which include the cell type, cause of demise as well as GC concentration and duration of application. The anti apoptotic role of GCs is most likely mediated by their ability to up regulate anti apoptotic proteins, transrepress proapoptotic proteins and also activate the neuroprotective PI3-Akt pathway [94, 95].

1.7. The Phosphatidylinositol 3-Akt kinase (PI3-Akt) pathway

Phosphatidylinositol 3-kinases are a family of intracellular signal transducer enzymes which are activated by several molecules via G protein-coupled receptors and tyrosine kinase receptors through the phosphorylation of 3 position hydroxyl groups of the inositol ring of phosphatidylinositol. These enzymes have the ability to activate Akt (protein kinase B) through phosphorylation of one or two amino acid residues leading to a "PI3-AKT" signalling pathway. The PI3-AKT pathway is known to mediate several cellular processes which help to maintain cell viability amongst which are; protein synthesis, inhibition of apoptosis, cell proliferation and transcription of survival genes [96-98].

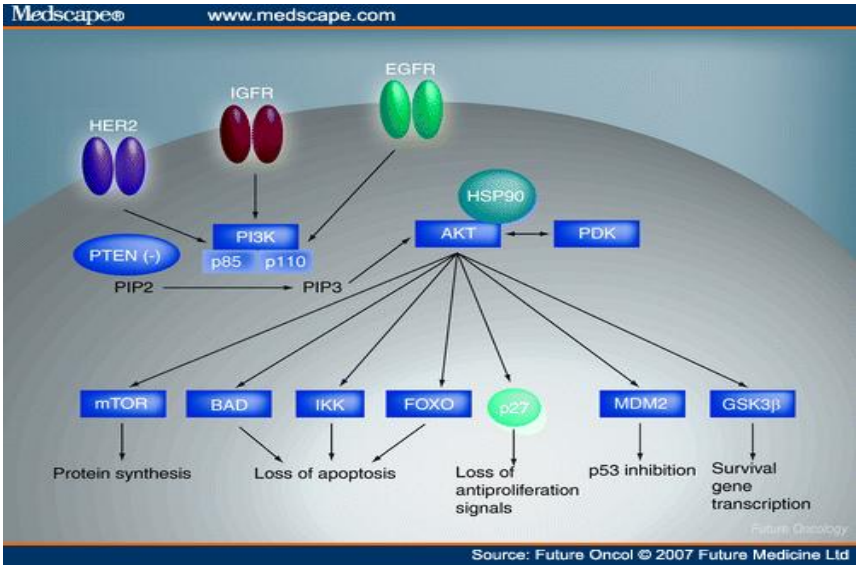

Figure 7: Overview of the PI3-k/AKT signalling pathway. Source: http://img.medscape.com.

2 AIM OF THE THESIS

Psychosocial stress is a frequent phenomenon in animal dwellings and is involved in the development and or exacerbation of several pathologies in humans [99-101]. An increase secretion of CORT is one of the hall marks of the stress response [102]. Once released, CORT has protective antiapoptotic as well as deleterious proapoptotic effects on different types of cells [85, 87, 88]. Following fasting mediated stress, a CORT surge has been reported to protect photoreceptors from apoptosis [86]. Therefore, we wondered if short-term psychosocial stress would also be protective on photoreceptors and what the effect would be when the stress duration is prolonged.

The first part of this thesis aimed to establish an appropriate experimental set up that can be used to investigate the effect of psychosocial stress on the damage on retinal neurons. CSC housing is a well established psychosocial stress paradigm in C57/Bl6 mice. The first part of this thesis was therefore dedicated to the re-establishment of CSC housing as an appropriate psychosocial stress paradigm in Balb/c mice owing to their suitability for light damage experiments.

The aim of the second part of the thesis was to characterize the effect of short-term and chronic psychosocial stress on induced neuronal cell death in the retina. This part focused on evaluating what a sharp increase in CORT levels following short-term psychosocial stress and sustained CORT levels followed by a blunted release following prolonged psychosocial stress imply for a damaged retina by analysing histological sections.

The third part of thesis was aimed at clearly pinpointing the molecule released during stress that confers the observed protective effect. Studies were designed to elucidate the role of CORT by performing exogenous injections and interrupting normal functioning of the HPA axis by prior adrenalectomy (ADX). Additionally, experiments in which exogenous CORT was injected into ADX mice to reproduce the neuroprotective effects of short-term psychosocial stress in ADX mice were performed in other to draw logically convincing conclusions.

In the fourth part of the thesis, *in vivo* and *in vitro* experiments were carried out to identify the mechanism underlying the protective effect of short-term psychosocial on light induced photoreceptor damage. Using molecular biology and protein biochemistry techniques, the up regulation of candidate genes, protein expression and the activation of a candidate cell signalling pathway were evaluated. Control experiments were performed to ascertain the involvement of the identified molecular signalling pathways by blocking this pathway and once more performing histological analysis to evaluate the impact such a treatment has on neuronal survival in the retina.

3 MATERIALS AND METHODS

3.1. Main materials and equipment.

Material/equipment	Supplier
BioPhotometer	Eppendorf, Hamburg
Centrifuges (5415D, 5415R, 5804R, 5810R)	Eppendorf, Hamburg
Glass pipettes	Schott, Roth, VWR
Glassware	Schott, Roth, VWR
Inolab pH-Meter	WTW GmbH, Weilheim
Latex gloves	Roth, Karlsruhe
Memmert water bad	Memmert GmbH, Schwabach
Mettler AE 163 fine balance	Mettler Toledo, Giessen
MilliQ Plus PF water purifier	Millipore Corporation, USA
Multi-reaction tubes 0.5, 1.5 and 2.0 ml	Roth, Karlsruhe
Nitrile gloves	VWR, Darmstadt
Parafilm	Pechiney Plastic, Chicago, USA
Pasteur pipettes	Brand, Wertheim
Pipetman pipettes	Gilson, Den Haag, Holland
Polymax 1040 shaker	Heidolph, Kelheim
Reaction tubes 15 ml, 50 ml	Sarstedt, Nürnbrecht
Research Pipettes	Eppendorf, Hamburg
Sunrise-Basic ELISA-Reader	Tecan GmbH, Austria
Systec V75 autoclave	Systec GmbH, Wettenburg
Vortex-Genie 2 mixer	Scientific Industries Inc., USA

Table I. Main Equipment.

3.2. Animal Models

3.2.1. Mice

To investigate the effects of psychosocial stress on retinal degeneration, Balb/c mice and male C57BL/6 mice were obtained from mice bred within the animal facility of the University of Regensburg, Germany and from the commercial supplier Charles Rivers (Sulzfeld, Germany) respectively. Adult Balb/c mice used for breeding in the animal facility were genotyped to confirm Balb/c lineage by looking at the *Rpe65* gene to be sure that the mice carried the *Rpe65*LEU450 variant and not the *Rpe65*Met450 variant which has been shown to be responsible for decreased susceptibility to light damage in mice [103]. For the isolation of Müller cells, Wistar rats from Charles River (Sulzfeld, Germany) were used.

3.2.1.1. Mice breeding

Breeding pairs for Balb/c mice were established and bred within the animal facility of the University of Regensburg. When they put to birth, offspring were separated from breeding pairs after 3 weeks. When male offspring attained 18 to 20 g body weight, they were numbered using thin metallic number plates pinned to their ears and single housed in standard polycarbonate mouse cages (16 X 22 X 14 cm) under standard laboratory conditions (12-h light, 12-h dark cycle, lights on at 0600h, 22°C, and 60 % humidity), with food and water *ad libitum* for at least five days before the start of the experiment. All procedures concerning mice were carried out in accordance with local and international guidelines on the ethical use of animals.

3.2.2. CSC housing

In order to induce psychosocial stress in Balb/c mice, male Balb/c (submissive experimental mice) weighing 18-24 g and male C57BL/6 mice weighing 30-35 g (aggressive dominant mice) were exposed to the CSC paradigm [64]. To this end, dominant mice were transferred into observation cages at least one day before the CSC procedure. Before the beginning of the CSC procedure, all potential dominant mice to be used for the CSC procedure were tested for aggressive behaviour. Dominant mice that started to injure their opponents by harmful bites were not used for the CSC procedure. On the day the CSC procedure began, experimental mice where weighed and divided into groups of four mice of equal mean weight per group. Groups were then randomly assigned to either the CSC or single housed controls (SHC) group. At the beginning of the dark phase, the four mice of each CSC group were transferred into the home cage of a large dominant mouse while SHC mice where let to stay in their cages. During the first 30 minutes after colony formation, the CSC housed mice were observed for behavioural analysis. In all colonies, the larger male mouse established a dominant status while it was chasing and attacking all four experimental mice. All four experimental mice were considered as subordinates based on exhibition of defensive behaviour which includes flight, retreat and a submissive upright posture as previously demonstrated in Bl/6 mice [64].

3.2.3. Short-term vs. Chronic CSC Housing

To investigate the effects of psychosocial stress on light or NMDA induced damage of retinal neurons, CSC was performed either acutely (for a short-term (10 hours)) or chronically (19 days). In the case of acute CSC, a random group of four CSC mice were housed together with one dominant male for 10 hours during the dark phase while control mice remained single in their home cages. At the end of 10 hours, body

weight was again measured. In the case of chronic CSC, CSC mice were housed with the dominant male for 19 days consecutively. To avoid habituation, the mice were transferred into the cage of a novel dominant male on day 8 and day 15. Control mice were singly housed and remained undisturbed in their home cages except for change of bedding once a week. Behavioural observation was again done upon change of the dominant mouse on day 8 and day 15 to ensure that the experimental mice were again subordinated by the new dominant mouse. To ascertain stress induction by CSC, stress parameters which include CORT levels, changes in body and adrenal weight were measured in a separate group of CSC and SHC mice during and or after short-term and chronic CSC housing. At the end of the 10 hours or 19 days CSC housing procedure, mice were weighed and either exposed to a treatment to induce neuronal damage (either NMDA injection or exposed to light damage) or killed for extraction of retinal tissue.

3.3. Intravitreal and intraperitoneal injections

3.3.1. Materials and Reagents

Substance	Function	Dosage	Company
Corticosterone	Glucocorticoid	52 µg/g	Sigma, Taufkirchen
Dimethyl sulfoxide	Solvent	-	Roth, Karlsruhe
N-Methyl-Aspartate (NMDA)	Glutamate analog	3 µl of 10 mM	Sigma, Taufkirchen
Ethanol	Solvent	-	Roth, Karlsruhe
PBS	Solvent	-	Life Technologies Karlsruhe
Triciribine	Akt inhibitor	3 µl of 1 ng/µl	Merck, Darmstadt

Narcotic/Antiseptic	Function	Company
Isoflurane	Anaesthesia	Baxter, Unterschleißheim
Iodine tincture	Antiseptic	Braun, Melsungen
Isoptomax. ointment	Antiseptic	Alcon Pharma, Freiburg

Material	Company
Needle (beveled needle 35 G)	W. P. I., Berlin
Hamilton syringe	Roth, Karlsruhe

Table II: Reagents and materials, i.v. and i.p. injections.

3.3.2. Intravitreal injection

In order to deliver desired substances into the eye, intravitreal injections were performed. To get this done, mouse were anaesthetised through inhalation of isoflurane narcotic and their eyes disinfected with a 10 % Iodine tincture solution. A needle (33 G) connected to 25 µl Hamilton syringe was introduced around the equator of the eyeball through the sclera in the direction of the optic nerve into the vitreous cavity and then a precise quantity (3 µl) of the test substance was injected through the Hamilton syringe. After about 20 seconds, the needle was withdrawn from the eye. This delay gives the eye the possibility to balance the increased intraocular pressure caused by the injection. After withdrawal of the needle, the eye was treated with antiseptic (isoptomax ointment). In this project, eyes and the optic nerve were investigated after intravitreal injection of triciribine and NMDA respectively. For each mouse, one eye received a control treatment composed only of the solvent in which the test substance was dissolved.

3.3.1. Intraperitoneal (ip) injection

To perform ip injections, mice were restrained with the abdomen facing upwards such that they could not move during the procedure. A needle connected to a syringe was introduced into the abdomen at about a 30 degree angle to a depth of approximately half a centimetre. Depending on the body weight of the mouse, a given volume of CORT (around 100 µl) dissolved in ethanol/saline, 1:1(vol/vol), was injected in a single intraperitoneal injection (52 µg/g) 15 minutes prior to light exposure or 7 hours prior to collection of retinal tissue for Western Blot. Vehicle-injected mice received a corresponding volume of ethanol/saline, 1:1(vol/vol), while a third group was left uninjected.

3.4. Animal surgery and blood sampling

3.4.1. Materials and Reagents

Substance	**Function**	**Company**
Isoflurane	Anaesthesia	Baxter, Unterschleißheim
Iso baxter	Antiseptic	Baxter, Unterschleißheim
Iodine tincture	Antiseptic	Braun, Melsungen

Material	**Company**
EDTA coated Tubes	Saarstedt, Nürnbrecht
PCR tubes	Biozym, Oldendorf
Beveled needle 35 G	W. P. I., Berlin

Table III : Reagents and materials for animal surgery and blood sampling.

3.4.2. Adrenalectomy (ADX)

The adrenal glands of mice were surgically removed as a means of disrupting the functioning of the HPA axis. To this end, mice were anesthetised through a continuous inhalation of isoflurane and fixed to a flat surface with the back facing upwards. The area on the back around the abdomen was shaved and disinfected using 70 % alcohol and a 2 cm skin incision performed on the back of the mice at the level of the kidneys (midline). The adrenals were removed bilaterally through two peritoneal incisions performed on the left and right side of the abdomen. Mice were then injected with isobaxter antiseptic in the area of the skin incision, the incisions sewed and iodine tincture applied. Sham mice underwent simple laparotomy. After surgery, both ADX and sham operated mice received 0.9 % saline in drinking water (until they were killed) to compensate for loss in mineralocorticoids. After the

operation, both ADX and sham operated mice were single housed for at least one week to allow for recovery before experiments started.

3.4.3. Dertermination of adrenal weight

As a stress indicator, adrenal weight after CSC was measured. In this regard, mice were killed by introducing them into a carbon dioxide exicator at the end of CSC housing. The abdomen was dissected open, both adrenal glands removed and carefully pruned of fat tissue and then weighed. The weight of both the left and right adrenals was expressed in relation to body weight (mg per g).

3.4.4. Blood sampling

To determine CORT and ACTH levels, mice were rapidly killed by decapitation under CO_2 anaesthesia within 1 minute after handling each mouse. Approximately 200 µl of trunk blood was collected in EDTA-coated tubes on ice (Sarstedt, Nümbrecth) containing 10 µl aprotinin (Trasylol, Bayer corp. AG, Leverkusen). CSC housed mice were killed immediately at the end of CSC housing, while CORT and vehicle-injected mice were killed 15 minutes after injection. Collected blood samples were centrifuged at 5000 rpm for 10 minutes and 120 µl plasma collected into PCR tubes for ACTH measurement while 20 µl was collected for CORT measurement. Plasma samples were stored at -20^0C until they were assayed using a commercially available ELISA Kit for CORT and ACTH.

3.5. Induction of retinal degeneration

Two well established methods were used to induce neuronal damage and subsequent degeneration. Here, photoreceptors were damaged via light induced photoreceptor damage [104], while RGC were damaged via NMDA mediated excitotoxicity [105].

3.5.1. Light induced damage of photoreceptors

To induce damage of photoreceptors, mice were first placed in transparent cylinders without bedding, food or water. The transparent cylinders were then placed in a circular pattern in the middle of the floor of the illumination box and exposed to diffuse white fluorescent light coming from the top of the illumination box. Luminance intensity was adjusted by moving the floor of the illumination box higher towards the light source to increase light intensity or lower towards the basement to reduce it as desired. Average luminance at the floor of the illumination box was measured using a lux meter. Illumination of the mice was performed at 5000 lux for 30 or 60 minutes as indicated. Control mice were left in their cages and kept under standard laboratory conditions. At the end of illumination, mice were re-housed in their single cages under standard laboratory conditions for up to three weeks. Eyes were then enucleated and fixed appropriately as indicated.

3.5.2. NMDA induced damage of RGC´s

The NMDA damage model is based on the specific excitotoxic damage of retinal ganglion cells upon an intravitreal injection of NMDA [106]. The glutamate analogue NMDA is a synthetic agonist for glutamate receptors. These receptors are coupled to a Ca^{2+} canal. Through a binding of the NMDA to its receptor, the ion canal gets opened leading to a Ca^{2+} influx. Given the fact that NMDA is not a natural ligand of this receptor, there is no natural mechanism to inactivate the NMDA-Receptor complex, leading to a prolonged opening of calcium channels. The excessive influx of the secondary messenger calcium influences several pathways which finally lead to an activation of the apoptotic-signal cascade thereby leading to apoptosis in RGC cells whose axons make up the optic nerve.

3.6. Histology

3.6.1. Paraffin sections

To quantify the number of apoptotic cells after a light induced damage by TUNEL labelling, enucleated eyes were embedded in paraffin.

3.6.1.1. Reagents and materials

Reagent	**Company**
Ethanol	Roth, Karlsruhe
Xylene	Merck, Damstadt
Paraformaldehyde	Merck, Damstadt
Paraffin	Engelbrecht, München
Equipment	**Company**
Embedding automat HMP110 (Paraffin)	Microm, Waldorf
Supercut 2050 (Paraffin)	Reichert-Jung, Kirchseeon

Buffer	**Composition**
4 % Paraformalaldhyde (PFA)	Weigh 4 g paraformaldehyde in a fume hood, add 0.1M PhP and bring to 100 ml. Dissolve by heating the closed bottle in a water bath at 65°C for 2 hours. Store the solution at 4°C,
Phosphate buffer (PhP). 0.1 M	P1: Na_2HPO_4 x H_2O: 35.6 g to 2 l P2: NaH_2PO_4 x H_2O: 13.8 g to 1 l P1:P2 = 5:1 pH 7.4

Table IV: Reagents and materials for paraffin embedding.

3.6.1.2. Preparation of eyes for Paraffin Embedding

To prepare the retina for paraffin embedding, mice were killed in a $C0_2$ exicator 24 hours after illumination. Eyes were marked using a tin needle that was inserted tangentially through the sclera at the 12 o'clock position. Using a pair of forceps, the tissue surrounding the eyeball was pushed down and the eye pulled out of the eye orbital and transferred into a 4 % PFA fixative solution.

3.6.1.3. Paraffin Embedding

In order to be able to make thin sections of the retina by paraffin cutting, eyes were allowed to stay in fixative (4 % PFA) for four hours after which samples were washed in 0.2 M phosphate buffer for 15 minutes repeated twice for a total of three washes. After washing, eyes were cut into two parts from the 12 o'clock position via the optic nerve to the 6 o'clock position. Eyes were placed in 50 % ethanol for 1 hour and then incubated in 70 % ethanol overnight. The next day, samples were incubated in 80 % ethanol for 1 hour followed by 96 % ethanol for 1 hour, repeated once for two incubations. After the last two incubations in 100 % ethanol, samples were transferred immediately into xylene for 1 hour 30 minutes two times. Eyes were then washed in three successive paraffin dishes as follows, paraffin 1 for 4 hours, paraffin 2 for 8 hours and paraffin 3 for 2 hours. At the end, samples were then brought into fresh paraffin and placed into an embedding mould.

3.6.1.4. Preparation of paraffin slides for TUNEL Labelling

To obtain paraffin slides for TUNEL labelling, paraffin blocks containing eye samples were fitted into a microtome and 6 µm thick slices prepared and then transferred into a warm water bath. Slices were then placed on glass slides and allowed to firmly attach overnight at a temperature of 37^oC. Good slices obtained from the centre of the retina had the following characteristics:

- Large retina ranging from one ora serata to the other ora serata,
- Presence of the optic nerve and an open pupil,
- Intact retinal layers without any folds.

Before staining, all slides were observed under the light microscope and slices that met quality criteria were chosen for TUNEL labelling.

3.6.2. TUNEL Labelling

3.6.2.1. Reagents and materials

Reagent	**Company**
Paraformaldehyde	Merck. Darmstadt
NaCl	Roth, Karlsruhe
Dapi	Linaris, Wertheim
Phosphate buffer saline (PBS)	Life Technologies, Karlsruhe
-Equilibration buffer, Proteinase K buffer, rTdT enzyme, Nucleotide mix, SSC	Promega, Maddison. USA
rTdT (51µl) incubation buffer	**quantity**
Equilibration buffer	45 µl
Nucleotide mix	5 µl
rTdT enzyme	1 µl

Table V : Materials and reagents TUNEL labeling.

3.6.2.2. Principle of the TUNEL assay.

Terminal deoxynucleotidyl transferase dUTP Nick End Labelling (TUNEL) was performed using the apoptosis detection kit “DEAD END” (Promega, Madison, USA). This method detects fragmented DNA by terminal end labelling of fragmented DNA through the addition of dUTPs that are secondarily labelled with fluorescent nucleotides. TUNEL labelling is a commonly used method for detecting apoptotic cell death. It is based on the fact that DNA fragmentation which is a major characteristic of cells that die by apoptosis does not occur when cells die by necrosis. The assay relies on the presence of nicks in the DNA which can be identified by Terminal deoxynucleotidyl transferase, an enzyme that catalyzes the addition of fluorescein -12- dUTP to the 3′-OH groups at the ends of fragmented DNA. Cells undergoing apoptosis therefore get fluorescent nucleotides attached to the nicks of their fragmented DNA. Labelled cells can be visualized by fluorescence microscopy.

3.6.2.3. The TUNEL Assay.

To perform TUNEL analysis, slices were deparaffinized by immersing slides in fresh xylene in a coplin jar for 5 minutes at room temperature. The process was repeated once for at least two xylene washes. After that, slides were immersed in 100 % ethanol for 5 minutes at room temperature. Samples were then rehydrated by sequentially immersing the slides through graded ethanol washes (100 %, 95 %, 85 %, 70 %, and 50 %) for five minutes each at room temperature. For each concentration, the process was repeated once for two ethanol incubations per concentration. After rehydration, slides were equilibrated by immersing the slides in 0.85 % NaCl for 5 minutes at room temperature followed by one PBS wash for 5 minutes at room temperature. After this, samples were fixed by immersing the slides in 4 % methanol solution in PBS for 15 minutes at room temperature. After that, slides were washed in

PBS for 5 minutes at room temperature two times. To permeabilize tissues, the liquid from the slides was removed and selected slices were encircled using a grease pen. Proteinase K solution was then added unto each slice for 8 minutes. After that, Samples were washed two times by immersing the slides in PBS for 5 minutes at room temperature in a coplin jar and fixed again by immersing the slides in 4 % formaldehyde solution in PBS for 5 minutes at room temperature. After tapping the slides to remove excess solution, the samples were covered with equilibration buffer for 10 minutes. The equilibration buffer was discarded and the incubation buffer containing recombinant terminal deoxyribosyl transferase added. For negative controls no recombinant terminal deoxyribosyl transferase was added to the incubation buffer. All slices were then placed on wet glass dishes and covered with aluminium foil to protect from direct light and placed in an incubation chamber at 37^0C for 60 minutes to allow the tailing reaction to occur. The tailing reaction was terminated by immersing the slides in 2X SSC in a coplin jar for 15 minutes at room temperature. After that, samples were washed by immersing the slides in fresh PBS 3 times for 5 minutes each at room temperature to remove unincorporated fluorescein-12-dUTP. At the end of the TUNEL assay, a mounting medium stain was added to each slice and the slice covered by a glass slide and then allowed to stay in the refrigerator until the two glass surfaces were firmly attached.

3.6.2.4. Microscopy and quantification of apoptotic cell.

Labelled slices were observed under a fluorescent microscope (Carl Zeiss, Jena, Germany) and typically fluorescent cells in the outer nuclear layer (ONL) were counted. The total area of the ONL was also measured using the Axio vision programme and the number of fluorescent cells was expressed per 1000 μm^2 of retinal ONL.

3.6.3. Preparation of semi-thin Sections

To analyse the morphological changes in the retina or the extent of loss of axons, optic nerves or eyes were prepared 3 weeks after light damage or NMDA injection respectively and embedded in epon and cut to produce 1 µm sections.

3.6.3.1. Materials and reagents for semi-thin sections

Reagent	**Company**
Acetone and Lead citrate	Merck, Darmstadt
Cacodylic acid Sodium trihydrate salt	Merck, Darmstadt
2-Dodecenylsuccinic-acid-anhydrate (DDSA)	Merck, Darmstadt
2.4.6-Tri(dimethylaminomethyl) Phenol (DPM-30)	Serva, Heidelberg
Epon	Serva, Heidelberg
Glutaraldehyde	Serva, Heidelberg
Glycidether	Merck, Darmstadt
Isopropanol	Roth, Karlsruhe
MNA	Carl Roth GmbH, Karlsruhe
Osmiumtetroxide	Merck, Darmstadt
1.4-p-phenylendiamine	Sigma, Taufkirchen
Pioloform	Plano, Marburg
Uranylacetate	Merck, Darmstadt
Equipment	**Company**
Embedding automat EM TP (Epon)	Leica, Wetzlar
Ultracut E-Ultramicrotom (Epon)	Reichert-Jung, Kirchseeon
Buffer	**Composition**

Cacodylate buffer	20.14 g Cacodylic acid, in 0.5 l distilled H_2O pH 7.2
EM-Fixant	2.5 % Paraformaldehyde 2.5 % Glutaraldehyde in Cacodylatpuffer
Phosphate buffer (PhP) 0.1 M	P1: Na_2HPO_4 x $2H_2O$: 35.6 g in 2 l P2: NaH_2PO4 x $1H_2O$: 13.8 g in 1 l P1:P2 = 5:1 pH 7.4
Stock solution A	62 ml Glycidether 100
Stock solution B	100 ml Glycidether 100

Table VI: Materials and reagents for semithin sections.

3.6.3.2. Preparation of eyes and optic nerves for Epon Embedding

To obtain eyes or optic nerves for histology, mice were killed by CO_2 asphyxiation and the eyes enucleated with the aid of forceps. To ensure proper fixation of the entire eye, the cornea was perforated with the aid of a thin needle before insertion into the EM fixant solution.

Epon embedding of enucleated eyes and optic nerves was performed as follows. Tissues were immersed into an EM fixant for 12-16 hours and then washed briefly in cacodylate buffer. The tissues were then fixed in 1 % osmium tetroxide in 100 mM phosphate buffer for 1-2 hours at 4°C followed by washing using cacodylate buffer for 2 hours. Samples were then stained with 2.0 % aqueous uranyl acetate for 2 hours at 4°C in the dark and drained by passing through increasing ethanol concentrations (70 %, 80 %, 90 %, and 100 %). Thereafter, samples were dehydrated by passing through a 1:1 and 1:2 mix of Epon: Aceton for 1 hour followed by incubation in 100

% Epon overnight. The next day samples where changed into fresh Epon for 1 hour and then hardened in an incubator for 24 hours at 60 °C followed by 48 hours at 90 °C. Semi-thin sections (1 µm) were then cut from the eyes and observed through light microscopy. Sixty nm slides were prepared from required regions with the help of the Ultracut E"-Ultramicrotome and stained.

3.6.3.3. Staining of Sagittal Eye Sections

Sagittal sections of the eye were stained with Richardson. Here, the slides were covered for 15 to 30 seconds at 60 °C with the staining solution and then cleaned with water.

Richardson staining solution

Stock solution I	1 % Azure II: 5 g in 500 ml distilled H_2O
Stock solution II	1 % Methyleneblue: 5 g Methyleneblue in 500 ml 1 % Borax
Final solution	1 vol Stock solution I + 1 vol Stock solution II + 2 volumes distilled H_2O

Table VII: Components of the Richardson staining solution.

3.6.3.4. Staining of optic nerves.

Optic nerves were contrasted as follows; samples were dissolved in Paraphenylendiamine (10 mg/ml) in ethanol solution and left for 3 days in day light until they became dark. Sections where then stained at room temperature for 2-3 minutes and washed with ethanol.

3.6.3.5. Analysis of semi-thin sections.

After treating optic nerves to give contrast, evaluation was done with the aid of a Zeiss light microscope and the Axio vision (3.0) software. Panorama pictures were made and axons counted using the counting function "Count-and-Tag" of the

windows free IT image tool program developed at the University of Texas health science center at San Antonio.

After staining sagittal sections of the eye, the surface of the inner plexiform layer was measured using the measuring tools of the Axiovision software (Carl Zeiss,). The data obtained was used to plot spider diagrams [107].

3.7. Molecular Biology

3.7.1. Reagents, Materials and Equipment

Reagent	Company
10 x PCR-buffer	Bioline, Luckenwalde
Agar	Merck, Darmstadt
Agarose	Biozym Scientific, Oldendorf
Ampicillin	Serva, Heidelberg
Borate (sodiumtetraborate)	AppliChem, Darmstadt
Bromophenol blue	Serva, Heidelberg
Chloroform	Roth, Karlsruhe
DMSO (Dimethylsulfoxide)	Roth, Karlsruhe
DNA-Standards	New England Biolabs, Frankfurt
dNTPs	Bioline, Luckenwalde
EDTA	Roth, Karlsruhe
Ethidium bromide	Serva, Heidelberg
Ficoll	Serva, Heidelberg
Fluorescein	Qiagen, Hilden
Hot star Taq	Qiagen, Hilden
iScript™ cDNA Synthesis Kit	BioRad, München
Isopropanol	Roth, Karlsruhe
Magnesium chloride (25 mM)	Qiagen, Hilden
Microseal®,, B“ Film	Biorad, München
PCR Plates, 96 Well iCycler IQ	Biorad, München

SYBR-Green I	Qiagen, Hilden
Taq DNA Polymerase	Bioline, Luckenwalde
Tris-HCl	Roth, Karlsruhe
TRIzol®-Reagent	Life Technologies, Karlsruhe
RNase-free water	Roth, Karlsruhe
Material / equipment	**Company**
Biosphere filter tips	Sarstedt, Nürnbrecht
Electrophoresis chamber	PeqLab Biotechnologie, Erlangen
IQ5 Multicolor Real-time PCR Detection System + iCycler	BioRad, München
Master cycler	Eppendorf, Hamburg
Power Supply	Consort, Turnhout, Belgium

Table VIII: Reagents and materials for molecular biology.

3.7.2. Genotyping of mice for Balb/c lineage

In order to confirm the genotype of Balb/c mice, breeding pairs in the animal facility were genotyped for the Leucine-Methionine variant *Rpe65 (Rpe65450Leu and Rpe65450Met)* that occurs at position 450 in mice of the *Rpe65* gene. DNA was extracted, amplified, the product digested using the restriction enzyme MWO and analysed on an agarose gel as described below.

3.7.2.1. Isolation of Genomic DNA from mouse tail biopsies

To obtain genomic DNA samples from tail biopsies to be used for genotyping of breeding pairs, mice were etherized, pierced with an ear mark and the tail cut for a 0.5 cm tail biopsy. DNA from the tail biopsy was extracted as described by Nexttec DNA isolation system as follows; Small samples of fresh tissue were obtained from the tails

of mice and 3 different buffers added to each sample as follows; 265 µl of buffer G1, 10 µl of buffer G2 and 25 µl of buffer G3 followed by incubation at 60^0C with shaking at 1200 rpm for 30 minutes in a thermo mixer. Thereafter, 120 µl of the lysate from each sample was transferred into an equilibrated Nexttec clean column and incubated for 3 minutes at room temperature. After incubation, samples were centrifuged at 700x g for 1 minute and the eluate which contained purified DNA collected.

3.7.2.2. Polymerase chain reaction (PCR)

Amplification of DNA was carried out by PCR technology in an optimised mix containing Taq (from Thermus aquaticus), dNTP´s, $MgCl_2$, primers and 10X buffer as follows.

PCR Mix.

Component	**Quantity**
10x Buffer	5 µl
$MgCl_2$	3 µl
dNTP´s (25 mM)	2 ul
Primers MWO	2 µl each
Taq	1 µl
H_20	29 µl
DNA (1:50)	100 ng
MWO forward primer	**MWO reverse primer**
CACTGTGGTCTCTGCTATCTTC	GGTGCAGTTCCACTTCAGTT

Table IX: PCR reaction mix for DNA amplification for LEU-MET mutation.

The following PCR program was used to run the PCR mix.

Step:	**Temperature:**	**Duration:**
Initial denaturation	94 °C	2 minutes
Denaturation	94 ° C	30 s
Primer annealing	55 °C – 65 °C	45 s
Elongation	72 °C	1 minute
Final elongation	72 °C	10 minutes

Table X: PCR Program for Balb/c mice genotyping.

35 cycles of denaturation, primer annealing and elongation were carried out.

3.7.2.3. Restriction digestion of PCR product

The product from the PCR reaction described above was digested by mixing 12 µl of PCR product, 8 µl of water and 0.3 µl MWO 1 restriction enzyme followed by incubation at 37°C for 3 hours.

3.7.2.4. Agarose Gel Electrophoresis

For analysis of digested DNA, digested products were separated by agarose gel electrophoresis. 1.0 % (w/v) agarose was dissolved in 150 ml of 1x TBE by boiling. The solution was cooled down to ~ 60°C and then EtBr was added at a concentration of 0.1 µg/ml and the mix poured into a gel rack for polymerization. The DNA samples were mixed with 5x loading buffer, loaded into the wells of the gel and electrophoresis performed for 2 hours in an electrical field of 120 - 140 V towards the cathode. To be able to evaluate the fragment size, 0.5 µg of an appropriate molecular weight marker was ran in parallel. For DNA analysis, the gel chamber equipment was rinsed with 0.5 M NaOH before use to reduce the risk of contamination. The nucleic

acids were visualized by UV irradiation and subsequent fluorescence of EtBr that intercalated with DNA.

3.7.3. RNA isolation from cells and tissue

For gene expression analysis, total RNA was isolated from Müller cells and retinal tissue. To obtain retinal tissues for RNA extraction, mice were killed by CO_2 asphyxiation immediately after CSC or 7 hours after illumination or CORT injection. Collected eyeballs were dissected immediately to obtain retinal tissue. At the time of dissection, excess fat, muscle and connective tissue surrounding the eyeball were removed, the cornea was excised and the lens removed. The remaining posterior eye segment was incised using a pair scissors from one side to the optic nerve. The attachment of the retina to the nerve was cut and retinal tissue collected by carefully picking it apart from the sclera with forceps into 500 µl TRIzol. In the case of Müller cells, cells were homogenized in 500 µl TRIzol by using a cell scrapper. RNA from tissue or Müller cells was extracted as described by Chomczynski and Sacchi [108], using TRIzol (Life Technologies) according to the following procedure.

To isolate RNA, obtained tissue was homogenized using a tissue shredder and samples incubated for 5 minutes at RT. After incubation samples were centrifuged at 12 000 g for 10 minutes at + 4 °C to pellet cell debris and contaminants. The supernatant was transferred into a fresh eppendorf tube and 1/5 vol of chloroform was added. The sample was mixed for 15 s, incubated for 2 - 3 minutes at RT and centrifuged at 12 000 g for 15 minutes at +4 °C. The aqueous phase was carefully transferred into a fresh eppendorf tube and 350 µl isopropanol were added. The sample was vortexed and stored at -20 °C overnight to enhance the yield of precipitation. RNA was precipitated by centrifugation at 12 000 g for 10 minutes at + 4 °C. The pellet was then washed twice by adding 700 µl of 75 % EtOH, vortexing

the mix and then centrifuging it at 7 500 g for 5 minutes at +4 °C. The pellet was air-dried and dissolved in 20 µl of sterile nuclease-free H_20. The quantity and purity of RNA was analysed spectrophotometrically and it was then stored at -80 °C until use.

The concentration of the isolated RNA was then measured by means of a spectrophotometer. To do this, 1 µl of each sample was placed on the tip of the photometer which automatically calculated the RNA concentration.

3.7.3.1. cDNA synthesis

To perform real time RT-PCR, RNA that had been stored at –80°C was reverse transcribed into cDNA by using the iScript™ cDNA Synthesis Kit (Bio-Rad, Munich). The kit takes advantage of an RNAse inhibited RNAse H+ reverse transcriptase (RT), as well as a blend of oligonucleotides and random hexamer primers to initiate the transcription of mainly polyA-tailed mRNA. Per sample, 1 µg of RNA was transcribed into cDNA by adding 4 µl of 5x iScript reaction mix, 1 µl of iScript RT and nuclease-free H_20 to fill up the volume to 15 µl. To control the sample for any DNA contaminants, a control sample without RT (referred to as the – RT reaction) was mixed in parallel. The reaction was allowed to proceed in a master cycler by using the reaction conditions below. After that the cDNA was stored at -20 °C until further use.

Step:	**Temperature**	**Duration**
1. Primer annealing	25 °C	5 minutes
2. Reverse transcription	42 °C	30 minutes
3. Inactivation of RT	85 °C	5 minutes
4. Cooling down reaction	4 °C	∞

Table XI: Reaction steps for transcription of cDNA by the iScript™ cDNA Synthesis Kit.

3.7.4. RT-PCR primer design

Primer pairs for quantitative RT-PCR that spanned intron boundaries of the mouse genome were designed by the Universal ProbeLibrary System from Roche (https://www.roche-applied-science.com/sis/rtpcr/upl/index.jsp?id=UP030000) for selected genes. Target gene names, species and primer sequences are listed below.

Primer	Species	Orientation	Sequence 5' to 3'
BDNF	Mus musculus	fw	AGTCTCCAGGACAGCAAAGC
		rev	TGCAACCGAAGTATGAAATAACC
CNTF	Mus musculus	fw	TTGATTCCACAGGCACAAAA
		rev	CCCTGCCTGACTCAGAGGT
Edn2	Mus musculus	fw	ACCTCCTCCGAAAGCTGAG
		rev	TTTCTTGTCACCTCTGGCTGTA
FGF2	Mus musculus	fw	CGGCTCTACTGCAAGAACG
		rev	TGCTTGGAGTTGTAGTTTGACG
GAPDH	Mus musculus	fw	TGTCCGTCGTGGATCTGAC
		rev	CCTGCTTCACCACCTTCTTG
GAPDH	Rattus norvegicus	fw	AATGTATCCGTTGTGGAT
		rev	GCTTCACCACCTTCTTGAT
GFAP	Rattus norvegicus	fw	GAGAGGGACAATCTCA
		rev	TGTGAGGTCTGCAAACTTGG
GFAP	Mus musculus	fw	ACAGACTTTCTCCAACCTCCAG
		rev	CCTTCTGACACGGATTTGGT
LIF	Mus musculus	fw	AAACGGCCTGCATCTAAGG
		rev	AGCAGCAGTAAGGGCACAAT

Table XII: Real time RT-PCR primers.

3.7.5. Quantitative Real-time PCR

To analyse the expression neurotrophic factors in mice after different treatments, a quantitative real-time PCR was performed using cDNA as a template. In an optimal RT-reaction, the amount of a given transcribed cDNA corresponds to the amount of copies of its mRNA in the original RNA sample. Therefore, the rate of amplification of a given gene from the cDNA template mix can be used to calculate the number of copies of its mRNA in the original sample. The PCR was carried out by using a combination of the multicolour iQ™5 RT-PCR Detection System and an iCycler® thermal cycler. The system takes advantage of SYBR-Green I, a fluorescent dye that binds non-specifically to dsDNA (Witzthum et al., 1999). As the amplification reaction proceeds into its exponential phase, the fluorescence intensity exceeds a background level. This time-point is called the cycle-threshold (CT) for that gene. The more cDNA for a given gene in the template the less cycles the reaction has to proceed until it reaches its CT. To get a relative quantification of the expression levels of tested genes, their CT-values were compared with those of GAPDH, a selected reference gene. Reference genes are referred to as genes that function as "house-keeping" genes in the investigated tissue and that, independent of treatment, show no transcriptional regulation between samples. Because of variance in composition, each amplicon has its individual melting temperature, resulting in an individual sharp melting curve. To avoid any false positive results caused by primer dimers or mispriming, the melting curves for each sample product were analysed for their purity.

To get reliable data, triplicates of each sample were investigated. For each investigated gene, one -RT reaction was run in parallel.

The RT-PCR was performed as follows.

Firstly due to a huge amount of samples, two different master mixes for the reagents were mixed.

- Master mix for 2x MM.
- Sg (SYBR-Green I) MM.

The 2x MM was made up first and was then used as a component in the SgMM. The 2x MM can be stored at -20 °C for later use.

A) 2x MM	
10 X buffer	300 µl
$MgCl_2$ (25 mM)	120 µl
dNTPs (25 mM each)	24 µl
H20	1006.5 µl
Total volume	1450.5 µl

B) Sg MM	
2X MM	752.96 µl
Taq Polymerase (5 U/µl)	6.24 µl
SYBR-Green I (7.4 % (w/v) in DMSO)	19.76 µl
Fluorescein (1:100 in H_20)	1.56 µl
Total volume	780.52 µl
Total volume	780.52 µl

In the next step, master mixes for primers, cDNAs and cDNA/-RT reactions were setup.

C) Primer mix (5 µl):

Primer fw	0.08 µl
Primer rev.	0.08 µl

D) cDNA / mix:

SgMM	97.5 µl
cDNA	3.25 µl
H_20	29.9 µl

E) cDNA/-RT mix:

SgMM	7.5 µl
H_20	2.5 µl
Total volume	10 µl

Table XIII: Real Time RT-PCR reaction mixes. A) 2x MM, B) Sg MM, **C**) Primer mix (5 µl) for one reaction. D) The cDNA reaction mix (10 µl) for one reaction. E) The cDNA/-RT-reaction mix (10 µl) for one reaction.

Finally, a cDNA or cDNA/-RT-reaction mix of 10 µl was added together with the 5 µl primer mix in a reaction well of a 96-well PCR plate to give a total reaction volume of 15 µl. For each sample, triplets were performed for cDNA mix and singlets for the cDNA/-RT mix. The PCR-plate was covered with a sealing film and the samples shortly centrifuged. The reactions were run by the following steps of reaction conditions (amplification + melting curve) (Table XIV).

Step:	Temperature:	Duration:
1. Taq polymerase activation	95 °C	15 minutes
2. Amplification 40 cycles	95 °C ↔ 60 °C	10 s ↔ 40 s
3. Final elongation	95 °C	1 minute
4. Transit to melting cycles	55 °C	1 minute
5. 81 cycles for melting curve	55 °C + 0.5 °C/cycle	6 s

Table XIV: Steps of reaction conditions for quantitative real-time PCR.

The data were calculated and evaluated by using the iQ Optical System Software version 2.0 to give the relative expression values for each sample. The relative expression values are calculated by the comparative CT method, ΔΔCT, according to the formula

ΔΔCT = ΔCT (sample) - ΔCT (reference gene) [109]

The relative expressions were graphically presented by transferring the obtained expression data into Microsoft® Excel. The statistical significance was calculated according to the student's t-test by assessing a p-value of $p < 0.05$ as significant.

3.8. Protein biochemistry techniques

3.8.1. Reagents and materials

Reagent	Company
Albumin fraction V (BSA)	Roth, Karlsruhe
Ammonium peroxide di sulphate (APS), 10 % (w/v)	Roth, Karlsruhe

BCA assay reagents A+B	Montlucon, France
Bromphenol blue	Serva, Heidelberg
Coomassie®Brillant blue R250	Sigma, Taufkirchen
Deoxycholic acid	Roth, Karlsruhe
DL-Dithiotreitol (DTT)	Sigma, Taufkirchen
Acetic acid	Merck, Darmstadt
Formaldehyde	Roth, Karlsruhe
Glutaraldehyde, 25 % in water	Serva, Heidelberg
Glycerine	Roth, Karlsruhe
Glycine	Roth, Karlsruhe
Heparin-Agarose (aqueous ethanol solution)	Sigma, Taufkirchen
HEPES	Roth, Karlsruhe
Potassium chloride (KCl)	Roth, Karlsruhe
Magnesium chloride ($MgCl_2$)	Roth, Karlsruhe
Methanol	Merck, Darmstadt
Sodium acetate ($Na(CH_3COO)$)	Roth, Karlsruhe
Sodium carbonate (Na_2CO_3)	Roth, Karlsruhe
Sodium choride (NaCl)	Roth, Karlsruhe
Sodium-EDTA	Roth, Karlsruhe
Soidium thio sulphate($Na_2S_2O_3$), penta hydrate	Sigma, Taufkirchen

PageRuler™Prestained protein ladder	MBI Fermentas, St. Leon
Protease inhibitor	Sigma, Taufkirchen
Rotiphorese® Gel 30	Roth, Karlsruhe
SDS (Sodium Dodecyl Sulphate)	Roth, Karlsruhe
Roti®-free stripping-buffer	Roth, Karlsruhe
ß-Mercaptoethanol	Roth, Karlsruhe
TEMED (N,N,N`,N`-Tetramethylethylendiamin)	Roth, Karlsruhe
Tris Ultrapure, MB grade	Usb Corporation, USA
Tween 20	Roth, Karlsruhe
Equipment/Material	**Company**
Aida Advanced Image Data Analyser version 4.06	Raytest, Straubenhardt
ELISA-reader	Tecan, Mainz
Empty columns	Biorad, München
LAS 3000	Fujifilm, Düsseldorf
Micro homogeniser	Roth, Karlsruhe
Power supply	Consort, Turnhout, Belgium
PVDF-Western Blot membrane	Roche, Mannheim
Semi-Dry electrophoretic transfer cell	Peqlab, Erlangen
Vertica gel electrophresis chamber	Peqlab, Erlangen
Cell scraper	Sarstedt, Nürnbrecht

Table XV: Reagents and materials for protein biochemistry.

3.8.2. Protein isolation for Western Blot

To perform Western Blot analysis, proteins were extracted from retinae and cultured Müller cells. Retinae were again extracted from eyes as previously described and homogenized with a tissue shredder. Meanwhile cells were obtained by using a cell scrapper.

Proteins were isolated by adding 500 µl of TRIzol® to the samples followed by incubation for 5 minutes at RT. The tissues were then homogenized with a tissue shredder and 1/5 vol of chloroform added. After homogenization, the homogenate was mixed for 15 s, incubated for 2 – 3 minutes at RT and centrifuged at 12 000 g for 15 minutes at + 4 °C. The aqueous phase was discarded, 450 µl of isopropanol added to the supernatant followed by incubation at room temperature for 10 minutes. The samples were then centrifuged at 12 000 g for 10 minutes at + 4 °C and the resultant pellet washed three times with 1 ml wash buffer (0.3M guanidine hydrochloride in 95 % ethanol) by incubation at RT for 20 minutes for each wash followed by centrifugation at 7600 g for 2 minutes. As a last wash step, samples were dissolved in 1 ml of 95 % ethanol, incubated at room temperature for 20 minutes and then centrifuged at 7600 g for 5 minutes at 4 °C. The resultant pellet was air dried and then dissolved by overnight incubation at 50°C in 200 ml water containing 1 % SDS, protease (1;1000, P8340) and phosphatase (1:100, P5326) inhibitors (Sigma Aldrich). The next day, samples were centrifuged at 10 000 g for 10 minutes and the supernatant that contained isolated proteins was collected and store at -20°C until usage.

3.9. Determination of protein concentration through the BCA-Assay

To allow equal amounts of each sample to be loaded during immunoblotting, the amount of protein in each protein sample was measured using the BCA assay.

The BCA assay is based on the reduction of Cu^{2+} to Cu^{1+} by protein in an alkaline medium and the selective colorimetric detection of the cuprous cation (Cu^{1+}) by bicinchoninic acid (BCA). In the first step, proteins present in the sample reduce Cu^{2+} to Cu^{1+} resulting to the development of a light blue complex .The quantity of reduced copper resulting from this reaction is proportional to the amount of available protein in the sample. In the second step of the reaction, BCA reacts with the reduced Cu^{1+} cation that was formed in step one resulting to the formation of an intense purple-colour which exhibits a strong linear absorbance at 560 nm.

To measure protein concentrations in samples, a standard curve is produced using several concentrations of Bovine serum albumin (BSA). A BSA (2 mg/ml) master solution was diluted with the same buffer to the following standard concentrations: 2000, 1500, 1000, 800, 600, 400, 200 and 100 µg/ml. 10 µl of each protein sample, (undiluted and 1:2 diluted) and the standard BSA concentrations were titrated into a 96 well plate. To each titre, 200 µl BCA solution (reagent A: reagent B = 50:1), was added. After 30 minutes incubation at 37°C, the proteins were measured in an ELISA reader. The extinction at 560 nM was measured photometrically and protein concentration was calculated by extrapolating the amount of absorbance of each sample from the standard curve.

BCA Reagents	
Bovine serum albumin	
Reagent A	1 gm sodium bicinchoninate (BCA) 2 gm sodium carbonate 0.16 gm sodium tartrate 0.4 gm NaOH, and 0.95 gm sodium bicarbonate
Reagent B	0.4 gm cupric sulfate (5 x hydrated) in 100 ml distilled water.

Table XVI: Composition of BCA reagents.

3.9.1. SDS PAGE

The separation of proteins for Western Blot analysis was done by means of SDS-Polyacrylamide gel electrophoresis (SDS PAGE). The gel electrophoresis procedure as well as the setting of the polyacrylamide gel were carried out using the method described by Laemmli [110].

Buffer/solution	**Components**
SDS-solution 10 % (w/v)	10 g SDS dissolved in distilled 100 ml H_2O
SDS-PAGE-Running buffer, (10x)	250 mM Tris/HCl 400 mM Glycine 1 % (w/v) SDS in distilled H_2O
SDS-sample buffer, 4x	0.25 M Tris/HCl, pH 6.8 30 % Glycerine 8 % (w/v) SDS

	0.02 % (w/v) Bromphenolblue 10 % β-Mercaptoethanol
10 x Electrode buffer	250 mM Tris/HCl 400 mM Glycine 1 % (w/v) SDS dissolved in distilled H_2O
Tris/HCl, 1.0 M, pH 6.8	121.14 g Tris dissolved in distilled H_2O
Tris/HCl, 1.5 M, pH 8.8	181.71 g Tris dissolved in distilled H_2O

Table XVII: SDS PAGE buffer compositions.

Preparation of the gel

A 10 % separating gel was prepared and used for the separation of retinal proteins. Briefly, two glass plates were cleaned with alcohol and fitted into a gel caster. The various components of the running gel were then mixed and quickly pipetted into the space between the two glass plates. Isopropanol was quickly poured over the gel and then it was allowed to polymerize. After polymerization of the running gel, the components of loading gel were mixed and placed over the running gel and a comb placed into it to about 1 cm close to the running gel to create sample wells. The loading gel was let to polymerise after which the comb was removed.

Polymerised gels were placed into the electrophoresis chamber and the buffer tanks were filled with 1x electrode buffer. The samples, containing equal amounts of proteins (15 – 40 µg according to attempt) were loaded into the slots. A molecular weight marker was pipetted into a separate slot. The separation of proteins by gel electrophoresis was done at 20 mA (per gel) for 60-90 minutes.

Components of the SDS gel

Component	Loading gel (1 ml volume)	Running gel 10 % (5 ml volume)
Distilled H_2O.	0.68 ml	1.9 ml
Rotiphorese® Gel 30	0.17 ml	1.7 ml
Tris/HCl, 1 M, pH 6.8	0.13 ml	-
Tris/HCl, 1.5 M, pH 8.8	-	1.3 ml
10 % SDS	0.01 ml	0.05 µl
10 % APS	0.01 ml	0.05 µl
TEMED	0.001 ml	0.002 µl

Table XVIII: Components of SDS gel.

Buffer/solution	Components
10 % (w/v) SDS	-10 g SDS -Add 100 ml dH_2O
Tris/HCl, 1.0 M, pH 6.8 (for stacking gels)	-121.14 g Tris -Dissolve in 1l dH_2O, adjust pH.
Tris/HCl, 1.5 M, pH 8.8 (for resolving gels)	-181.71 g Tris -Dissolve in 1l dH_2O, adjust pH,
SDS loading dye, 4x	-0.25 M Tris/HCl, pH 6.8 -30 % Glycerol -8 % (w/v) SDS -0.02 % (w/v) Bromphenol blue -0.3 M DTT
SDS-PAGE Electrode buffer	-250 mM Tris/HCl -1.92 M Glycin -1 % (w/v) SDS -dissolve in 1l dH_2O

Table XIX: Composition of SDS PAGE gel and buffer components.

Components 10x Transfer buffer	
Tris	5.8 g
Glycine	2.9 g
Methanol	200 ml
SDS	3.7 ml 10 % (w/v) dissolved in 1 l dH_2O

Table XX: Transfer buffer components.

3.9.1.1. Semi-dry blotting

For the transfer (Blotting) of proteins onto a PVDF membrane, the membrane was first cut according to the size of the gel (9X7 cm). The membrane was then pre-treated for some seconds with methanol, washed subsequently for two minutes in distilled H_2O and then equilibrated for 5 minutes in transfer buffer. Additionally, 5 pieces of filter paper immersed in transfer buffer were used. To transfer proteins from gel to the PVDF membrane, a semi-dry blot was setup as outlined below and ran at 25 V for 90 minutes.

Semi-dry Blot layout

cathode (-)
3 buffer soaked filter papers
Separating gel with proteins
PVDF-Membrane
2 buffer soaked filter papers
Anode (+)

Table XXI: Outline Semi dry blot layout.

3.9.2. Western Blot analysis.

For Western Blot analyses, 20 µg - 40 µg of protein from retinae were subjected to a 8 % SDS-PAGE and transferred onto a PVDF membrane (Roche) by Semi-dry blotting. After blocking with 5 % low-fat milk in PBS-T, membranes were incubated overnight with primary antibodies (diluted 1:1000 in 5 % BSA in PBS-T). These antibodies reacted with the corresponding antigen to form an antibody antigen complex. Membranes were washed 3x with TBS-T for 10 minutes per wash. After washing, membranes were hybridized with HRP-conjugated secondary antibodies (diluted 1:5000 in PBS-T with 5 % BSA) specific for the primary antibody. The membranes were then washed 3x with TBS-T for 10 minutes per wash and incubated with Luminol Reagent and HRP peroxide aces Solution (1:1 mixed) (Millipore corporation, Billerica, USA) in foil paper for 5 minutes at room temperature. The formed antibody-antigen-complex could be detected in presence of luminol due to the oxidation of luminol to give a chemiluminescence signal in a reaction catalysed by HRP. Membranes were visualized on a BAS 3000 Imager work station (Fujifilm). Western Blot signals were evaluated by densitometry with the Aida Image Analyser v.4.06 software (Raytest).

The following antibodies were used for Western Blotting.

Primary Antibody	**Clone**	**Supplier**
pAkt	monoclonal	Cell signaling
Akt	monoclonal	Cell signaling
Secondary Antibody	**Clone**	**Supplier**
Goat anti rabbit	polyclonal	Cell signaling

Table XXII: Antibodies for western blotting.

3.9.3. Protein quantification by ELISA

To determine CORT levels in mice, an ELISA was performed on obtained blood samples. As an alternative method to quantify apoptosis after light damage, free histones were also measured using a free histones ELISA assay.

3.9.3.1. CORT measurement.

To measure CORT levels, mice were weighed and introduced into a $C0_2$ exicator. Immovable CO_2 anaesthetised mice were decapitated and trunk blood collected into an eppendorf tube. The collected blood was centrifuged at 5000 rpm for four minutes. Ten µl of the supernatant was collected into a 150 µl tube containing 4 µl of PBS for CORT measurement. The rest of the supernatant was collected into a 200 µl tube for ACTH measurement. Samples were stored at -20^0C until the ELISA was performed and CORT concentrations determined by measuring the absorption at 405 nm.

3.9.3.2. The free histones ELISA.

To perform this ELISA, obtained retinae were weighed and dissolved in a corresponding volume of lysis buffer. The ELISA was performed as follows:

Equal volumes of the lysate were made up to 20 µl in provided wells and 80 µl of immunoreagent added. The wells were then covered using a cover foil and incubated on a gentle shaker for 2 hours. Thereafter, the solutions were removed by gentle tapping and each well rinsed 3 times with 250 µl of incubation buffer. 100 µl of ABTS solution was then pipetted into each well and the wells incubated on a plate shaker until the colour development was sufficient for photometric analysis. At this point 100 µl of ABTS stop solution was pipetted into each well and absorbance measured at 405 nm against ABTS solution plus 100 µl ABTS stop solution as blank. The enrichment factor of each sample was calculated by subtracting the background (blank) and dividing the value by the enrichment factor of the negative control.

3.10. Immunohistochemistry

Using immunohistochemistry, specific proteins can be localised and quantified in cells by use of indirect immunofluorescence which is quantified using a primary antibody which binds to the sought antigen on the protein while a secondary antibody binds itself to an epitope of the primary antibody. A streptavidin molecule coupled to the fluorochrom Alexa 488 then gets coupled to the secondary antibody through biotinylation.

3.10.1.1. Reagents and materials

Reagent/material	**company**
Cover glass	Menzel-Gläser, Braunschweig
Fluorescent Mounting Medium	Dako, Hamburg
Cuvettes	Schott, Mainz
Vectashield Mounting Medium with 10 % DAPI	Linaris, Wertheim

Table XXIII: Reagents and materials for immunohistochemistry.

3.10.2. Embedding and Cryosectioning

To prepare sections for immunohistochemistry, mice were killed, eyes extracted using forceps and fixed in 4 % PFA for at least four hours. Thereafter, eyes underwent three successive washes using 0.1 M phosphate buffer for 15 minutes per wash. Eyes were then successively treated for 4–24 hours each in 10 %, 20 % and 30 % sucrose in 0.1 M $NaPO_4$ buffer. The eyes were then embedded in Tissue-Tek, snap-freezed in liquid nitrogen and stored at –20 ° C until sectioning. Embedded eyes were sectioned by cutting sagittal cryosections of 12 µm thickness in using a Microtom HM 500 OM

cryostat. For storing, the sections were placed on SuperFrost®Plus object-plates, wrapped in aluminium foil and stored at -20 °C until immunostaining was performed.

The following antibodies were used for immunohistochemistry.

Primary Antibody	**Clone**	**Supplier**
Rabbit anti pAkt	monoclonal	Cell signalling
GFAP	polyclonal	Signet laboratories USA
Secondary Antibody	**Clone**	**Supplier**
Biotinylated goat anti rabbit	polyclonal	Vector laboratories USA

Table XXIV: Antibodies for immunohistochemistry.

3.10.3. Protocol immunohistochemistry

Cryosections were treated with 0.1 M $NaPO_4$ buffer containing 0.05 % Tween-20 for 5 minutes, blocked with 0.5 % BSA diluted in 0.1 M $NaPO_4$ buffer for 45 minutes and then incubated with a rabbit-derived antibody diluted 1:50 in 0.1 M $NaPO_4$ buffer containing 0.5 % BSA in a moist chamber at + 4 °C overnight. Control slides were incubated with 0.1 M $NaPO_4$ containing 0.5 % BSA alone. Slides were then washed three times for 5 minutes in 0.1 M $NaPO_4$ and incubated with a green fluorescing goat-derived anti-rabbit secondary antibody diluted 1:1000 in 0.1 M $NaPO_4$ containing 0.5 % BSA in dark for 1 hour at RT. Thereafter, slides were washed 3 times for 5 minutes in 0.1 M $NaPO_4$ buffer and mounted by coverslips with a few drops of 1:10 DAPI (4'-6-diamidine-2-phenyl indole) mounting medium. The slides were stored in the dark at +4 °C until viewed under a fluorescent microscope.

3.10.4. Fluorescence microscopy

DAPI stained nuclei and GFP-labelled GFAP or pAkt were analysed by an Axio Imager Z1 fluorescence microscope. Images were documented in a Carl Zeiss Axio Vision format (.zvi) at 20 and 40 X magnifications. The data were converted into TIF-format.

3.11. *In vitro* studies

3.11.1. Reagents and materials for cell culture

Reagent/Medium	Supplier
DMEM 4500	PAA, Pasching, Austria
DMEM + Glutamax II	PAA, Pasching, Austria
Ethanol, absolute	Roth, Karlsruhe
Fetal Bovine Serum	Life Technologies, Karlsruhe
Collagenase A	Sigma, Taufkirchen
Gentamycin (5 mg/ml)	Life Technologies, Karlsruhe
Penicillin-Streptomycin	Life Technologies, Karlsruhe
Phosphate Buffered Saline (PBS)	Life Technologies, Karlsruhe

Table XXV: Reagents, materials and equipment for cell culture.

3.11.2. General cell culture procedures

The cultivation and treatment of cells was carried out under sterile conditions. The materials used were autoclaved and the solutions and buffers sterilised. The use of sterile solutions and media as well as the change of the medium and the treatment of the cells was carried out under a sterile work bench. The cultivation of cells was carried out in special compartments of constant temperature and constant carbon dioxide concentration. Cells were viewed under a microscope to assess the degree of confluency and to confirm the absence of bacteria and fungi every second day.

When cells became confluent, spent medium was removed and the cell monolayer was washed twice with PBS without Ca^{2+}/Mg^{2+}. Three ml of trypsin was then pipetted

into the culture flask and rotated to cover monolayer with trypsin so that they started floating. Cells were then transferred into a falcon tube containing culture medium. The cells were pelleted by centrifugation at 1000 rpm for 5 minutes and then re-suspended in 5 ml of culture medium. An aliquot of the suspension was transferred into a new culture flask containing 12 ml culture medium. For long-term storage, cells were suspended in appropriate culture medium containing 10 % DMSO and stored in a cryovial in liquid nitrogen.

Cell quantification was performed using a casy machine (Innovatis, Reutlingen, Germany). Firstly, the cell counter was cleaned using casyton solution. Ten ml of casyton and 50 µl of the cell suspension were brought into a tube that was then placed in the CASY machine to perform the cell count.

3.11.3. Isolation and culture of Müller cells

Composition of culture medium and digest solution

Culture medium
500 ml DMEM + GlutaMax™-II
50 ml 100 % FCS
5 ml L-Glutamin (200 mM)
5 ml Penicillin/ Streptomycin
Digesting solution
DMEM + GlutaMax™-II
0.1 % Trypsin/EDTA
70 µg/ml collagenase

Table XXVI: Composition of culture medium and digest solution for Müller cell isolation and culture.

3.11.3.1. Procedure Müller cell isolation

The isolation and enrichment of Müller cells was done as described by Hicks and Courtois [111]. Wistar rats were killed between the postnatal days 8 and 12 (p 8-12) and the eyes enucleated. The prepared eyes were left overnight in the dark at 4^{o}C in Müller cell medium. The next day, the cornea was pierced and the eyes incubated in digest solution for 60 minutes at 37°C. The cornea, ciliary body and lens were removed. The retina was separated carefully from the pigment epithelium, homogenised by continuous in and out suction using a pipette, distributed on the bottom of a cell culture plate and then filled with 2.5 ml serum containing Müller cell medium. After multi-day incubation, retinal aggregates and deposits were rinsed through pipetting with medium. After performing multiple repeats of this process under microscopic inspection, a clean population of Müller cells remained in the culture dish. These remaining cells were trypsinized and cultivated in cell culture bottles with serum containing Müller cell medium.

3.11.4. Viability of 661 W cells after CORT treatment

In order to investigate the neuroprotective effects of GCs on photoreceptor cells *in vitro*, the immortalised mouse photoreceptor cell line (661W) [112] was used. Cells were cultured in Dulbeco/Vogt modified Eagle's minimal essential medium (DMEM) containing 10 % FCS until confluence. One hundred µl of the cell suspension was used to perform a cell count. A volume corresponding to 25 000 cells was then pipetted into each well of a 96 well plate and allowed for at least four hours to let attach. After this, the cells were observed under the microscope to check for adhesion. Two hours before the start of the experiment, cells were briefly treated with 0.5 nM staurosporine for 15 minutes to induce differentiation [113].

The wells were shared into 4 groups and treated as follows:

1) Normal growth medium containing two percent DMSO as negative control,

2) Normal growth medium with 20 nM CORT dissolved in DMSO,

3) Normal growth with 50 nM CORT dissolved in DMSO,

4) Untreated cells.

Ten hours later, the spent medium was removed and the cells of the three DMSO treated groups received cell culture medium without FCS to induce apoptosis. Untreated cells were cultured again in cell culture medium containing 10 % FCS.

3.11.4.1. The WST Viability Assay.

The assay works on the principle that tetrazolium salts are reduced to formazan by NADH which is found in the enzyme mitochondrial dehydrogenase. Given that the number of viable cells correlates with the activity of mitochondrial dehydrogenases in the sample. The enzyme activity determines the amount of formazan dye formed which directly correlates to the number of metabolically active cells in the culture. The amount of formazan dye produced by metabolically active cells in the culture is then quantified by a scanning multi well spectrophotometer where the absorbance of the dye solution is measured at 405 nm.

The assay was performed according to the following procedure:

After cells had been serum starved, the medium was removed and replaced with 70 µl medium that had been diluted with WST-1 (Roche) in a 1:10 ratio. Cells were then incubated at 37^{o}C for 30 minutes. Cell viability was measured by measuring absorption at 405 nM using an ELISA reader (Tecan GmbH, Grödig, Austria). The

plate was returned to the incubator for a further one hour period after which cell viability was measured again.

3.11.5. CORT treatment of Müller and 661 W cells

The effect of CORT on the expression of GFAP and the phosphorylation of Akt was investigated after treatment of these cells with CORT for 10 hours. Protein and RNA was extracted from CORT treated Müller and 661 W cells and then used for Western Blot analysis and real time RT-PCR as already described.

3.12. Statistics

All Statistics were carried out using the student's t test with two unpaired independent variables which is part of the Microsoft excel 2010.

4 RESULTS

4.1. Ten hours CSC alters physiological parameters of stress in Balb/c mice

CSC housing was originally established as a chronic stress paradigm spanning a 19 day period [64]. However, an important facet of this project was aimed at analysing the effect of a short-term psychosocial stress on retinal damage. Therefore, the efficacy of CSC as a short-term psychosocial stressor was investigated. As aforementioned, during 10 hours CSC Balb/c mice already portrayed behavioural sings of psychosocial stress. Nevertheless, observation of behavior solely does not suffice to justify psychosocial stress, therefore in order to ascertain that 10 hours CSC induces short-term psychosocial stress in Balb/c mice, it was necessary to evaluate other physiological indicators of stress. These indicators which included change in body weight, plasma CORT concentration and change in adrenal weight were analysed and compared to those measured of C57BL/6 mice.

4.1.1. Ten hours CSC causes body weight loss in Balb/c Mice

Most often stress causes body weight loss. Moreover, it has been published that psychosocial stress in mice leads to significant body weight loss [114], a phenomenon that was also validated in the CSC housing paradigm. For this reason, change in body weight due to 10 hours CSC in Balb/c mice was measured. To this end, mice were weighed before and after 10 hours CSC to obtain mean body weight per group. The mean body weight at the beginning CSC was deducted from the mean body weight immediately after CSC housing to obtain the mean body weight change per group.

The results showed that after 10 hours CSC housing, CSC housed mice had a 0.9 g mean body weight loss whereas SHC mice increased their body weight by about 0.5 g, a difference that was statistically significant ($P < 0.05$), (Figure 8A).

4.1.2. Ten hours CSC causes a rise in CORT levels in Balb/c mice

An optimum way to assess the stress level of an organism is by measuring parameters that denote the activity state of the HPA axis notably plasma CORT levels [115] as they are an indisputable stress indicator. Hence, to confirm psychosocial stress in Balb/c mice following 10 hours CSC housing, plasma CORT levels were measured in CSC housed Balb/c mice and compared to those of SHC. For this purpose, CSC housed and SHC were immediately decapitated after 10 hours CSC, trunk blood collected and CORT levels measured by ELISA.

The data showed that SHC mice had mean CORT values of 32 ng/ml while the CSC housed mice had a more than 10-fold increase in CORT levels as compared to SHC, a difference that was statistically significantly ($P \leq 0.001$), (Figure 8B).

4.1.3. Ten hours CSC causes mild increase of adrenal weight in Balb/c mice

Adrenal hyperplasia is a well-established indicator of prolonged stress [116]. Despite its relatively short duration, the effect of 10 hours CSC on adrenal weight was investigated to see if any signs of stress could already be observed. To this end, after 10 hours CSC, mice were sacrificed and the adrenals carefully excised, pruned of fat and their weights determined. The weights of both adrenals were equated to the body weight to give a relative adrenal weight (mg organ weight/g body weight) and the mean relative adrenal weight per group calculated. Data from two independent experiments showed a consistent trend of higher relative adrenal weight in CSC housed (0.16 ± 0.03 g) compared to SHC mice (0.13 ± 0.01 g), (Figure 8C).

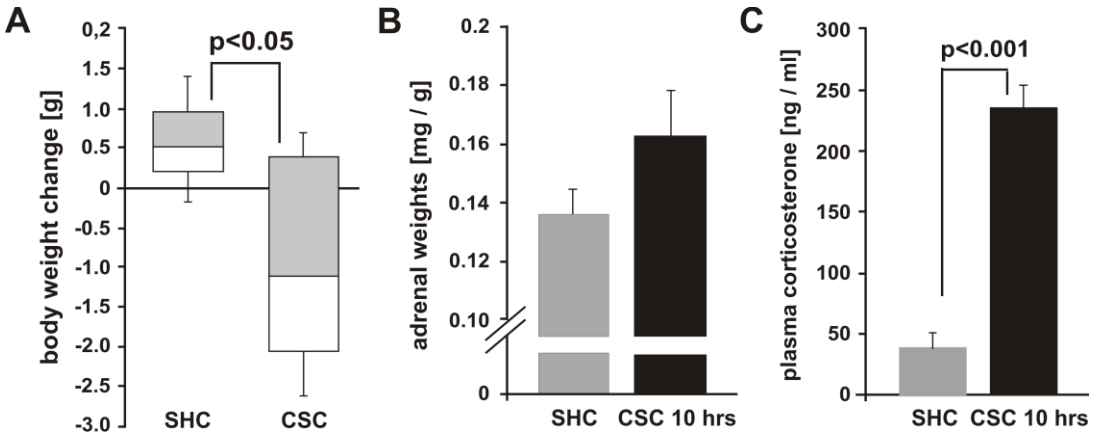

Figure 8: 10 hours CSC induced psychosocial stress in Balb/c Mice. Balb/C mice were exposed to the CSC for 10 hours to analyse whether an acute (10 hours) psychosocial stress could be induced in this mouse strain. As indicators for psychosocial stress, mean body weight gain (A), adrenal weights (B) and plasma CORT levels (C) were analysed immediately after stress exposure. In 10 hours CSC housed mice, body weight gain (A) was markedly decreased when compared to single housed controls (SHC) while adrenal weight (B) increased when compared to single housed controls (SHC). A huge increase in plasma CORT was measured in acute psychosocially stressed mice compared to SHC (C). The data shown are combined from two independent experiments, $n \geq 8$, mean ± SEM.

4.2. Nineteen days CSC influences physiological parameters of stress in Balb/c mice

Although acute and chronic stress more often than not affect the same systems, the way the body responds to them can differ distinctly [117]. As such, albeit the data so far revealed that changes in physiologic indicators of stress after 10 hours CSC observed in Balb/c mice corresponded to those observed in C57BL/6 mice, it couldn't be assumed that the same will hold true after 19 days of CSC. For this reason, it was compelling to verify if chronic stress indicators in Balb/c mice after 19 days CSC housing conformed to those established in C57BL/6 mice. For this reason, Balb/c mice were submitted to 19 days CSC housing in exactly the same way as established in C57BL/6 mice and physiologic indicators of stress before, during and after 19 days CSC housing measured. Parameters assessed included: body weight

evolution during the 19 days of CSC housing, adrenal hyperplasia and CORT levels at the end of 19 days CSC in CSC housed compared to SHC mice.

4.2.1. Nineteen days CSC affects body weight gain in Balb/c mice

It has been established in C57BL/6 mice that body weight evolution varies between SHC and CSC housed mice during 19 days CSC. SHC mice were shown to gain weight steadily whereas CSC housed mice showed an irregular pattern of weight gain. To see if Balb/c mice would show a similar pattern, body weight evolution in these mice during 19 days CSC was analysed. To achieve this goal, mice were submitted to 19 days CSC housing. At the onset of CSC (day 0), and on days 1, 7, 15 and the end of day 19, body weight was measured. The change in body weight on each day was calculated by subtracting the weight on day one from the weight on that day.

At the beginning of the CSC housing procedure (day 0), both the SHC and CSC housed groups had an average body weight of 21.0 g and were assigned a net body weight gain of 0 g. The next day (day 1) the SHC group had a mean body weight gain of 0.5 g whereas CSC housed mice had a 0.1 g mean body weight loss, a difference that was statistically significant ($P \leq 0.02$). On day 7, both SHC and CSC housed mice were found to have gained weight, with SHC having a mean body weight increase of 1.1 g as opposed to 0.6 g in CSC housed mice. Despite the body weight gain by CSC housed mice, the difference in mean body weight gain still remained statistically significant ($P \leq 0.01$). On day 15, SHC were found to have gained an average 2.2 g, as opposed to a 1.1 g gain in CSC housed mice, a difference that was again statistically significant ($P \leq 0.01$). After 19 days CSC, it was found that SHC mice had gained a mean body weight of 3.2 g as compared to a mean gain of 1.4 g in CSC housed mice. Throughout the 19 days, SHC had a rather continuous increase in weight, gaining an average of 0.16 g/day to end up with a mean weight of 24.2 g, meanwhile CSC

housed mice show an average weight gain of 0.7 g to end up with a mean weight of 22.4 g. Despite starting on equal mean body weight, there was a statistically significant difference in body weight between both groups at the end of 19 days CSC housing ($P \leq 0.05$), (Figure 9A).

4.2.2. CORT levels re-normalize following 19 days CSC in Balb/c mice

Having demonstrated that after 10 hours CSC housing, CSC housed Balb/c mice experience a tremendous increase in CORT levels, it was necessary to know what the CORT levels are following prolonged stress. In C57BL/6 mice it has been established that CORT levels after 19 days CSC are not different from those of SHC mice. To investigate if the same holds true for Balb/c mice, the difference in CORT levels between subordinated and SHC Balb/c mice after 19 days CSC was investigated. For this reason after performing 19 days CSC as earlier described chronically subordinated mice and SHC mice were decapitated, trunk blood collected and plasma CORT levels measured by ELISA.

The data shows that there was no difference in CORT levels between both groups at the end of 19 days CSC as SHC mice had mean CORT levels of 27.29 ± 3.8 ng/ml while CSC housed mice had mean CORT levels of 28.05 ± 6.1 ng/ml, (Figure 9B).

4.2.3. Nineteen days CSC causes adrenal hyperplasia in Balb/c mice

Chronic stress is known to induce adrenal hyperplasia in rodents [116] and confirmed to occur in C57BL/6 mice after 19 days CSC housing. Therefore, this indicator of hyperactivity of the HPA axis was investigated after 19 days CSC housing in Balb/c mice to see if it concurs to what is described in other chronic stress paradigms. For this purpose, after 19 days CSC, the weight of the left and right adrenal gland for both

CSC housed and SHC mice were measured and calculated to give a relative adrenal weight (mg organ weight/g body weight) as previously described.

The data showed that CSC mice had a mean left relative adrenal weight of 0.95 ± 0.04 g compared to SHC which had 0.80 ± 0.24 g, a difference that was statistically significant. For the right adrenal, CSC mice again had a higher mean relative adrenal weight of 0.87 ± 0.05 g compared to SHC which had 0.73 ± 0.05 g, a difference that was also statistically significant ($P \leq 0.05$). When both adrenals were considered, CSC housed mice had a higher mean relative adrenal weight of 1.82 ± 0.09 g, compared to SHC mice which had 1.53 ± 0.04 g, a difference that was also statistically significant ($P \leq 0.05$), (Figure 9C).

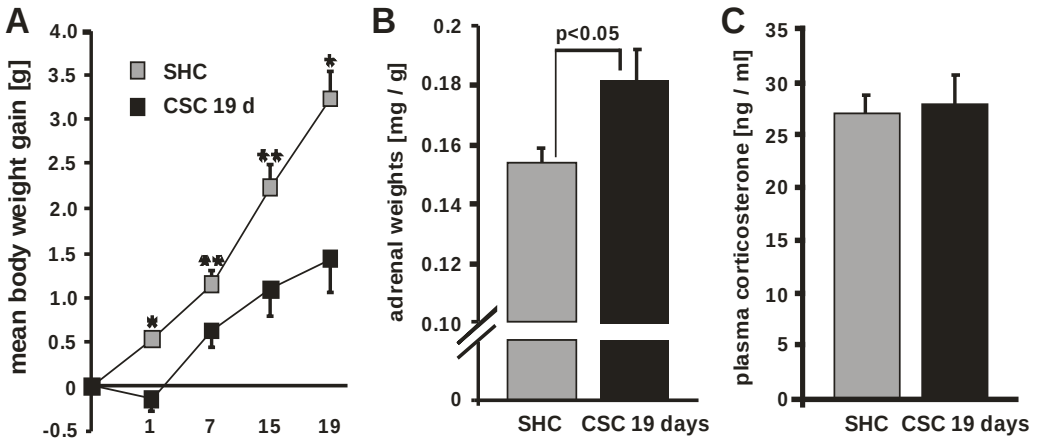

Figure 9:19 days CSC induced psychosocial stress in Balb/c Mice. Balb/c mice were exposed to CSC housing for 19 days to analyse whether a chronic psychosocial stress could be induced in this mouse strain. As indicators for psychosocial stress, mean body weight gain (A), adrenal weights (B) and plasma CORT levels (C) were analysed after chronic stress exposure. In CSC housed mice, body weight gain was markedly lower when compared to single housed controls (SHC) while adrenal weight significantly increased when compared to the SHC group. Plasma CORT levels were not different in both groups. The data shown are combined from two independent experiments, $n \geq 8$, mean ± SEM.

4.3. Balb/c mice were genetically susceptible to light damage

As the data so far altogether showed that both 10 hours and 19 days CSC are capable of inducing short-term and chronic psychosocial stress, respectively, in Balb/c mice, the next important data point necessary to validate the animal model was to ensure Balb/c mice at hand were genetically susceptible to light damage.

Using different mice species, it has been demonstrated that susceptibility to light damage depends on the genetic background [118], more precisely on the variant of the *Rpe65* gene which the mice carry [119]. The *Rpe65* gene codes for the retinal pigment epithelium protein *Rpe65*. Codon 450 of this gene exists in two variants being; *Rpe65Met450* and *Rpe65LEU450*. Mice carrying the *Rpe65Met* variant of *Rpe65* are resistant to light induced retinal degeneration while those carrying the Leucine variant are more susceptible [103]. To ascertain that the Balb/c mice carried the *Rpe65LEU450* variant, breeding pairs were genotyped. The *Rpe65Met* variant has no restriction site for the restriction enzyme MWO 1, meanwhile the *Rpe65LEU450* variant contains the restriction site of MWO 1 and yields two fragments of 437 and 236 base pairs upon digestion with this restriction enzyme.

To determine the variant in breeding pairs, mouse tail biopsies were obtained from all breeding pairs and DNA extracted from them. The extracted DNA was amplified and the amplification product digested using the restriction enzyme MWO 1 and then run on an agarose gel.

Image analysis of the agarose gel revealed that, MWO 1 digestion of the amplification product effectively yielded two fragments of 437 and 236 base pairs for all breeding pairs as shown in Figure 10.

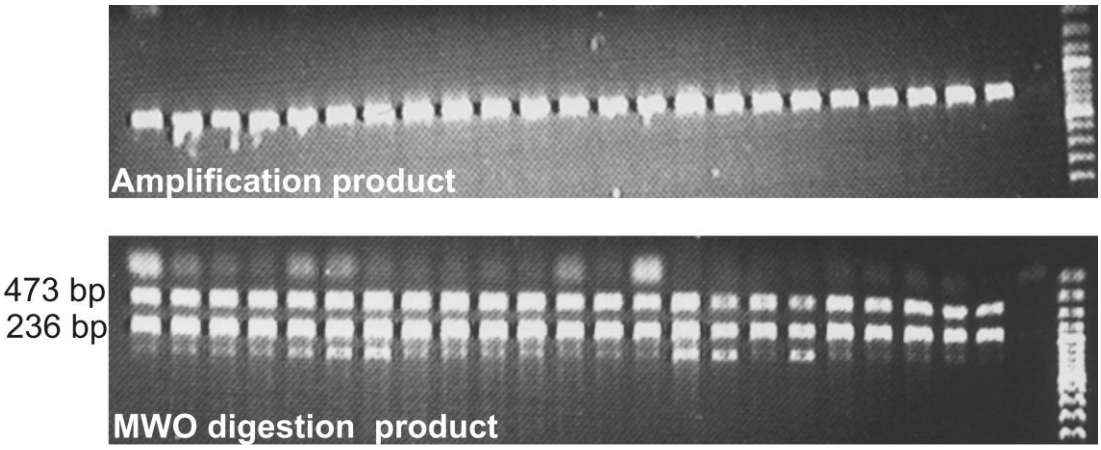

Figure 10: Breeding pairs carried the *Rpe65* LEU 450 variant of the *Rpe* 65 gene. DNA from mouse tail biopsies was amplified and the amplification product digested using the restriction enzyme MWO and run on an agarose gel. An image of the agarose gel showed that digestion yielded two products of 473 and 236 bp for all samples.

4.4. Effects of short-term psychosocial stress on induced retina neurodegeneration

4.4.1. Prior short-term psychosocial stress decreased apoptosis in the retina

Elevated systemic GC levels via fasting mediated stress have previously been shown to protect photoreceptors from light damage [86]. Given that short-term psychosocial stress due to 10 hours of CSC housing resulted to a significant increase in CORT levels in Balb/c mice, the effect of short-term psychosocial stress on light induced damage of photoreceptors was investigated.

To this end, immediately after 10 hours CSC housing, SHC and CSC housed mice were illuminated at 5000 lux for 1 hour. Twenty four hours after light damage, mice were sacrificed and the eyes prepared. Enucleated eyes were then embedded in paraffin and sagittal sections prepared. Using the obtained sagittal sections, apoptotic cells in the retina were labelled for TUNEL analysis.

As expected after a light damage, TUNEL revealed apoptotic cells predominantly in the ONL. The number of apoptotic cells in this layer was counted and expressed per 1000 μm^2. The data showed that SHC had a mean of 50.12 ± 5.11 cells / 1000 μm^2 ONL, meanwhile CSC housed mice showed about a 27 % decrease in apoptotic cells (36.5 ± 5.2 cells / 1000 μm^2), a difference that was statistically significant ($P \leq 0.05$), (Figure 11).

To analyse best experimental conditions, this experiment was done with a lower duration of illumination (30 min). After 24 hours, eyes were enucleated, sections prepared, TUNEL labelling performed and the number of apoptotic cells were quantified. Again, CSC housed mice showed a 25 % decrease of apoptotic cells (35.7 ± 1.74 cells / 1000 μm^2) compared to SHC (47.8 ± 4.6 cells / 1000 μm^2), a difference that was also statistically significant ($P \leq 0.05$), (Figure 11C).

4.4.2. Short-term psychosocial stress decreases free histone release following light damage

The release of free histones when DNA fragmentation occurs is a hallmark for apoptosis [120] and so the quantity of free histones released from fragmentized DNA is an index of the amount of cells undergoing apoptosis. Since TUNEL data showed a significantly less number of apoptotic cells after a light damage when mice were treated by short-term psychosocial stress, the release of free histones following light damage after 10 hours CSC was investigated.

To this end, 24 hours after light damage that was preceded by 10 hours CSC, mice were killed and a free histones ELISA performed. The absorbance at 405 nm was read by use of a spectrophotometer and used to calculate the free histones enrichment factor for each sample.

In CSC housed mice a 45 % less intense signal was detected when compared to SHC mice, a difference that was statistically significant ($P \leq 0.05$), (Figure 11D).

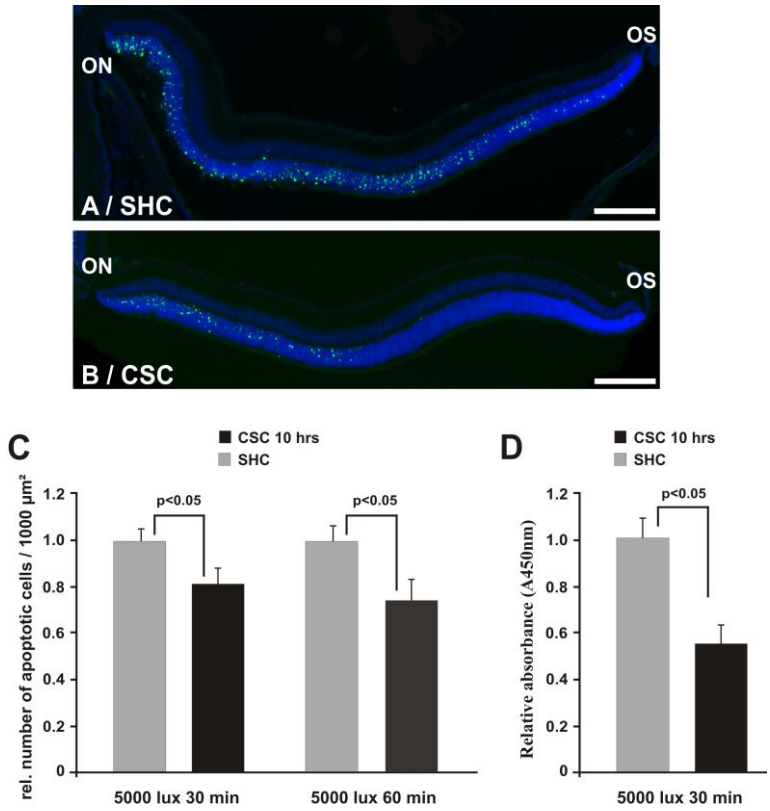

Figure 11: Short-term psychosocial stress protected photoreceptors from light induced damage. A, B. Representative TUNEL staining (green) of sagittal sections through retinae 24 hours after illumination with 5000 lux for 60 minutes. Before light exposure, acute psychosocial stress was induced by 10 hours CSC housing (B) whereas control mice were kept under single house conditions (A). The number of TUNEL-positive cells on sagittal sections was quantified and plotted as the relative number of apoptotic cells per 1000 µm^2 ONL (C). In acute psychosocially stressed mice, the number of TUNEL positive cells is markedly decreased in the ONL when compared to SHC. The quantity of released free histones was quantified by ELISA (D). The data shown are combined from two independent experiments for each treatment, $n \geq 8$, mean ± SEM. Scale bars: A, B, 100 µm.

4.5. Effects of chronic psychosocial stress on induced retinal degeneration

Given that an increase in CORT after short-term psychosocial stress correlated with a protective effect on photoreceptors, it was necessary to verify what happens following prolonged stress. After 19 days CSC, CORT levels in mice show a circadian rhythm, at the end of the active dark phase both stressed and SHC mice have the same CORT levels (Figure 9). On the other hand, 19 days CSC housed mice are known to experience hypocortisolism at the end of the active light phase compared to their SHC counterparts [64].

4.5.1. Chronic psychosocial stress (19 days) does not protect photoreceptors.

Since 19 days CSC housed Balb/c mice were found to have comparable systemic CORT levels like their SHC counterparts during the dark phase, it was pertinent to investigate what occurs when light damage is administered at this time point. To fulfil this, at the end of the dark phase following 19 days CSC, both SHC and CSC housed mice were illuminated at 5000 lux for 30 minutes, sacrificed 24 hours later and a TUNEL assay performed.

Just like in the case of 10 hours CSC, TUNEL labelling revealed numerous apoptotic cells in the ONL. The numbers of apoptotic cells were counted and expressed per 1000 μm^2 ONL. The data showed no difference between both groups as SHC had a mean of 21.90 ± 5.7 cells /1000 μm^2 while CSC housed mice had a mean of 22.79 ± 6.5 cells /1000 μm^2, (Figure 12).

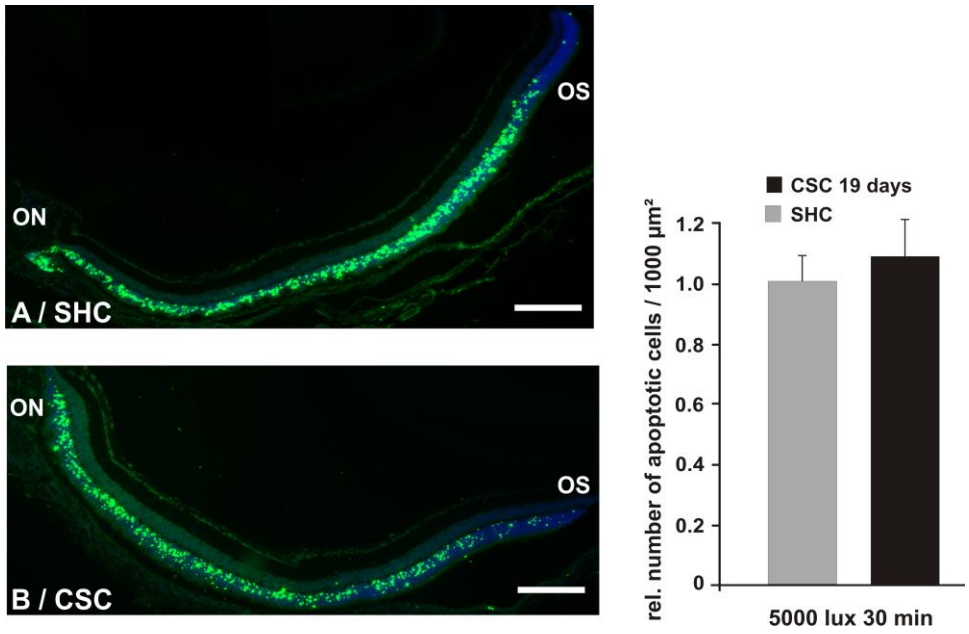

Figure 12: 19 days CSC housing does not protect photoreceptors from light induced damage. A, B Representative TUNEL staining (green) of sagittal sections from retinae 24 hours after illumination with 5000 lux for 30 min. Before light exposure, chronic psychosocial stress was induced by 19 days CSC housing (B) whereas control mice were kept under single house conditions (SHC, A). The number of TUNEL-positive cells on sagittal sections was quantified and plotted as the relative number of apoptotic cells per 1000 µm^2 (ONL). The data shown are combined from two independent experiments, n ≥ 8, mean ± SEM. Scale bars: A, B, 100 µm.

4.5.2. Chronic psychosocial stress (19 days) exposes the retina to increased damage

When light damage was performed in the morning after chronic stress, there was no significant difference in retinal apoptosis between SHC and CSC housed mice (Figure 9). This data correlated to equal CORT values in both groups. However, it has been shown that, 19 days CSC housed mice can not increase their CORT levels during the day and so they suffer from hypocortisolism at the end of the light phase. As such, the effect of this chronic stress induced hypocotisolism on retinal apoptosis was investigated to see if less CORT levels at the end of the light phase will in turn have deleterious effects for the retina. To get this done, after 19 days of CSC housing, both

SHC and CSC housed mice were illuminated at 5000 lux for 30 minutes during the light phase, sacrificed 24 hours later and a TUNEL assay performed. CSC housed mice showed a 51 % increase of apoptotic cells (10.2 ± 1.28 cells /1000 µm²) compared to SHC (6.4 ± 2.14 cells /1000 µm²), a difference that was statistically significant ($P \leq 0.05$), (Figure 13).

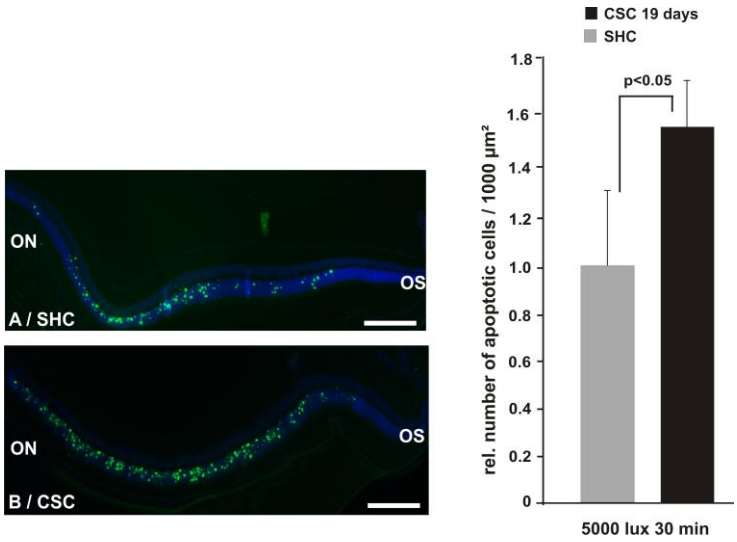

Figure 13: 19 days CSC enhances damage of photoreceptors after illumination: A, B. Representative TUNEL staining (green) of sagittal sections from retinae 24 hours after illumination with 5000 lux for 30 min. Light exposure was performed at the beginning of the dark phase. Before light exposure, chronic psychosocial stress was induced by 19 days CSC housing (B) whereas control mice were kept under single house conditions (SHC, A). The number of TUNEL-positive cells on sagittal sections was quantified and plotted as the relative number of apoptotic cells per 1000 µm^2 ONL. The data shown are combined from two independent experiments, $n \geq 4$, mean ± SEM. Scale bars: A, B, 100 µm.

4.6. Exogenous CORT protects photoreceptors from light damage

So far, the data consistently showed a correlation between CORT levels and protection of photoreceptors against light damage. Therefore, to further investigate the role of CORT in the protective effect of short-term psychosocial stress, exogenous CORT was administered prior to light damage and apoptosis quantified 24 hours later

to evaluate if exogenous CORT could confer the same protective effect as short-term psychosocial stress on photoreceptors following light damage.

4.6.1. CORT injection increases systemic CORT levels

To investigate the role of CORT on photoreceptor cell protection against light damage, it was fundamental to determine to which extent CORT levels rise in blood following an exogenous CORT injection into the peritoneal cave. For this purpose, mice were divided into two groups and one group injected with 52 µg/g of CORT, while the other received a vehicle injection as described. Fifteen minutes after injection, mice were decapitated, trunk blood collected and CORT levels measured by ELISA.

Values obtained from ELISA measurements showed that CORT-injected animals had mean CORT levels of 309 ng/ml which were significantly higher as compared to vehicle-injected animals (mean of 44 ng/ml) which in turn had higher levels than measured basal CORT levels (32 ng/ml) of Balb/c mice, (Figure 14D).

4.6.2. CORT injection before illumination protects photoreceptors from light damage

As an exogenous injection of CORT effectively resulted to a high increase in systemic CORT levels in mice, the effect of exogenous CORT on photoreceptors following light damage was investigated. For this purpose, mice were divided into 3 groups of equal body weight and the groups randomly assigned to the CORT injection, vehicle or no injection group. Fifteen minutes after administering the corresponding injection, mice were exposed to 5000 lux for 60 minutes. Twenty four hours after light damage, mice were sacrificed, the eyes embedded in paraffin and sagittal sections prepared for TUNEL.

As expected, TUNEL labelling revealed numerous apoptotic cells in the ONL. The data showed that uninjected mice had about 64.28 ± 9.61 apoptotic cells /1000 µm² ONL, which was significantly different ($P \leq 0.01$) from vehicle-injected mice (52.42 ± 10.91 apoptotic cells /1000 µm² ONL). CORT-injected mice had about 34 % less apoptotic cells (42.2 ± 6.67 cells /1000 µm² ONL) than uninjected mice, a difference that was also statistically significant ($P \leq 0.01$), (Figure 14D).

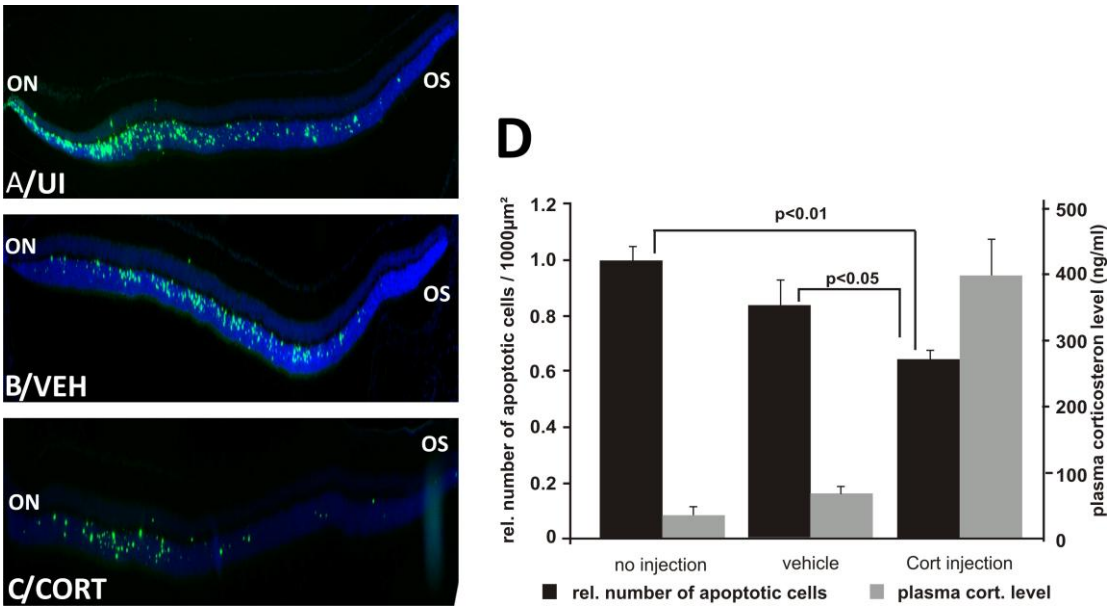

Figure 14: Exogenous CORT protected photoreceptors from light induced damage. Single housed mice were injected with CORT [52 µg /g body weight] (C) or its vehicle 15 minutes prior to light damage (B) (D: gray bars). TUNEL staining of sagittal sections from retinae 24 hours after an illumination with 5000 lux for 60 minutes of uninjected mice (A), vehicle-injected mice (B) and CORT injected mice (C). The number of TUNEL positive cells on sagittal sections was quantified and plotted as the relative number of apoptotic cells per 1000 µm^2 ONL (D: black bars). The data shown are combined from two independent experiments, $n \geq 7$, mean ± SEM. Scale bars: A, B, 100 µm.

4.6.3. Effect of CORT on 661W cell apoptosis

Following a robust CORT effect on photoreceptor survival *in vivo*, an interesting question worth investigating was whether CORT would produce the same effects on photoreceptors *in vitro*. In this light, the effect of CORT on photoreceptor apoptosis *in vitro* was investigated on the 661W immortalised cell line which is an appropriate model for photoreceptor cells *in vitro* [112].

To perform the above experiment, 661W cells were cultured in 6 well plates and treated with staurosporine which is known to induce differentiation in immortalised cells [113]. Morphologically, 24 hours after treatment with staurosporine, 661W cells adopted a more neuronal structure as dendrites and axons having synapse-like structures at their ends, which outgrew from the cell body (Figure 15B).

As staurosporine is also known to induce apoptosis in immortalised cells [113], several concentrations of staurosporine were tested for different durations of incubation to get the minimum concentration and corresponding duration that induced high differentiation as seen by morphological changes at the least toxicity as evidenced by cell death. 0.5 nM staurosporine for 10 minutes was found to be the most suitable as cells showed a more neuronal structure with axon like structures extending from the cell body. Therefore, 661W cells were differentiated with 0.5 nM staurosporine for 10 minutes and then incubated with 20 nM CORT for 10 hours. After 10 hours of CORT incubation cells were then exposed to serum starvation which is an established method of inducing cell apoptosis *in vitro* [121]. Thereafter, apoptosis was quantified using the Wst-1 cell viability assay.

The data showed that after serum starvation, a significant 27 % of cells underwent apoptosis. However, pre-treatment with 20 nM CORT did not influence cell survival of serum starvation, (Figure 15C).

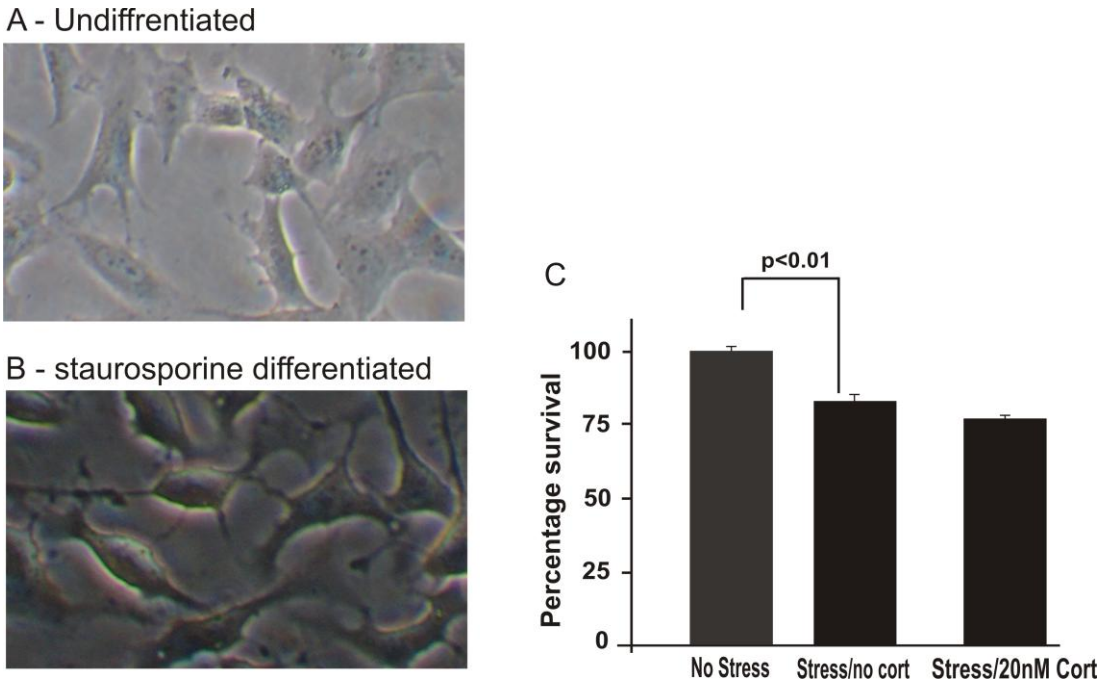

Figure 15: CORT does not prevent 661 W apoptosis *in vitro*. 661W cell normal morphology (A): 661W cells show a more neuronal appearance following differentiation with 0.5 nM staurosporine for 10minutes(B): Following serum starvation stress, a significant number of cells underwent apoptosis but pre-treatment with 20 nM CORT for 10 hours did not confer any protective effect (C).The data shown are combined from three independent experiments, mean ± SEM.

4.7. Adrenalectomy and light damage

In vivo, the release of CORT due to stress is regulated by the HPA axis [102]. Final production and release of CORT occurs at the level of the adrenal gland and so adrenalectomy makes it impossible for any CORT to be produced during a stress reaction, making the adrenal an indispensable part of the HPA axis.

4.7.1. Adrenalectomy exacerbates light induced damage of photoreceptors

To analyse if a CORT deficiency following adrenalectomy would shut off the protective effect of short-term psychosocial stress, mice were adrenalectomised

(ADX) while control mice underwent a sham operation (sham). Both groups were allowed to recover for two weeks after which each group was subdivided into two groups, a CSC group and a SHC group followed by 10 hours CSC housing. Immediately after CSC housing, all groups sham/CSC, sham/SHC, ADX/CSC and ADX/SHC were exposed to 5000 lux for 30 minutes and then subjected to TUNEL analyses.

As expected, TUNEL staining revealed numerous apoptotic cells in the ONL of sham/SHC mice. The number of apoptotic cells in the sham/SHC group was counted and normalised to 100 %. In conformity with previous data between SHC and CSC housed mice, relative to sham/SHC, sham/CSC mice showed an about 30 % significant decrease in the number of apoptotic cells ($P \leq 0.05$). On other hand, relative the sham/CSC group, ADX/CSC mice showed an about 41 % increase in the number of apoptotic cells, a difference that was also significant ($P \leq 0.05$). There was no relative difference between sham/SHC and ADX/SHC group (Figure 16).

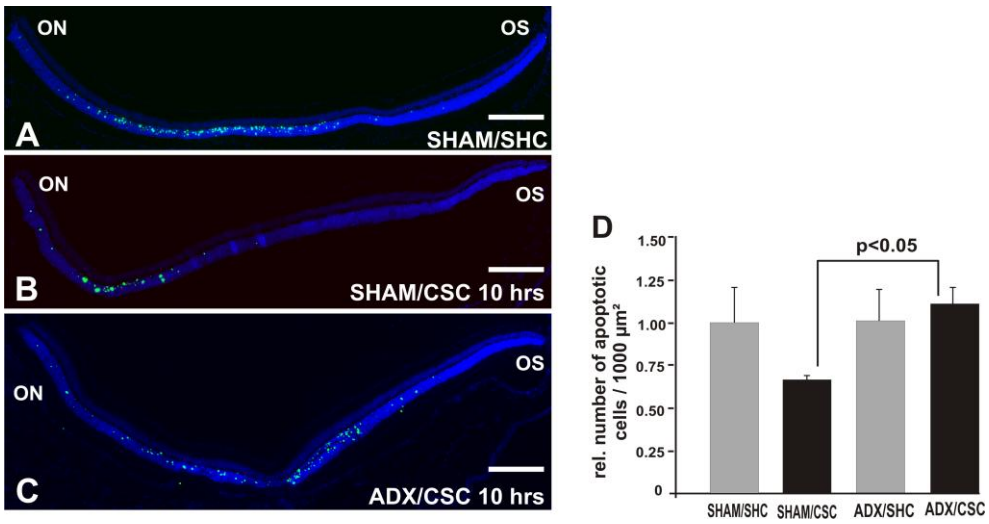

Figure 16: Adrenalectomy impeded stress-mediated protection against light induced damage of photoreceptors.A-D. Representative TUNEL staining (green) of sagittal sections from retinae 24 hours after illumination with 5000 lux for 30 minutes from mice 2 weeks after adrenalectomy (C; ADX) or

sham surgery (A, B; sham), and 10 hours CSC housing (B, C) or single housed controls (A; SHC) immediately prior to light exposure. The number of TUNEL-positive cells on sagittal sections was quantified and plotted as the relative number of apoptotic cells per 1000 μm^2 ONL (D). The data shown are combined from two independent experiments, $n \geq 4$, mean ± SEM. Scale bars: A, B, 100 µm.

4.7.2. Prior adrenalectomy worsens retinal degeneration

Given the extremely high apoptosis in ADX mice as compared to sham operated mice after 10 hours CSC, it was probable that upon further retinal degeneration there would be a huge decrease in the thickness of the ONL of ADX mice as compared to sham operated mice. As such, the rate of retinal degeneration following ADX was analysed. To this end, Sham and ADX mice were submitted to 10 hours CSC and illuminated at 5000 lux for 1 hour immediately after 10 hours CSC while a third group of ADX mice was left unilluminated. Three weeks after light damage, eyes were prepared and embedded in epon. A quantitative morphometry of the thickness of the ONL of the retina was performed. The data obtained were plotted on a spider diagram.

After 10 hours CSC housing, Sham operated mice were almost completely protected against a light induced loss of photoreceptors as they were similar to unilluminated mice. On the other hand, there was a very high damage in ADX mice as indicated by a thinner ONL, a difference that was statistically significant for most regions of the ONL ($P \leq 0.05$), (Figure 17A).

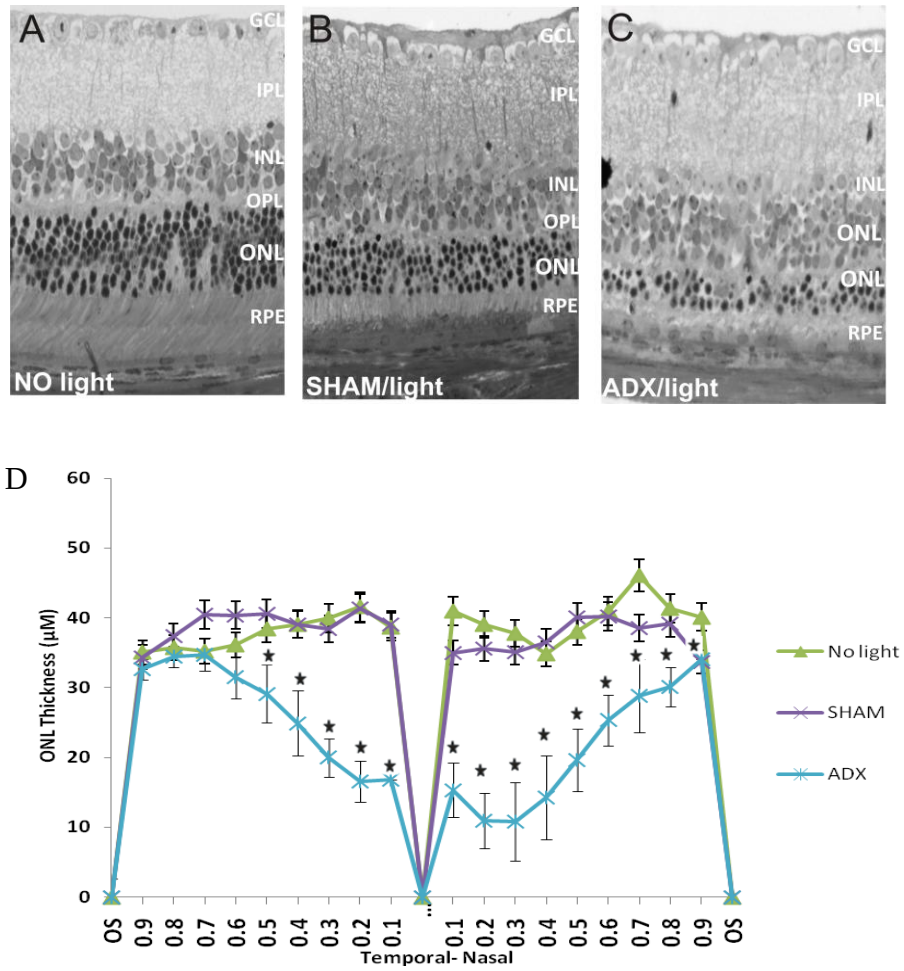

Figure 17: Adrenalectomy promotes retinal degeneration. A, B,C. Representative plastic sections from retinae 3 weeks after illumination with 5000 lux for 1 hour. Adrenalectomy was performed 2 weeks before light exposure (ADX, C), while control mice underwent simple laparotomy (sham, B). All groups were exposed to 10 hours CSC housing and then light damage performed (B and C) while control mice were left unilluminated (A). The thickness of the ONL was measured 3 weeks after light damage and plotted on a spider diagram (D), $n \geq 5$, mean ± SEM.

4.7.3. CORT injection rescues adrenalectomised mice from severe light damage

From the experiments this far, exogenous CORT was shown to protect photoreceptors against light damage while ADX mice turned out to be extremely susceptible to light damage than sham controls. As such, it was logical to investigate if an exogenous CORT injection would rescue adrenalectomised mice from a severe light damage.

For this purpose, adrenalectomy was performed in Balb/c mice. After a two weeks recovery period, one group received a 52 µg/g CORT injection while the other group received a vehicle injection. Fifteen minutes after injection, mice were exposed to 5000 lux for 60 minutes. After 24 hours eyes were prepared and subjected to TUNEL staining.

As expected after a light damage, TUNEL staining revealed apoptotic cells predominantly in the ONL. The numbers of apoptotic cells were counted and expressed per 1000 µm^2 ONL. The results showed that ADX/VEC mice had a mean of 15.69 ± 2.6 cells / 1000 µm² ONL, meanwhile ADX/CORT mice showed a 50.7 % decrease in apoptotic cells (7.73 ± 0.9 cells / 1000 µm² ONL), a difference that was statistically significant ($P \leq 0.05$), (Figure 18).

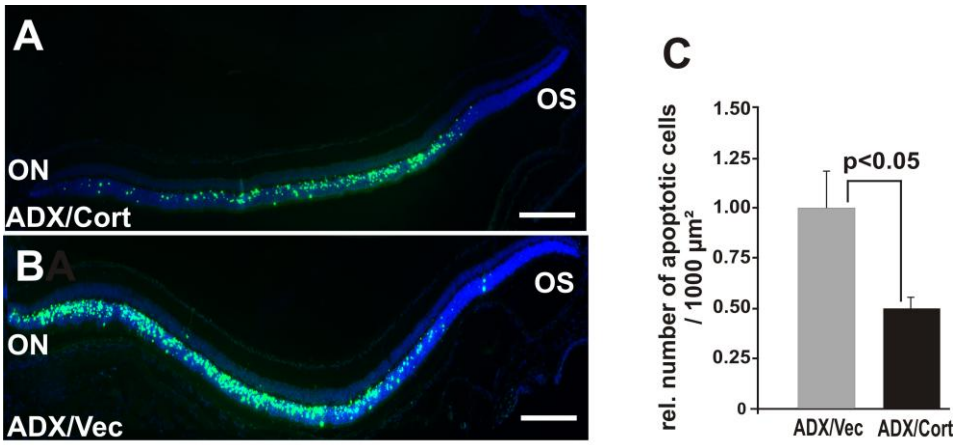

Figure 18: CORT injection rescues the exacerbating effect of adrenalectomy on light damage. To prove that stress-induced neuroprotective effects are mediated via increased CORT levels, adrenalectomised mice were treated with CORT [52 µg/g body weight] or injected with vehicle 15 minutes prior to illumination with 5000 lux for 60 min. A, B. Representative TUNEL staining (green) of sagittal sections through retinae 24 hours after illumination, A (CORT injection) and B (Veh injection). The number of TUNEL-positive cells on sagittal sections was quantified and plotted as the relative number of apoptotic cells per 1000 µm^2 ONL (C). The data shown are combined from two independent experiments, $n \geq 8$, mean ± SEM. Scale bars: A, B, 100 µm.

4.8. Effect of short-term psychosocial stress and *in vitro* CORT treatment on Müller cell gliosis

As the data from experiments conducted this far summarily confirmed a neuroprotective effect of acute psychosocial stress via a CORT surge on light induced photoreceptor damage, the next intriguing aspect was to elucidate the mechanisms involved in this protective effect.

It has previously been published that, when the retina is under stress such as in the event of light damage, Müller cells can be activated leading to the activation of pathways that subsequently promote the secretion of neuroprotective factors that in turn activate signals which confer a protective effect on photoreceptors [122]. As such, the activation state of Müller cells following 10 hours CSC was analysed by evaluating GFAP expression as a marker for Müller cell gliosis [123].

4.8.1. Short-term psychosocial stress induces Müller cell gliosis

To investigate if Müller cell activation occurred following 10 hours CSC, CSC housing was performed as earlier described. Immediately after CSC, mice were sacrificed, retinae extracted and a real time RT-PCR for GFAP performed. In a separate set of mice, cryosections were made from eyes and used for GFAP immunostaining.

Analysis of RT-PCR data showed that immediately after 10 hours CSC, CSC housed mice had a 2.1-fold increase in GFAP expression when compared to SHC, a difference that was statistically significant ($P \leq 0.05$). GFAP immunostaining revealed a more intense GFAP staining in Müller cells after 10 hours CSC compared to SHC, (Figure 19B).

As it is known that light damage results in a higher expression of GFAP [122], it was not obvious if CSC housed mice would still have higher GFAP expression levels after

light damage compared to their SHC counterparts and so this was investigated in a separate set of experiments. To this end, real time RT-PCR was performed 7 hours after light damage that was preceded by 10 hours CSC. Data analysis showed that after light damage there was no difference in GFAP expression between CSC housed and SHC mice (Figure 19A).

4.8.2. CORT injection did not induce Müller cell gliosis

Since 10 hours CSC resulted in Müller cell activation, the ability of a CORT injection to induce GFAP expression was also investigated. For this reason, mice were shared into 2 groups. One group received a 52 µg/g CORT injection, while the other received a vehicle injection. Seven hours after CORT injection mice were sacrificed and real time RT-PCR for GFAP performed. The data showed that there was no difference in GFAP mRNA expression between both groups (Figure 19A).

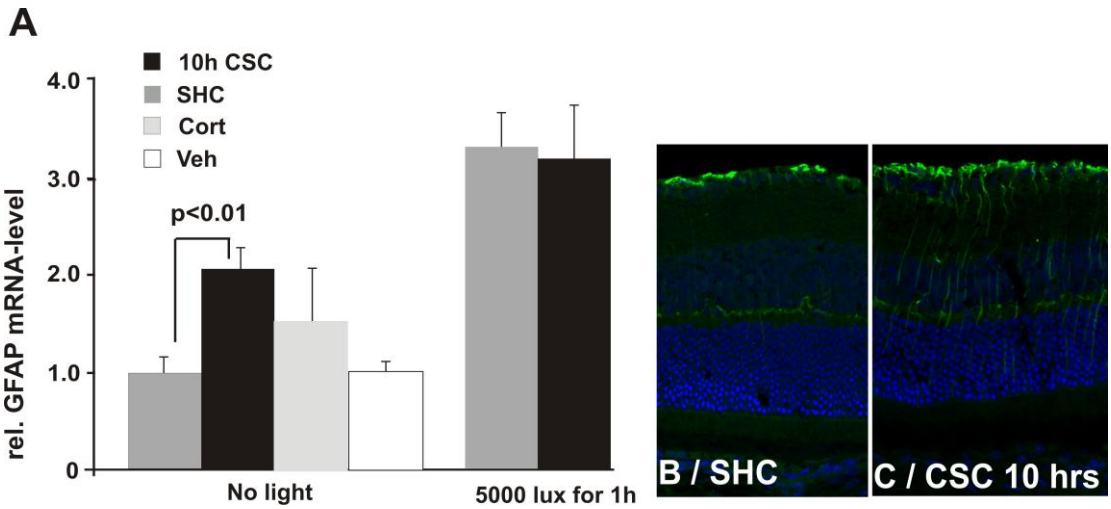

Figure 19: Short-term psychosocial stress activates Müller cell gliosis. Quantitative real-time RT-PCR for GFAP (A), mRNA in RNA from retinae of 10 hours CSC housed and SHC animals immediately after 10 hours CSC as well as 7 hours after illumination for 60 minutes with 5000 lux. 10 hours CSC induced a 2.1-fold increase in GFAP mRNA in CSC compared to SHC immediately after 10 hours CSC, an effect that is lost when this is followed by light damage The data shown are combined from

two independent experiments, n ≥ 7, mean ± SEM. B, C. Representative immunostaining for GFAP (green) of retinal sagittal sections in 10 hours CSC housed (C) and SHC mice (B).

4.8.3. CORT activates Müller cells in vitro

Based on the fact that Müller cell activation occurred following 10 hours CSC, the next logical question was whether this was also a CORT-mediated effect. A reasonable way to check this was to investigate if CORT treatment would exert similar effects on Müller cells *in vitro*. For this purpose, Müller cells were extracted from Wistar rats and seeded into 6 well plates. A group of 6 wells were incubated with 2 nM CORT for two hours while another group of 6 wells received control treatment. Immediately after CORT incubation, cells well harvested, RNA extracted and subjected to real time RT-PCR for GFAP.

The data showed that after CORT incubation, Müller cells showed an about 4-fold increase in GFAP mRNA expression compared to control treated cells, a difference that was statistically significant ($P \leq 0.05$), (Figure 20).

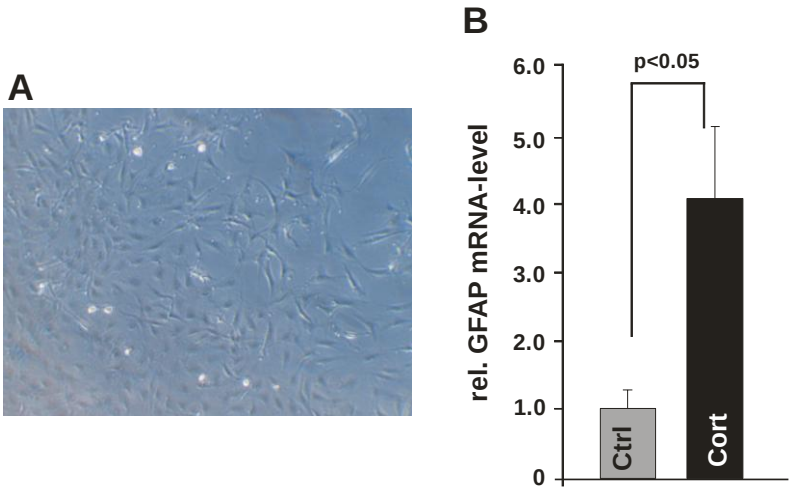

Figure 20: CORTincubation induces Müller cell gliosis *in vitro* A. Image of cultured Müller cells. B. To check if CORT will also activate Müller cells *in vitro* cells were incubated with 2 nM CORT for 2 hours. Real time RT-PCR data showed that CORT incubation induced an about 4-fold increase in

GFAP mRNA in CORT treated cells when compared to untreated controls (B). The data shown are combined from two independent experiments, n ≥ 7, mean ± SEM.

4.9. Neither short-term psychosocial stress nor CORT increases neurotrophic factor secretion

One of the ways by which Müller cells are known to exert their effects on photoreceptor survival is via an activation of the Lif-End 2 cycle which then leads to the secretion of neuroprotective growth factors [124, 125]. As data showed that 10 hours CSC can activate Müller cells, an effect which was also observed following *in vitro* incubation of Müller cells with CORT, there was a chance that this could lead to increased neurotrophic factor secretion via activation of the Lif-End-2 cycle. To check this, the expression of Lif and End-2 and other neurotrophic factors following 10 hours CSC and CORT injection was investigated.

4.9.1. Neither short-term psychosocial stress nor CORT injection activates the Lif/End-2 cycle

It has previously been shown that the secretion of neurotrophic factors, following Müller cell activation could be preceded by an activation of the Lif-End-2 cycle [124, 125]. As the data showed an activation of Müller cells following 10 hours CSC, it was interesting to investigate a possible activation of the Lif-End-2 cycle by short-term psychosocial stress or CORT injection. To this end, immediately after 10 hours CSC or 7 hours after CORT injection, retinae from CSC and SHC/uninjected, CORT_injected and vehicle-injected mice were extracted and RNA isolated. The obtained RNA was transcribed into cDNA and real time RT-PCR for Lif and End-2 performed.

The results showed no difference in Lif and End-2 mRNA expression between either the 10 hours CSC compared to SHC group or CORT compared to either the vehicle-injected group or uninjected (SHC) mice, (Figure 21).

There was a possibility that Lif/End-2 secretion could occur at a later time point. For this reason, the expression of Lif and End-2 was evaluated 7 hours after 10 hours CSC. Furthermore, there was also a possibility that Müller cell activation by 10 hours CSC could rather prime the retina so that Lif and End-2 secretion are activated in the event of a light damage. As such, the expression of Lif and End-2 was investigated 7 hours after light damage preceded by 10 hours CSC. To this end, CSC housed and SHC mice were again shared into two groups each and one group from each illuminated at 5000 lux for 1 hour, 7 hours after light damage retinae from all four groups (SHC/ No Light, SHC/Light, CSC/No light and CSC/ Light) were extracted and RNA isolated. The obtained RNA was transcribed into cDNA and real time RT-PCR for Lif and End-2 performed.

As expected, there was a significant increase in Lif and End-2 mRNA levels between light damaged and unilluminated retinae from mice for both SHC and CSC groups. The data again showed no difference in Lif and End-2 mRNA expression between either the CSC/No light compared to SHC/No light group 7 hours after 10 hours CSC or between the SHC/light and CSC/light 7 hours after light damage (Figure 21).

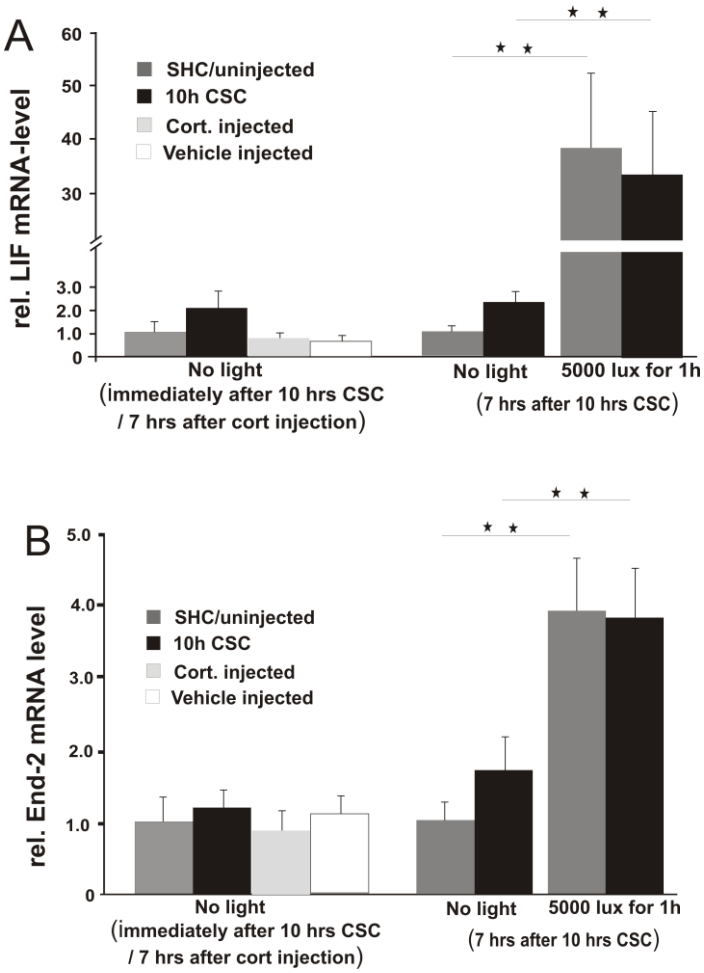

Figure 21: Short-term psychosocial stress or CORT injection does not induce Lif/End-2 mRNA expression.A, B. Quantitative real-time RT-PCR for Lif (A) and End-2 (B) mRNA from retinae of 10 hours CSC housed and SHC animals immediately after 10 hours CSC as well as 7 hours after illumination for 60 minutes with 5000 lux. Data analysis showed no difference for the various time points between SHC and CSC housed or CORT and vehicle-injected mice for both neurotrophic factors. The data shown are combined from two independent experiments, $n \geq 7$, mean ± SEM.

4.9.2. Neither short-term psychosocial stress nor CORTinjection activated the secretion of neuroprotective factors

An increase in neurotrophic growth factors during light damage is known to protect photoreceptors from light damage [126]. As such, to see if this was involved in their mechanisms of protection of photoreceptors from light damage, the expression of neurotrophic factors following 10 hours CSC or CORT injection was investigated. For

this reason, immediately after 10 hours CSC or 15 minutes after CORT injection, retinae from CSC and SHC/Uninjected, CORT-injected and vehicle-injected mice were extracted and subjected to real time RT-PCR for Fgf-2 and Cntf.

Data analysis showed no difference in Fgf-2 and Cntf expression between either the 10 hours CSC compared to SHC group or CORT compared to the Vehicle-injected group, (Figure 22).

An exogenous increase in neurotrophic growth factors after damage of photoreceptors has already occurred has previously been shown to be able to rescue these cells [10, 124]. As such, the expression of Fgf-2 and Cntf was investigated 7 hours after light damage that was directly preceded by 10 hours CSC. To verify previously obtained data at another time point, the expression of Fgf-2 and Cntf was investigated 7 hours after CSC without light damage. For this purpose, CSC housed mice and SHC were again shared into two groups each and one group from each illuminated at 5000 lux for 1 hour. Seven hours after illumination, retinae from all four groups; SHC/ No Light, SHC/Light, CSC/No light and CSC/ Light were extracted and subjected to real time RT-PCR for Fgf-2 and Cntf.

As expected, there was a significant increase in Fgf-2 levels between light damaged and unilluminated mice for both the SHC and CSC groups (Figure 22). But no difference was detected in Fgf-2 and Cntf mRNA expression between either the CSC/No light compared to SHC/No light group 7 hours after 10 hours CSC or between the SHC/light and CSC/light 7 hours after light damage (Figure 22).

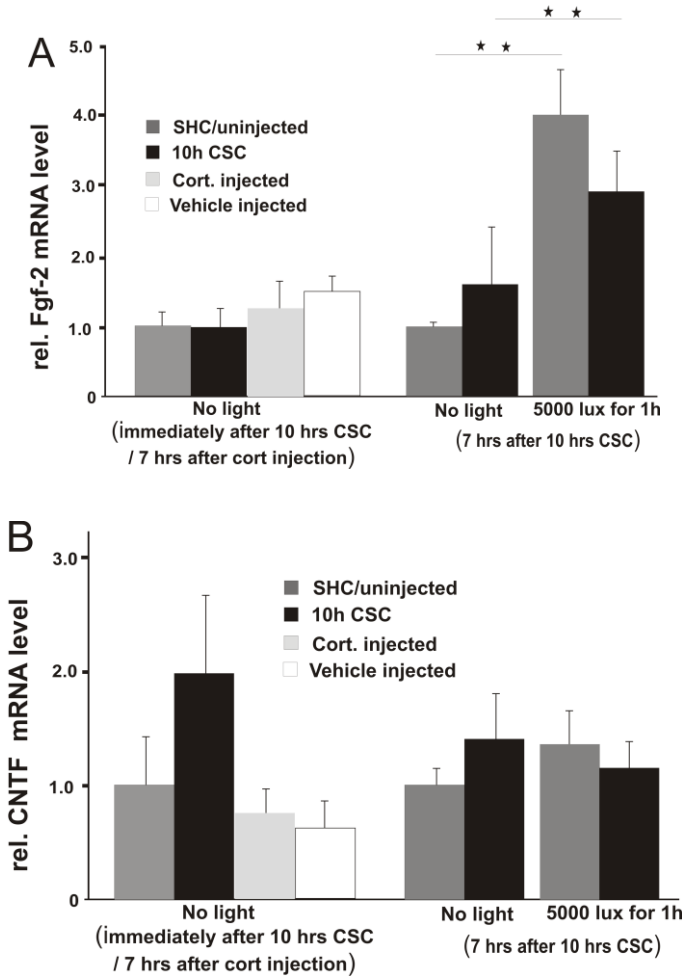

Figure 22: Neither short-term psychosocial stress nor CORT injection induces the expression of neurotrophic factor. A, B. Quantitative real-time RT-PCR for Fgf-2 (A) and Cntf (B) mRNA from retinae of 10 hours CSC housed and SHC animals immediately after 10 hours CSC as well as 7 hours after illumination for 60minuteswith 5000 lux. Data analysis showed no difference for the various time points between SHC and CSC housed or CORT and vehicle-injected mice for both neurotrophic factors. The data shown are combined from two independent experiments, $n \geq 7$, mean ± SEM.

4.10. The role of the PI3-Akt pathway in the neuroprotective effect of short-term psychosocial stress

It is known that CORT can have direct effects on neurons via Akt phosphorylation [95]. As the data showed that the neuroprotective effect of 10 hours CSC is not mediated via an increase secretion of neuroprotective growth factors, it made sense to investigate if the effect could be directly mediated via an activation of Akt

phosphorylation. As such, the influence of 10 hours CSC on Akt phosphorylation was investigated.

4.10.1. Short-term psychosocial stress activates Akt phosphorylation

To investigate if 10 hours CSC influences Akt phosphorylation, mice were once more exposed to 10 hours CSC as earlier described. Immediately after CSC mice were sacrificed, total retinal protein extracted and subjected to western blot analyses for pAkt and Akt.

In SHC mice, a specific band for pAkt was detected at approximately 61 kDa. The intensity of the pAkt signal was substantially increased in retinal protein from mice that had been subjected to 10 hours CSC housing prior to preparation. The intensity of the Akt signal that was used as loading control was almost similar in both groups. Densitometry revealed a 2.6-fold increase in the pAkt/Akt ratio in short-term psychosocially stressed mice when compared to SHC mice, a difference that was statistically significant ($P \leq 0.05$), (Figure 23).

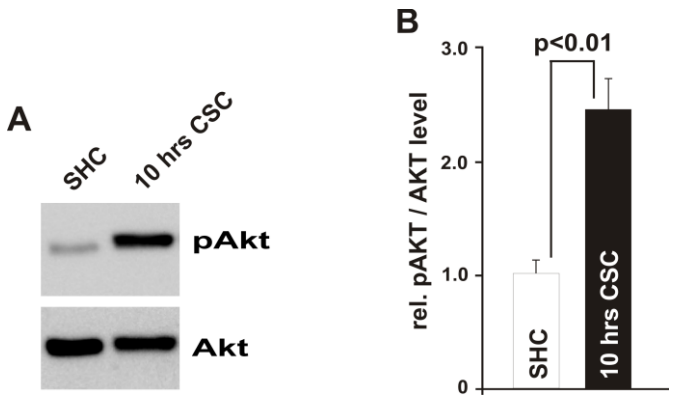

Figure 23 :Short-term psychosocial stress induces Akt phosphorylation. Western blot analyses (A) and relative densitometry (B) for phosphorylated Akt or total Akt in retinal proteins after 10 hours CSC housing. The data shown are combined from two independent experiments, $n \geq 8$, mean ± SEM.

4.10.2. CORT injection promotes Akt phosphorylation

Following a significantly higher Akt phosphorylation after 10 hours CSC, it became necessary to verify if this increase in Akt phosphorylation was mediated via CORT. An appropriate way to do this was by investigating if exogenous CORT would also activate this pathway. To get this done, mice were shared into two groups, one for CORT injection (CORT group) and the other for vehicle injection (veh group). Two hours after a CORT injection, mice were sacrificed and total retinal proteins were subjected to western blot analysis for pAkt and total Akt.

In vehicle-injected mice a specific band for pAkt was detected at approximately 61 kDa. The intensity of the pAkt signal was substantially increased in retinal protein from mice that received a CORT injection prior to preparation. The intensity of the Akt signal that was used as loading control was almost similar in both groups. Densitometry revealed that a 2.6-fold increase in the pAkt / Akt ratio in CORT injected mice when compared to SHC mice, a difference that was statistically significant ($P \leq 0.05$), (Figure 24).

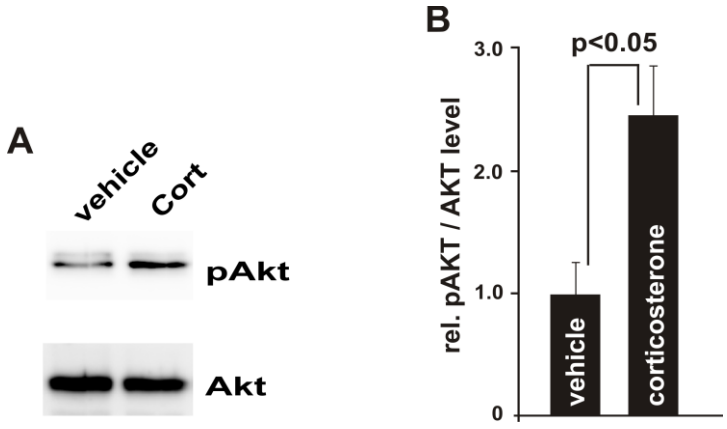

Figure 24: Exogenous CORT induces Akt phosphorylation Western blot analyses (A) and relative densitometry (B) for phosphorylated Akt and total Akt in retinal proteins 2 hours after CORT (52 µg/g) or vehicle injection. The data shown are combined from two independent experiments, $n \geq 8$, mean ± SEM.

4.10.3. Adrenalectomy attenuates Akt phosphorylation

As the data following 10 hours CSC and exogenous CORT injection suggest that both an endogenous and exogenous increase in CORT activated Akt phosphorylation which in turn mediates neuroprotection properties of photoreceptors, it was hypothesised that a lack of CORT following an ADX and a loss of neuroprotective effects could be due to less Akt phosphorylation. For this purpose, ADX and sham operated control mice were exposed to 10 hours CSC housing. Immediately after CSC, mice were sacrificed and total retinal proteins were subjected to western blot analyses for pAkt and total Akt.

The results showed that the intensity of the pAkt signal was substantially decreased in retinal protein from ADX mice compared to sham mice. The intensity of the Akt signal that was used as loading control was almost similar in both groups. Densitometry revealed mice a 2.6-fold decrease in the pAkt/Akt ratio in ADX mice when compared to sham, a difference that was statistically significant ($P \leq 0.05$), (Figure 25).

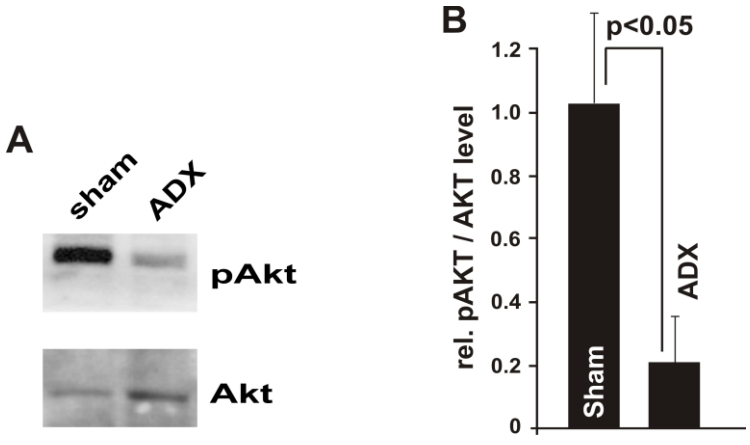

Figure 25: ADX inhibits Akt phosphorylation retina. Western blot analyses (A) and relative densitometry (B) for pAkt or total Akt in retinal proteins from retinae of short-term psychosocial stressed ADX and sham operated mice. The data shown are combined from two independent experiments, $n \geq 4$, mean ± SEM.

4.10.4. CORT incubation promotes Akt phosphorylation in Müller cells in vitro

Following a CORT activation of Akt phosphorylation *in vivo*, an intriguing question was whether CORT would exert similar effects on Müller cells *in vitro*. To investigate this, cultured Müller cells from Wistar rats were incubated with 2 nM CORT for two hours. Immediately after CORT treatment, cells were harvested, total retinal protein extracted and subjected to western blot analyses for pAkt and total Akt.

In control treated Müller cells, a specific band for pAkt was detected at approximately 61 kDa. The intensity of the pAkt signal was substantially increased in protein from CORT incubated Müller cells. The intensity of the Akt signal that was used as loading control was almost similar in both groups. Densitometry revealed a 2.6-fold increase in the pAkt/Akt ratio in CORT treated cells when compared to vehicle treated, a difference that was statistically significant ($P \leq 0.05$), (Figure 26).

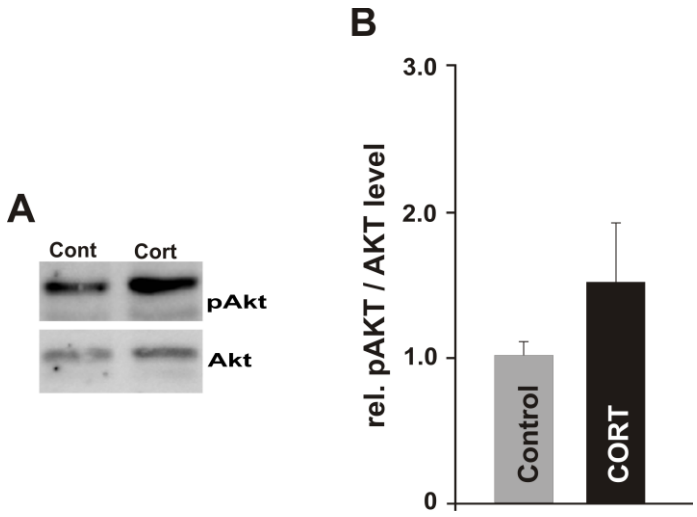

Figure 26: CORT induces Akt phosphorylation in Müller cells. Western blot analyses (A) and relative densitometry (B) for phosphorylated Akt or total Akt in retinal proteins after 2 hours CORT incubation. The data shown are combined from two independent experiments, $n \geq 5$, mean ± SEM.

4.10.5. Light damage does not influence Akt phosphorylation

As the data showed that increased phosphorylation of Akt following high CORT levels is followed by neuroprotection of photoreceptors against light damage, it was likely that this pathway can be activated as a protective mechanism by light or could be a pathway that is inhibited after light damage leading to an increase in apoptosis. Therefore, the influence of light damage on Akt phosphorylation was evaluated. Here, mice were illuminated with 5000 lux for 1 hour (Light group) while control mice were left unilluminated (No Light group). Immediately after light damage, mice were sacrificed and total retinal proteins subjected to western blot analyses for pAkt and total Akt.

The intensity of the pAkt signal was not different between the illuminated and non illuminated mice. The intensity of the Akt signal that was used as loading control was almost similar in both groups. Densitometry revealed no significant effect on Akt phosphorylation, (Figure 27).

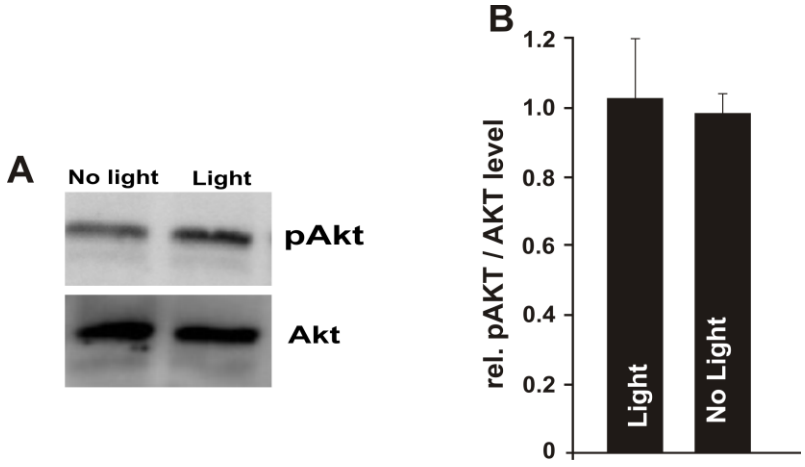

Figure 27: Light damage does not influence Akt phosphorylation in retina. SHC mice were submitted to 5000 lux light damage for 1 hour. Representative western blots for Akt phosphorylation (A) and densitometry showing the pAkt/total Akt ratio of two independent experiments (B). n = 6, mean ± SEM.

4.11. Triciribine inhibits the protective effect of short-term psychosocial stress and CORT injection

Given that increased CORT levels due to CSC correlate with an increase Akt phosphorylation which in turn correlates to a protective effect on photoreceptors, it became imperative to investigate if Akt phosphorylation plays an important role in the protective effect of CSC housing or is just a side event of increased systemic CORT. For this purpose, the phosphorylation of Akt was inhibited using the inhibitor triciribine.

4.11.1. Triciribine inhibits Akt phosphorylation in retina

Before using triciribine as an inhibitor of Akt phosphorylation, its inhibitory effect on this pathway was verified. To this end, mice received an intravitreal injection of 3 µl of 1 ng/µl triciribine into the right eye (Triciribine) and vehicle into the left eye (Veh) followed by a CORT injection two hours later. After 2 additional hours, mice were sacrificed and total retinal proteins were subjected to western blot analyses for pAkt and total Akt.

The intensity of the pAkt signal was substantially decreased in retinal protein from triciribine-injected eyes compared to vehicle-injected eyes. The intensity of the Akt signal that was used as loading control was almost similar in both groups. Densitometry revealed a 36 % decrease in the pAkt/Akt ratio in triciribine-injected eyes when compared to vehicle-injected eyes, a difference that was statistically significant ($P \leq 0.05$), (Figure 28).

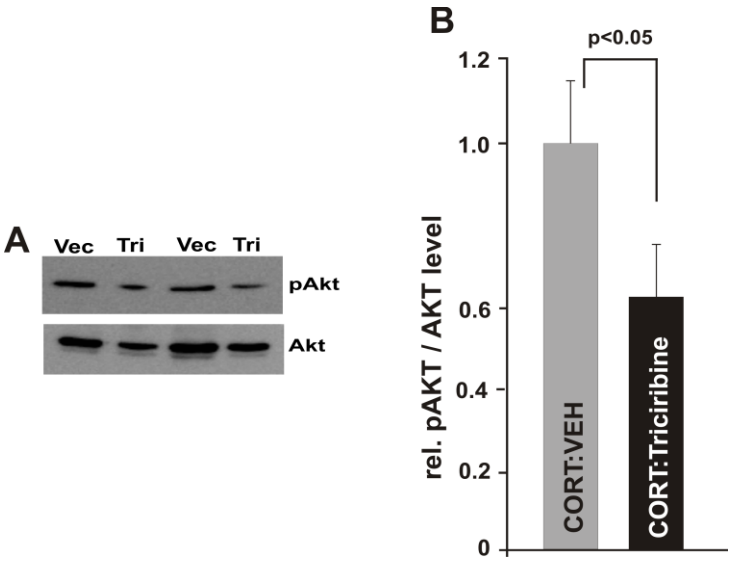

Figure 28: Triciribine inhibits Akt phosphorylation in the retina. To evaluate the importance of Akt phosphorylation in the protective effect of 10 hours CSC, this pathway was inhibited via intravitreal injection of 3 µl of 1 ng/µl triciribine. Western blot analyses (A) and relative densitometry (B) for phosphorylated Akt or total Akt in retinal proteins from triciribine or vehicle-injected mice after CORT injection. The data shown are combined from two independent experiments, $n \geq 8$, mean ± SEM.

4.11.2. Short-term psychosocial stress mediates its neuroprotective effects via Akt phosphorylation

To analyse if 10 hours CSC mediates its neuroprotective effect on damaged photoreceptors via an increase in Akt phosphorylation, 3 µl of 1 ng/µl triciribine was intravitreal injected into one eye whereas the fellow eye received the vehicle only. After 10 hours CSC, mice were illuminated with 5000 lux for 30 minutes. 24 hours after light damage, mice were sacrificed and subjected to TUNEL labelling.

In the retina of vehicle-injected eyes, several TUNEL positive cells were detected in the ONL but this was more pronounced in retinae of triciribine treated eyes. The number of apoptotic cells per 1000 μm^2 ONL were counted and normalised to 100 %. The data revealed that triciribine-injected had a 21 % relative increase in apoptotic

cells compared to vehicle-injected eyes, a difference that was statistically significant ($P \leq 0.05$), (Figure 29).

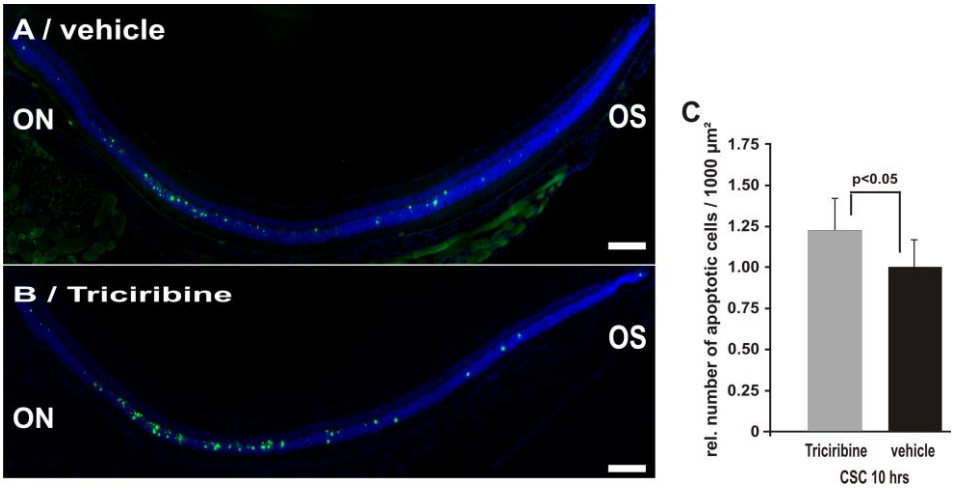

Figure 29: Triciribine blocks the neuroprotective effect of short-term psychosocial stress on damaged photoreceptors. A, Representative TUNEL staining (green) of sagittal sections through retinae 24 hours after illumination with 5000 lux for 60 min. Before acute psychosocial stress, 3 µl of 1 ng/µl triciribine was injected into the right eye (B) whereas the left eye received a vehicle injection. B. The number of TUNEL positive cells on sagittal sections was quantified and plotted as the relative number of apoptotic cells per 1000 μm^2 ONL. The data shown are combined from two independent experiments, n $\geq$ 8, mean ± SEM.

4.11.3. Triciribine injection blocks protective effect of CORT injection

Following the fact that triciribine-injected eyes had significantly higher apoptosis compared to the vehicle-injected fellow eye after 10 hours of CSC, an important data point to fulfil was to investigate if triciribine would also block the protective effect of CORT injection as this would provide conclusive evidence that CSC and CORT injection provide their protective effects by activating the same pathways. To this end, two hours before CORT injection, 3 µl of 1 ng/µl triciribine were injected intravitreally into the right eye and a vehicle solution into the left eye. Fifteen minutes

after CORT injection, mice were illuminated at 5000 lux for 30 minutes. Again the number of apoptotic cells was analysed by TUNEL staining.

In the retina of vehicle-injected eyes, several TUNEL positive cells were detected in the ONL but this was more pronounced in retinae of triciribine-treated eyes. The number of apoptotic cells per 1000 µm^2 ONL were counted and normalised to 100 %. The data revealed that triciribine-injected eyes had a 42 % relative increase in apoptotic cells compared to vehicle-injected eyes, a difference that was statistically significant ($P \leq 0.05$), (Figure 30).

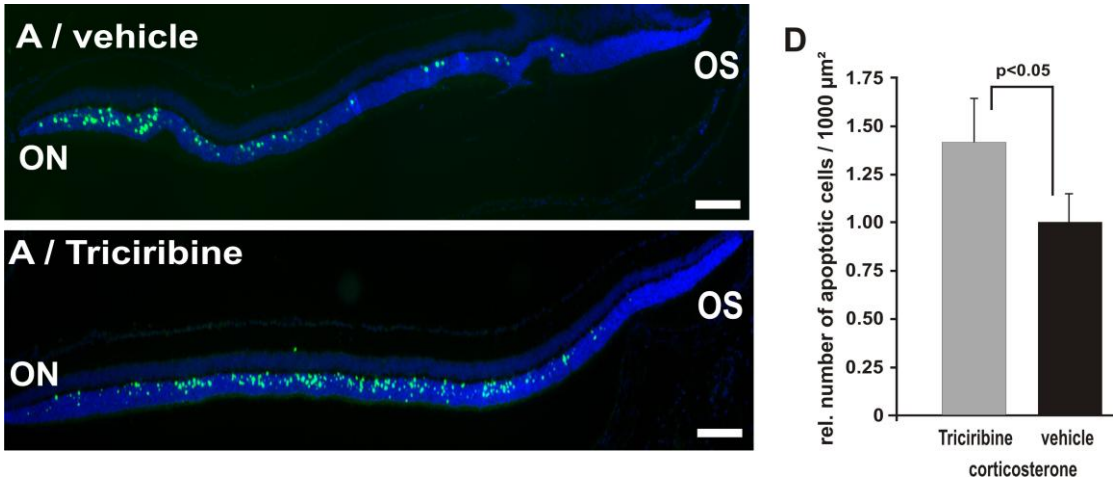

Figure 30: Triciribine blocks the protective effect of exogenous CORT on light damage. A, B. Representative TUNEL staining (green) of sagittal sections through retinae 24 hours after illumination with 5000 lux for 60 min. Before CORT injection, 3 µl of 1 ng/µl triciribine were injected into the right eye (B) whereas the left eye received a vehicle injection (A). The number of TUNEL-positive cells on sagittal sections was quantified and plotted as the relative number per 1000 µm^2 ONL (C). The data shown are combined from two independent experiments, $n \geq 8$, mean ± SEM.

4.12. Short-term psychosocial stress has no effect on NMDA mediated RGC excitotoxicity

After injury, an intravitreal injection of GCs has been shown to ameliorate RGC loss by promoting survival and regeneration [127]. Since the TUNEL and ELISA data demonstrated that acute psychosocial stress via 10 hours CSC has protective effects on photoreceptor apoptosis, it was worth investigating if this systemic increase in CORT could also protect against RGC apoptosis induced via NMDA injection as NMDA is known to induce excitotoxicity and cause a subsequent apoptosis in these cells [105]. To this end, immediately after performing 10 hours CSC as previously described, both CSC and SHC received a 3 µl PBS injection into the vitreous of the left eye while the right eye received 3 µl of 10 mM NMDA (a concentration that is enough to cause a substantial but not complete damage of RGC´s [128]).

Three weeks after treatment with NMDA, the structure of optic nerves was essentially normal in the PBS injected left eyes (Figure 31a), meanwhile a loss of axons and the formation of an excessive glial scarring were observed in semithin sections through optic nerves of NMDA-treated right eyes (Figure 31b). The total number of axons in the right eye were counted and compared to the number of axons in the left eye. The data showed that the NMDA eyes from the SHC group had 15512 ± 2672 surviving axons compared to 32846 ± 2426 axons in PBS eyes meanwhile CSC showed a trend of an increase in the number of surviving axons with 17017 ± 1788 surviving axons compared to 29035 ± 1998 axons in PBS-treated eyes (Figure 31c).

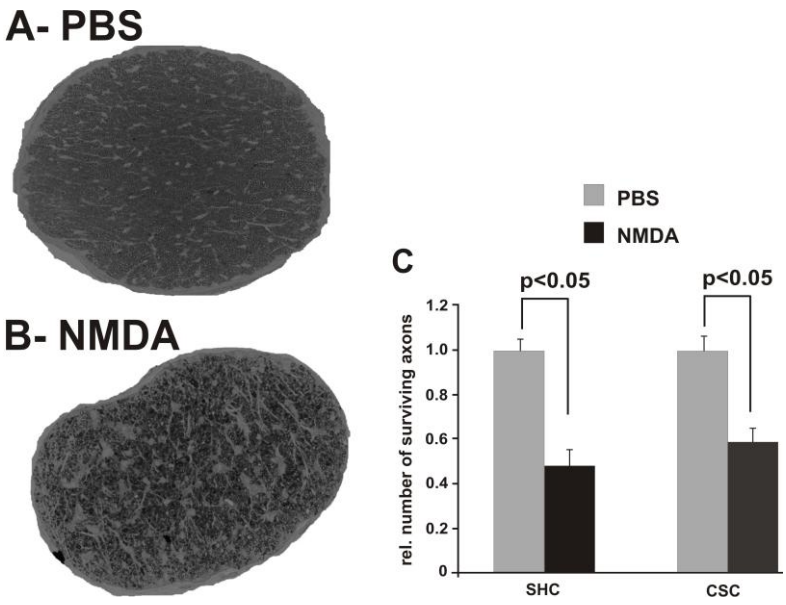

Figure 31: Short-term psychosocial stress has no effect on NMDA induced loss of retinal ganglion cells. A-B: Representative sagittal plastic sections through the optic nerve. After an injection of 3 µl PBS in the vitreous body, light microscopy showed no abnormality in the optic nerve, (A). In comparison, after an intravitreal injection of NMDA (10 mM), glial scarring and an excessive loss of axons can be observed (B). Quantification showed no difference in the number of surviving axons between CSC housed and SHC mice (E). n = 6, mean ± SEM.

5 DISCUSSION

5.1. CSC housing in Balb/c mice: An appropriate model

To investigate the effects of psychosocial stress on induced damage of retinal neurons, the first challenge was to establish an appropriate animal model for psychosocial stress in an animal species that allows for the induction of substantial neuronal damage using well established methods of choice.

As an animal model for psychosocial stress, the CSC paradigm which was originally established in C57BL/6 mice was chosen as it has been shown to robustly induce psychosocial stress in mice as evidenced by profound alterations in quantifiable stress parameters [64]. Moreover, it has also been used to investigate the effects of psychosocial stress on different disorders ranging from simple psychopathologies like mood to complicated inflammatory disorders in mice [129, 130]. Additionally, another advantage of using CSC housing in this project was that it gave the opportunity to separately investigate the effect of acute and chronic stress on neuronal damage using the same animal model.

To induce retinal degeneration *in vivo,* light exposure was used to damage photoreceptors as it has been demonstrated to substantially induce photoreceptor apoptosis in mice and rats [86, 131] and has widely been used to study retinal degeneration owing to several advantages it offers over other animal models [126].

Given the fact that C57BL/6 mice are very resistant to light, hence necessitating high light intensities, Balb/c mice were chosen for experiments as they are extremely susceptible to light damage compared to C57BL/6 mice [132].

It is known that, Balb/c mice are more responsive to both acute and chronic stressors than C57BL/6 mice [133]. Therefore, it wasn't obvious that CSC housing will induce psychosocial stress as in Balb/c mice. As such, CSC housing was first replicated in these mice.

During the first 30 minutes of CSC housing in Balb/c mice, subordinated mice all manifested behavioural attitudes of flight, retreat and a submissive upright posture which are established indicators of psychosocial stress in rodents [134].

As behavioural observation alone does not suffice to ascertain psychosocial stress, additional parameters which included body weight, adrenal weight and changes in CORT levels were analysed and compared in SHC versus CSC housed Balb/c mice.

It was shown that subordinated Balb/c mice significantly lost body weight after 10 hours CSC. Meanwhile in the case of 19 days CSC, after an initial body weight loss, subordinated mice gradually began to gain minimal amounts of weight, a phenomenon that can be explained by a habituation effect that occurs following prolonged subordination, reason why the dominant mouse was again changed on days 7 and 15.

Several factors do contribute to body weight loss following subordination. Firstly, once subordinated, mice have been shown to have a lower food intake than controls [135], this is because they don't have access to food due to constant harassment from the dominant mouse which also spends most of its time around the food. Moreso, an integral part of the stress response is a stimulation of the sympathetic nervous system that mobilises more energy for the fight or flight response by increasing metabolism [136]. Lastly, increased release of CRH due to HPA axis activation during stress causes an increase in colonic motility, a process that leads to an emptying of the

bowels [137]. Summarily, less food consumption, higher metabolism and higher defecation are responsible for weight loss following 10 hours CSC.

Adrenal hyperplasia is an indicator of stress [67]. Results from both short-term and long term CSC showed that both acute and chronic psychosocial stress via CSC housing affected the adrenal gland of Balb/c mice. The insignificant increase in adrenal weight after 10 hours CSC reflects the short period of stress. On the other hand, a significant increase in adrenal weight after 19 days CSC housing corresponds to what has been shown in other chronic stress paradigms such as overcrowding and repeated restrain in rats [138, 139]. Adrenal hyperplasia is explained by the fact that prolonged stress exposure leads to increased ACTH [140] which induces both cellular hypertrophy and hyperplasia in the zona fasciculata of the adrenal cortex [116] thereby leading to an increase in adrenal weight.

After 10 hours of CSC, the observed significant increase in CORT led to a definite conclusion that Balb/c mice were considerably stressed after CSC as this is in line with other studies where acute stressors like immobilization and forced swimming were shown to cause an increase secretion of CORT [141]. Generally, elevated GC levels following acute stress are a well established component of the acute stress response since they indicate the activity level of the HPA axis [115]. Following the extension of stress duration to a 19 day period, obtained data showed that CORT levels “re-normalized” to basal levels despite the on going stressful situation. This data is consistent with data from other researchers who have shown that chronic restrain stress accompanied by forced swimming produced a significant elevation only in basal plasma ACTH, but not in CORT [142]. A probable reason for this is a down regulation of HPA activity during chronic stress aimed at minimizing the deleterious effects of chronic CORT release on normal body functions [143-145]. More

specifically, it has been shown that following chronic CSC adrenal response to ACTH is attenuated [64] and so CORT production is compromised.

5.2. Effect of short-term psychosocial stress on photoreceptor apoptosis

A major factor that determines the effect of stress is the duration of exposure, generally classified as acute (short-term) and chronic. After short-term psychosocial stress via 10 hours of CSC housing, a protective effect was observed on photoreceptors following light damage. This result was again replicated by data which showed that prior short-term stress reduces the release of free nucleosomes following light damage. Put together, these results correspond to studies that have shown beneficial effects of fasting mediated acute stress via a CORT surge on light damaged photoreceptors [86] and also general beneficial effects of acute stress on neurons of the CNS [146, 147].

In an acute stress reaction several molecules including; GCs, CRF, ACTH, Aldosterone and Catecholamines get secreted. It was therefore necessary to identify which of them is particularly responsible for the protective effect of acute psychosocial stress. The prime candidate was CORT as GCs have been shown to protect against apoptosis induced by different ways in several types of retinal neurons [86, 127]. Evidence implicating GCs was provided by the next experiments in which a dose response relationship between CORT and photoreceptor survival of light damage was demonstrated. Furthermore, a convincing approach to assert the function of a molecule is to eliminate it and analyse the effects that ensure. By performing adrenalectomy mice were rendered incapable of producing CORT in response to stress and this turned out to be very deleterious to the retina as adrenalectomised mice showed significantly higher apoptosis and retinal degeneration after light damage

preceded by 10 hours CSC. As adrenalectomy on its own can induce cellular apoptosis [148], an interesting argument that could be raised is that the observed increase in apoptosis in ADX mice was an ADX effect and not a light damage effect. However, such as objection is counteracted by the fact that no difference in apoptosis was found between ADX SHC and sham SHC mice, meaning ADX on its own was not harmful to photoreceptors. Furthermore, it could be argued that the adrenal gland secretes other molecules like aldosterone and catecholamines, therefore the absence and presence of one or more of these molecules could be responsible for the deleterious effect of ADX and the stress mediated neuroprotection of damaged photoreceptors respectively. However, by injecting exogenous CORT into adrenalectomised mice the deleterious effects of adrenalectomy were rescued, clearly pointing out that CORT mediates the protective effect on photoreceptors. Data obtained after 10 hours CSC housing, CORT injection, adrenalectomy and CORT injection of adrenalectomised mice summarily confirm that the neuroprotective effect of short-term psychosocial stress is mediated by a surge in CORT.

The absence of any protective effect of CSC following NMDA mediated damage is mostly likely due to two reasons. The first is the fact that NMDA induced death was very severe so much so that a potential neuroprotective effect of short-term psychosocial stress could be concealed. Furthermore, given that CORT levels rise tremendously after 10 hours CSC, a second reason is supported by data which show that at very high concentrations (310-650 nM), CORT potentiates NMDA excitotoxicity whereas slightly elevated plasma CORT (10-90 nM) exerts neuroprotective effects against excitotoxic insults [90].

In vitro studies carried out didn’t reveal any GC effect on 661W cell apoptosis induced by serum starvation. The reason for this observation may lie in the used cell

culture model. Although 661W cells are photoreceptor derived, they are cancerous immortalized cells and do not express most of the proteins that are expressed by photoreceptors [112]. Secondly, the mode by which cellular apoptosis was induced *in vitro* was completely different from what was utilized *in vivo*.

5.3. Effect of chronic stress on photoreceptor degeneration

Although several studies have examined the deleterious effects of chronic stress in different pathologies, the effect of chronic psychosocial stress on damaged photoreceptors has not been investigated before now. Chronic stress otherwise referred to as distress results to a physiologic stress response that either persist long after stressor exposure has subsided or is continuously activated by a stressor resulting to a sustained exposure of the organism to stress hormones. After prolonged psychosocial stress (19 days), this study demonstrated that there was no protective or deleterious effect on photoreceptors when light damage is performed at the end of the active dark cycle. As CORT levels at this point in time are the same in 19 days CSC housed and SHC mice, this result is in full support of the conclusion after the first set of experiments in which CORT is indexed as the fundamental factor for photoreceptor protection. By performing light damage at the end of the light phase, a time point at which CSC housed mice are known to suffer from hypocortosolism, it was demonstrated that exposure to chronic stress could have deleterious consequences for the retina as 19 days CSC housed mice had a significantly higher light damage. In principle, this result corresponds to other studies which showed that 3 weeks chronic restraint stress or continuous exogenous administration of GCs for long duration increases vulnerability to neuronal damage [92, 93]. However, a necessary clarification to make is that, unlike in the studies cited above the deleterious effect of 19 day CSC on photoreceptors when light damage is performed at the end of the light

phase is due to less CORT levels, not a sustained CORT increase following chronic stress. This is clear as 19 day CSC housed mice illuminated at the end of the dark phase following chronic stress didn't show increased susceptibility to light damage.

5.4. The effect of CORT on photoreceptor demise

The overall conclusion that CORT is responsible for the protective effect of short-term psychosocial stress on damaged photoreceptors is in line with studies in which synthetic GC analogues triamcinolone and dexamethasone prevented both secondary and primary photoreceptor cell damage in rabbits and mice [4, 86] and others which show enhanced neuronal vulnerability to apoptosis in the absence of GCs [90].

It has been shown that GCs can bind to MRs at low concentrations or GRs at high concentrations and provide an anti apoptotic effect [149] via a wide range of mechanisms both *in vivo* and *in vitro* [150, 151]. Since the GR is expressed by all cell types in the retina [152], GCs have the possibility to mediate both receptor dependent and direct actions in the retina.

The GR can regulate genes by two main mechanisms termed type 1 and type 2. In the type 1, the activated GR interacts with transcription factors either directly by physical contact or indirectly via "bridging" and enhance transcription [153, 154] or cause inhibition [155]. Important antiapoptotic genes regulated by GCs through type 1 binding include the cyclin dependent kinase inhibitor (p21) [95], GC-inducible protein kinase-1 (SGK-1) and Mitogen-activated protein kinase phosphatase-1 (MKP-1) [156].

The type 2 mechanism is used by GCs to achieve gene inhibition of genes which do not contain any nGRE sequences or any other GR-binding sites [157]. This is possible through the transrepressive action of the GR on other transcription factors such as

activating protein-1 (AP-I) via a protein–protein interaction mechanism which is void of DNA binding. The genes involved are positively regulated by AP-1 which binds to specific AP-1 binding site target sequences within responsive promoters. AP-1 forms a complex containing several components such as (c-fos, Fra-1, c-Jun, Jun-B and Jun-D etc [158], with c-fos being an essential component of AP-I mediated light induced apoptosis in photoreceptors as it initiates mitochondrial activation of apoptosis [159].Through the type two mechanism, the GC-GR interaction has been shown to lead to the inhibition of proapoptotic c-fos thereby protecting photoreceptors from light induced apoptosis [86]. Another, transcription factor involved in apoptosis which is transrepressed by GCs is NF-KB [160], which is necessary for p53-mediated cell death [161].

Apart from the type 1 and type 2 mechanism of action, intracellular binding of GCs to the GR activates some rapid non genomic neuroprotective pathways such as the phosphoinositide 3-kinase (PI3K) pathway [95, 162] and lead to a wide range of anti apoptotic signals that occur within minutes and are insensitive to inhibitors of transcription.

GCs are also known to regulate several cellular processes like ion cycling and substrate oxidation that influence apoptosis through physicochemical interactions with cellular membranes independent of the GR [163, 164].

5.5. Müller glial activation *in vivo* and *in vitro*

There was a chance that the protective effect of short-term psychosocial stress and CORT on photoreceptors could be mediated by the ability of GCs to induce the expression of neurotrophic factors like bFGF and NGF [165, 166] which are capable of protecting photoreceptors from light damage [126]. It has been shown that there is

usually an increased GFAP expression which is indicative of Müller cell gliosis following injury or light damage to the retina [167, 168]. Such an activation of Müller cells permits them to produce and secrete neurotrophic factors [125], which delay apoptotic RGC death and prevent photoreceptor cell death in inherited retinal degenerations or following light-induced photoreceptor injury [15, 131, 169-171]. Both *in vivo* after 10 hours CSC and *in vitro* after 2 hours CORT incubation, GFAP expression was found to be up regulated. However, GFAP itself has no neuroprotective effect, so the question was whether the observed Müller cell gliosis could lead to increased neurotrophic factor secretion. For all time points investigated, none of the examined neurtrophic factors (Lif, End-2, Fgf-2, Cntf and BDNF) were found to be upregulated. This result simply points to the fact that the observed Müller cell activation doesn't seem to play any active role in the observed stress mediated protective effect on photoreceptors and is supported by the fact that the protective effect observed 15 minutes after CORT injection was not preceded by Müller cell gliosis

Though demonstrated to be of no significance in the observed neuroprotective effect, the observed activation of Müller cells following 10 hours CSC cannot simply be waved as an insignificant side event especially as the data could be replicated following 2 hours CORT incubation *in vitro*. Since no Müller cell activation was observed 15 minutes after CORT injection, both data points put together suggest that prolonged exposure to CORT may be necessary to stimulate Müller cell gliosis.

After 2 hours of Müller cell incubation with CORT, an activation of Akt phosphorylation was observed. However, it is worth noting that the time point of two hours after incubation doesn't correspond to the illumination time point *in vivo* where Akt phosphorylation was found to be elevated and protective. Summarily, these

results showing Müller activation *in vivo* and *in vitro* suggests that apart from its immediate effect on photoreceptors, a delayed effect of GCs may involve genomic actions which activate the expression of survival genes resulting to delayed processes such as glial activation and other secondary effects which could again be mediated by Akt phosphorylation.

5.6. Activation of the PI3K-Akt pathway

Independent of neurotrophic factors, GCs are known to activate the neuroprotective phosphoinositide 3-kinase (PI3-K) pathway in a ligand dependent non genomic manner leading to the activation of the serine/threonine kinase Akt [95, 162]. Akt exists in three isoforms all of which are present in the retina [172] and is a key mediator of signal transduction processes downstream of PI3-K [173, 174]. This study showed that in 10 hours CSC housed and CORT injected mice, Akt phosphorylation increased whereas it decreased following adrenalectomy. This strongly suggested that Akt phosphorylation is linked to CORT levels which in turn show a negative correlation with apoptosis. This result is in line with other studies which show an increased Akt phosphorylation in cultured neurons when they are treated with CORT for about the same duration as in this study [95]. Additionally, these results are in line with a recent study which showed that photoreceptor survival in several RP models is enhanced by PI3-K activation [175].

5.7. The neuroprotective effect of the PI3K-Akt pathway

By blocking Akt phosphorylation using triciribine, the protective effects of short-term psychosocial stress and CORT injection was lost in the triciribine-injected eye compared to the vehicle-injected fellow eye. This result ascertained that the protective effect of short-term psychosocial stress and CORT injection is mediated via an

activation of the neuroprotective PI3-Akt pathway. This results is in accordance with other studies which showed that Akt2 knock-out mice exhibit a significantly greater sensitivity to light-induced cell death than heterozygous or wild-type mice [176]. Furthermore, the importance of this pathway has been demonstrated by *in vitro* studies which show that the ability of NGF to prevent apoptosis can be inhibited by blocking the PI3-Akt pathway. This same study showed that platelet-derived growth factor prevented apoptosis of PC-12 cells expressing the wild-type PDGF receptor, but not of cells expressing a mutant receptor that failed to activate PI3-Akt kinase [177].

One of the main observations of this study is the ability of CORT to provide a neuroprotective effect on photoreceptors just 15 minutes after injection. This implies that the pathway through which this protective effect is mediated is really rapid. As such, the direct inhibitory phosphorylation of proapoptotic proteins like those of the Bcl-2 family such as BAD by Akt seems to be the most likely pathway involved in stress mediated neuroprotection of photoreceptors. The rapidity of this pathway is favoured by the fact that none of its down stream effects requires gene transcription.

Bcl-2 is normally anti apoptotic as it forms a dimmer with pro apoptotic Bax and prevents it from inducing apoptosis. Though GCs are known to cause an increased expression of Bcl-2 thereby reducing apoptosis [94], their action via the P13-Akt pathway on other Bcl-2 family proteins like BAD is a non genomic inhibitory one. BAD a heterodimeric partner for Bcl-2 is known to displace Bax from its dimmer with Bcl-2 and promote cell death [178]. When GCs induce Akt phosphorylation this can lead to BAD phosphorylation and inhibition which prevents it from dimerising with Bcl-2 proteins thereby blocking the release of the apoptotic signal protein Bax [179]. Another antiapoptotic molecule whose expression is increased by GCs but on

which GCs also exhibit non genomic actions is the cyclin-dependent kinase inhibitor (p21) [95], in this case unlike the case of Bcl-2 family proteins which are inhibited by phosphorylation, CORT activation of the P13-Akt kinase pathway leads to a phosphorylation and activation of p21 thereby permitting it to regulate caspases [180]. Additionally, once activated by CORT, Akt has the ability to phosphorylate and diminish the proteolytic activity of caspases [181].

A second non genomic mechanism through which GC activation of Akt inhibits apoptosis is through its interaction with IκBkinase (IKK). Although Akt can phosphorylate and activate NFκB through IKK in a non genomic manner, this pathway is relatively slower as it necessitates more intermediates and its downstream effects require gene transcription. In the context of the rapidity of the observed CORT protective effect, it is less likely for this pathway to take precedence over the previously described direct inhibition of antiapoptotic proteins by PI3-Akt.

The NFκB transcription factor is normally sequestered in the cytoplasm by proteins of the IκB family and gets translocated to the nucleus upon activation. Even though GCs have the ability to transrepress NFκB expression [160], an additional way GCs interact with NFκB is via Akt. When GCs activate Akt, it interacts with IKK and causes it to phosphorylate and activate the p65 subunit of the transcription factor NFκB [182]. Activated NFκB is known to activate the transcription of anti-apoptotic members of the Inhibitor of apoptosis (IAP) family (c-IAP1, c-IAP2, XIAP and surviving) which then inhibit various pro-apoptotic proteins through cell-cycle regulation, protein degradation and caspase independent signal transduction cascades [183].

5.8. Time lapse and specificity of the protective effect of CORT

Amongst the most salient inferences from this study is the necessity of an increase in CORT levels before light damage actually begins. This is logical as data show that CORT levels rise significantly following light damage [86]. The relevance of Wenzel´s data for this study is that, CORT levels rise significantly in CSC housed as well as SHC/uninjected mice upon exposure to light, however only 10 hours CSC housed and CORT injected mice got protected. The study further showed that injecting CORT just 15 minutes prior to light damage provided a protective effect which is as intense as that observed in short-term stressed mice where CORT levels rise for an about 10 hour duration. The rapid action of injected CORT favours the argument for a direct non genomic effect of CORT and is supported by the fact GCs have previously been shown to have direct effects on photoreceptors [184].This is consolidated by the fact that the activation of the PI3-Akt pathway was shown to be necessary for this effect.

Another important inference from this study is that the observed neuroprotection is mostly likely occurs on photoreceptors directly. First of all the rapidity of the protective effect makes the involvement of other cell types very less likely. Moreso, the data dismisses any possible involvement of Müller cell which are the main cell type that provide support to photoreceptors. First line evidence in this direction is provided by data which show that the observed Müller cell gliosis is not followed by a secretion of neurotrophic factors. Secondly, there was no increase in GFAP mRNA 15 minutes after CORT injection which is a time point at which CORT was shown to already be able to mediate neuroprotection. These two data points make any arguments in favour of Müller cell involvement in the neuroprotective effect of CORT

unfounded. Put together, the rapid nature of the CORT effect and the non involvement of Müller cells strongly suggest a direct effect on photoreceptors.

5.9. Implications of this study for retinal degeneration patients

The conclusions arrived at from this study have several possible implications for patients of retinal degenerative diseases involving progressive loss of photoreceptors (RP and AMD).

First and foremost, the study demonstrates that a short-term stress (acute) could have beneficial effects for patients. However, the stress episodes need to be considerably spaced to allow for optimal and sustained rise and fall in CORT levels that allow for an activation and deactivation of the GR without desensitising it, thereby permitting it to effect Akt phosphorylation when CORT levels rise subsequently.

Unlike with short-term stress, this study shows that chronic stress has possible negative effects for retinal degeneration patients. Chronic stress leads to hypocortisolism via diverse effects including an attenuation of the HPA axis (less CORT release) and a down regulation of GRs which conduces to decreased CORT potency [185, 186]. Both effects are in disfavour of GC mediated protection of photoreceptors and so they could probably be unhealthy for a degenerating retina. This can be elaborated by examining the effect of chronic stress on gradual retinal degeneration in the VPP mouse. The VPP mouse overexpresses three point mutations in the murine opsin gene that had been identified in patients suffering from RP. This over expression leads to moderate degeneration of photoreceptor cells that starts approximately four weeks after birth. During the following weeks retinal damage increases continuously and leads at the age of two months to a substantial reduction in

the number of photoreceptors and only a few photreceptors remain at the age of seven months [187, 188].

Another important deduction from this study is that, for retinal degeneration patients , an additional abnormally in the functioning of the GR as in hereditary or acquired GC insensitivity [189, 190] could promote a faster progression of their disease. On the other hand, for patients suffering from GC hypersensitivity, this could paradoxically be an advantage at least in the context of their progressive loss of sight.

5.10. Summary and conclusion

Living together with members of same or different species in the same ecological niche is a common phenomenon in the animal kingdom. As such, several relationships such as predator-prey, boss-employee, alongside monumental events such as bereavement and issues like divorce etc make psychosocial stress extensively common in humans and other animals. Thus, psychosocial stress provides a relevant model to investigate the consequences of stress for the body especially in disease states. To the best of our knowledge, the influence of psychosocial stress on retinal degeneration has not been investigated this far.

Using a well established psychosocial stress paradigm, we investigated the effect of both acute and chronic psychosocial stress on induced photoreceptor apoptosis which is a predicament for neurons in many retinal degenerative diseases. Firstly, we identified beneficial neuroprotective effects of short-term psychosocial stress on damaged photoreceptors. Secondly, in line with many other studies showing diverse deleterious effects of chronic stress, we showed that prolonged psychosocial stress could have adverse effects for damaged photoreceptors. In subsequent experiments,

we could establish beyond doubt that, the neuroprotective effect of psychosocial stress is mediated through a CORT surge which elicits an activation of the PI3-Akt pathway via a rapid GR based direct action on photoreceptors themselves.

Overall this study suggests that for a retinal degeneration patient (RP and AMD), normal life with occasional rise in CORT following adequately spaced stress episodes could have beneficial effects compared to a quiet life where CORT is maintained at basal levels. However, a quiet life is in turn better than a chronically stressful life which conduces to deleterious hypocortisolism or acquired GC insensitivitity.

SUPPLEMENTARY

5.11. References

1. Slominski, A., *A nervous breakdown in the skin: stress and the epidermal barrier.* J Clin Invest, 2007. **117**(11): p. 3166-9.

2. Foulds, W.S., *The retinal-pigment epithelial interface.* Br J Ophthalmol, 1979. **63**(2): p. 71-84.

3. Maeda, H., et al., *Apoptosis of photoreceptor cells in ornithine-induced retinopathy.* Graefes Arch Clin Exp Ophthalmol, 1998. **236**(3): p. 207-12.

4. Bhisitkul, R.B., et al., *Neuroprotective effect of intravitreal triamcinolone acetonide against photoreceptor apoptosis in a rabbit model of subretinal hemorrhage.* Invest Ophthalmol Vis Sci, 2008. **49**(9): p. 4071-7.

5. Foster, R.G., et al., *Circadian photoreception in the retinally degenerate mouse (rd/rd).* J Comp Physiol A, 1991. **169**(1): p. 39-50.

6. Resnikoff, S., et al., *Global data on visual impairment in the year 2002.* Bull World Health Organ, 2004. **82**(11): p. 844-51.

7. Mitchell, P., W. Smith, and J.J. Wang, *Iris color, skin sun sensitivity, and age-related maculopathy. The Blue Mountains Eye Study.* Ophthalmology, 1998. **105**(8): p. 1359-63.

8. Lange, C., et al., *Retina-specific activation of a sustained hypoxia-like response leads to severe retinal degeneration and loss of vision.* Neurobiol Dis. **41**(1): p. 119-30.

9. Portera-Cailliau, C., et al., *Apoptotic photoreceptor cell death in mouse models of retinitis pigmentosa.* Proc Natl Acad Sci U S A, 1994. **91**(3): p. 974-8.

10. LaVail, M.M., et al., *Multiple growth factors, cytokines, and neurotrophins rescue photoreceptors from the damaging effects of constant light.* Proc Natl Acad Sci U S A, 1992. **89**(23): p. 11249-53.

11. Gao, H. and J.G. Hollyfield, *Aging of the human retina. Differential loss of neurons and retinal pigment epithelial cells.* Invest Ophthalmol Vis Sci, 1992. **33**(1): p. 1-17.

12. Curcio, C.A., et al., *Aging of the human photoreceptor mosaic: evidence for selective vulnerability of rods in central retina.* Invest Ophthalmol Vis Sci, 1993. **34**(12): p. 3278-96.

13. Boughman, J.A., P.M. Conneally, and W.E. Nance, *Population genetic studies of retinitis pigmentosa.* Am J Hum Genet, 1980. **32**(2): p. 223-35.

14. Bunker, C.H., et al., *Prevalence of retinitis pigmentosa in Maine.* Am J Ophthalmol, 1984. **97**(3): p. 357-65.

15. Hartong, D.T., E.L. Berson, and T.P. Dryja, *Retinitis pigmentosa.* Lancet, 2006. **368**(9549): p. 1795-809.

16. Hong, D.H., et al., *A retinitis pigmentosa GTPase regulator (RPGR)-deficient mouse model for X-linked retinitis pigmentosa (RP3).* Proc Natl Acad Sci U S A, 2000. **97**(7): p. 3649-54.

17. Liu, H., et al., *Severe retinal degeneration caused by a novel rhodopsin mutation.* Invest Ophthalmol Vis Sci. **51**(2): p. 1059-65.

18. Boughman, J.A., M. Vernon, and K.A. Shaver, *Usher syndrome: definition and estimate of prevalence from two high-risk populations.* J Chronic Dis, 1983. **36**(8): p. 595-603.

19. Maugeri, A., et al., *Mutations in the ABCA4 (ABCR) gene are the major cause of autosomal recessive cone-rod dystrophy.* Am J Hum Genet, 2000. **67**(4): p. 960-6.

20. Haines, J.L., et al., *Complement factor H variant increases the risk of age-related macular degeneration.* Science, 2005. **308**(5720): p. 419-21.

21. Hageman, G.S., et al., *A common haplotype in the complement regulatory gene factor H (HF1/CFH) predisposes individuals to age-related macular degeneration.* Proc Natl Acad Sci U S A, 2005. **102**(20): p. 7227-32.

22. Kortvely, E., et al., *ARMS2 is a constituent of the extracellular matrix providing a link between familial and sporadic age-*

related macular degenerations. Invest Ophthalmol Vis Sci. **51**(1): p. 79-88.

23. Mahley, R.W. and S.C. Rall, Jr., *Apolipoprotein E: far more than a lipid transport protein.* Annu Rev Genomics Hum Genet, 2000. **1**: p. 507-37.

24. Cideciyan, A.V., et al., *Disease sequence from mutant rhodopsin allele to rod and cone photoreceptor degeneration in man.* Proc Natl Acad Sci U S A, 1998. **95**(12): p. 7103-8.

25. Heckenlively, J.R., J.A. Rodriguez, and S.P. Daiger, *Autosomal dominant sectoral retinitis pigmentosa. Two families with transversion mutation in codon 23 of rhodopsin.* Arch Ophthalmol, 1991. **109**(1): p. 84-91.

26. LaVail, M.M., et al., *Increased susceptibility to constant light in nr and pcd mice with inherited retinal degenerations.* Invest Ophthalmol Vis Sci, 1999. **40**(5): p. 1020-4.

27. Wang, M., et al., *Expression of a mutant opsin gene increases the susceptibility of the retina to light damage.* Vis Neurosci, 1997. **14**(1): p. 55-62.

28. Organisciak, D.T., et al., *Light-induced damage in the retina: differential effects of dimethylthiourea on photoreceptor survival, apoptosis and DNA oxidation.* Photochem Photobiol, 1999. **70**(2): p. 261-8.

29. Keller, C., et al., *Protective effect of halothane anesthesia on retinal light damage: inhibition of metabolic rhodopsin regeneration.* Invest Ophthalmol Vis Sci, 2001. **42**(2): p. 476-80.

30. Lamb, T.D. and E.N. Pugh, Jr., *Dark adaptation and the retinoid cycle of vision.* Prog Retin Eye Res, 2004. **23**(3): p. 307-80.

31. Hao, W., et al., *Evidence for two apoptotic pathways in light-induced retinal degeneration.* Nat Genet, 2002. **32**(2): p. 254-60.

32. Sieving, P.A., et al., *Inhibition of the visual cycle in vivo by 13-cis retinoic acid protects from light damage and provides a mechanism for night blindness in isotretinoin therapy.* Proc Natl Acad Sci U S A, 2001. **98**(4): p. 1835-40.

33. Crabb, J.W., et al., *Drusen proteome analysis: an approach to the etiology of age-related macular degeneration.* Proc Natl Acad Sci U S A, 2002. **99**(23): p. 14682-7.

34. Gu, X., et al., *Carboxyethylpyrrole protein adducts and autoantibodies, biomarkers for age-related macular degeneration.* J Biol Chem, 2003. **278**(43): p. 42027-35.

35. Scholl, H.P., et al., *Systemic complement activation in age-related macular degeneration.* PLoS One, 2008. **3**(7): p. e2593.

36. Lin, J.H., et al., *IRE1 signaling affects cell fate during the unfolded protein response.* Science, 2007. **318**(5852): p. 944-9.

37. Padnick-Silver, L., et al., *Retinal oxygenation and oxygen metabolism in Abyssinian cats with a hereditary retinal degeneration.* Invest Ophthalmol Vis Sci, 2006. **47**(8): p. 3683-9.

38. McMahon, A. and W. Kedzierski, *Polyunsaturated very-long-chain C28-C36 fatty acids and retinal physiology.* Br J Ophthalmol. **94**(9): p. 1127-32.

39. Bernstein, P.S., et al., *Diverse macular dystrophy phenotype caused by a novel complex mutation in the ELOVL4 gene.* Invest Ophthalmol Vis Sci, 2001. **42**(13): p. 3331-6.

40. West, J.D. and L.J. Marnett, *Endogenous reactive intermediates as modulators of cell signaling and cell death.* Chem Res Toxicol, 2006. **19**(2): p. 173-94.

41. Wolfrum, U. and A. Schmitt, *Rhodopsin transport in the membrane of the connecting cilium of mammalian photoreceptor cells.* Cell Motil Cytoskeleton, 2000. **46**(2): p. 95-107.

42. Mockel, A., et al., *Pharmacological modulation of the retinal unfolded protein response in Bardet-Biedl syndrome reduces apoptosis and preserves light detection ability.* J Biol Chem.

43. Ron, D. and P. Walter, *Signal integration in the endoplasmic reticulum unfolded protein response.* Nat Rev Mol Cell Biol, 2007. **8**(7): p. 519-29.

44. Halliwell, B., ***Free radicals in Biology and Medicine 4th edition***. Oxford univ

2007.

45. Chang, G.Q., Y. Hao, and F. Wong, *Apoptosis: final common pathway of photoreceptor death in rd, rds, and rhodopsin mutant mice.* Neuron, 1993. **11**(4): p. 595-605.

46. Wong, F., *Photoreceptor apoptosis in animal models. Implications for retinitis pigmentosa research.* Arch Ophthalmol, 1995. **113**(10): p. 1245-7.

47. Dunaief, J.L., et al., *The role of apoptosis in age-related macular degeneration.* Arch Ophthalmol, 2002. **120**(11): p. 1435-42.

48. Wyllie, A.H., *Glucocorticoid-induced thymocyte apoptosis is associated with endogenous endonuclease activation.* Nature, 1980. **284**(5756): p. 555-6.

49. Gavrieli, Y., Y. Sherman, and S.A. Ben-Sasson, *Identification of programmed cell death in situ via specific labeling of nuclear DNA fragmentation.* J Cell Biol, 1992. **119**(3): p. 493-501.

50. Petrin, D., et al., *Structural and functional protection of photoreceptors from MNU-induced retinal degeneration by the X-linked inhibitor of apoptosis.* Invest Ophthalmol Vis Sci, 2003. **44**(6): p. 2757-63.

51. Dragunow, M., et al., *In situ evidence for DNA fragmentation in Huntington's disease striatum and Alzheimer's disease temporal lobes.* Neuroreport, 1995. **6**(7): p. 1053-7.

52. Troost, D., et al., *Apoptosis in amyotrophic lateral sclerosis is not restricted to motor neurons. Bcl-2 expression is increased in unaffected post-central gyrus.* Neuropathol Appl Neurobiol, 1995. **21**(6): p. 498-504.

53. Li, Y., et al., *Temporal profile of in situ DNA fragmentation after transient middle cerebral artery occlusion in the rat.* J Cereb Blood Flow Metab, 1995. **15**(3): p. 389-97.

54. Kerr, J.F., A.H. Wyllie, and A.R. Currie, *Apoptosis: a basic biological phenomenon with wide-ranging implications in tissue kinetics.* Br J Cancer, 1972. **26**(4): p. 239-57.

55. Kaufmann, S.H., et al., *Analysis of caspase activation during apoptosis.* Curr Protoc Cell Biol, 2001. **Chapter 18**: p. Unit 18 2.

56. Wenzel, A., et al., *Molecular mechanisms of light-induced photoreceptor apoptosis and neuroprotection for retinal degeneration.* Prog Retin Eye Res, 2005. **24**(2): p. 275-306.

57. Cruickshanks, K.J., R. Klein, and B.E. Klein, *Sunlight and age-related macular degeneration. The Beaver Dam Eye Study.* Arch Ophthalmol, 1993. **111**(4): p. 514-8.

58. Taylor, H.R., et al., *Visible light and risk of age-related macular degeneration.* Trans Am Ophthalmol Soc, 1990. **88**: p. 163-73; discussion 173-8.

59. Simons, K., *Artificial light and early-life exposure in age-related macular degeneration and in cataractogenic phototoxicity.* Arch Ophthalmol, 1993. **111**(3): p. 297-8.

60. Bessero, A.C. and P.G. Clarke, *Neuroprotection for optic nerve disorders.* Curr Opin Neurol. **23**(1): p. 10-5.

61. Lommer, D. and H.P. Wolff, *Stimulation of the in vitro biosynthesis of corticosteroids by angiotensin II.* Experientia, 1966. **22**(10): p. 699-700.

62. Dhabhar, F.S. and B.S. McEwen, *Acute stress enhances while chronic stress suppresses cell-mediated immunity in vivo: a potential role for leukocyte trafficking.* Brain Behav Immun, 1997. **11**(4): p. 286-306.

63. Santos, I.N. and R.C. Spadari-Bratfisch, *Stress and cardiac beta adrenoceptors.* Stress, 2006. **9**(2): p. 69-84.

64. Reber, S.O., et al., *Adrenal insufficiency and colonic inflammation after a novel chronic psycho-social stress paradigm in mice: implications and mechanisms.* Endocrinology, 2007. **148**(2): p. 670-82.

65. Padgett, D.A., P.T. Marucha, and J.F. Sheridan, *Restraint stress slows cutaneous wound healing in mice.* Brain Behav Immun, 1998. **12**(1): p. 64-73.

66. Swiergiel, A.H., I.L. Leskov, and A.J. Dunn, *Effects of chronic and acute stressors and CRF on depression-like behavior in mice.* Behav Brain Res, 2008. **186**(1): p. 32-40.

67. Berton, O., et al., *Differential effects of social stress on central serotonergic activity and emotional reactivity in Lewis and spontaneously hypertensive rats.* Neuroscience, 1998. **82**(1): p. 147-59.

68. Biondi, M. and L.G. Zannino, *Psychological stress, neuroimmunomodulation, and susceptibility to infectious diseases in animals and man: a review.* Psychother Psychosom, 1997. **66**(1): p. 3-26.

69. Blanchard, D.C., et al., *Visible burrow system as a model of chronic social stress: behavioral and neuroendocrine correlates.* Psychoneuroendocrinology, 1995. **20**(2): p. 117-34.

70. Blanchard, R.J., K.J. Flannelly, and D.C. Blanchard, *Life-span studies of dominance and aggression in established colonies of laboratory rats.* Physiol Behav, 1988. **43**(1): p. 1-7.

71. Uschold-Schmidt, N., et al., *Chronic psychosocial stress results in sensitization of the HPA axis to acute heterotypic stressors despite a reduction of adrenal in vitro ACTH responsiveness.* Psychoneuroendocrinology. **37**(10): p. 1676-87.

72. McEwen, B.S., E.R. De Kloet, and W. Rostene, *Adrenal steroid receptors and actions in the nervous system.* Physiol Rev, 1986. **66**(4): p. 1121-88.

73. Keller-Wood, M.E. and M.F. Dallman, *Corticosteroid inhibition of ACTH secretion.* Endocr Rev, 1984. **5**(1): p. 1-24.

74. Hauger, R.L., et al., *Corticotropin-releasing factor receptors and pituitary adrenal responses during immobilization stress.* Endocrinology, 1988. **123**(1): p. 396-405.

75. Holmes, M.C., et al., *Magnocellular axons in passage through the median eminence release vasopressin.* Nature, 1986. **319**(6051): p. 326-9.

76. Andrews, R.C. and B.R. Walker, *Glucocorticoids and insulin resistance: old hormones, new targets.* Clin Sci (Lond), 1999. **96**(5): p. 513-23.

77. Fain, J.N., J.H. Ihle, and S.W. Bahouth, *Stimulation of lipolysis but not of leptin release by growth hormone is abolished in adipose tissue from Stat5a and b knockout mice.* Biochem Biophys Res Commun, 1999. **263**(1): p. 201-5.

78. Sebaldt, R.J., et al., *Inhibition of eicosanoid biosynthesis by glucocorticoids in humans.* Proc Natl Acad Sci U S A, 1990. **87**(18): p. 6974-8.

79. Almawi, W.Y., et al., *Regulation of cytokine and cytokine receptor expression by glucocorticoids.* J Leukoc Biol, 1996. **60**(5): p. 563-72.

80. Buttgereit, F. and A. Scheffold, *Rapid glucocorticoid effects on immune cells.* Steroids, 2002. **67**(6): p. 529-34.

81. Oakley, R.H., et al., *The dominant negative activity of the human glucocorticoid receptor beta isoform. Specificity and mechanisms of action.* J Biol Chem, 1999. **274**(39): p. 27857-66.

82. Geley, S., et al., *Genes mediating glucocorticoid effects and mechanisms of their regulation.* Rev Physiol Biochem Pharmacol, 1996. **128**: p. 1-97.

83. Northrop, J.P., G.R. Crabtree, and P.S. Mattila, *Negative regulation of interleukin 2 transcription by the glucocorticoid receptor.* J Exp Med, 1992. **175**(5): p. 1235-45.

84. Paliogianni, F. and D.T. Boumpas, *Glucocorticoids regulate calcineurin-dependent trans-activating pathways for interleukin-2 gene transcription in human T lymphocytes.* Transplantation, 1995. **59**(9): p. 1333-9.

85. Cox, G. and R.C. Austin, *Dexamethasone-induced suppression of apoptosis in human neutrophils requires continuous stimulation of new protein synthesis.* J Leukoc Biol, 1997. **61**(2): p. 224-30.

86. Wenzel, A., et al., *Prevention of photoreceptor apoptosis by activation of the glucocorticoid receptor.* Invest Ophthalmol Vis Sci, 2001. **42**(7): p. 1653-9.

87. Bailly-Maitre, B., et al., *Dexamethasone inhibits spontaneous apoptosis in primary cultures of human and rat hepatocytes via Bcl-2 and Bcl-xL induction.* Cell Death Differ, 2001. **8**(3): p. 279-88.

88. Smets, L.A., G. Salomons, and J. van den Berg, *Glucocorticoid induced apoptosis in leukemia.* Adv Exp Med Biol, 1999. **457**: p. 607-14.

89. Sapolsky, R.M., *Stress, Glucocorticoids, and Damage to the Nervous System: The Current State of Confusion.* Stress, 1996. **1**(1): p. 1-19.

90. Abraham, I., et al., *Chronic corticosterone administration dose-dependently modulates Abeta(1-42)- and NMDA-induced neurodegeneration in rat magnocellular nucleus basalis.* J Neuroendocrinol, 2000. **12**(6): p. 486-94.

91. Sapolsky, R.M. and W.A. Pulsinelli, *Glucocorticoids potentiate ischemic injury to neurons: therapeutic implications.* Science, 1985. **229**(4720): p. 1397-400.

92. Hibberd, C., J.L. Yau, and J.R. Seckl, *Glucocorticoids and the ageing hippocampus.* J Anat, 2000. **197 Pt 4**: p. 553-62.

93. Arbel, I., et al., *The effects of long-term corticosterone administration on hippocampal morphology and cognitive performance of middle-aged rats.* Brain Res, 1994. **657**(1-2): p. 227-35.

94. Schorr, K. and P.A. Furth, *Induction of bcl-xL expression in mammary epithelial cells is glucocorticoid-dependent but not signal transducer and activator of transcription 5-dependent.* Cancer Res, 2000. **60**(21): p. 5950-3.

95. Harms, C., et al., *Phosphatidylinositol 3-Akt-kinase-dependent phosphorylation of p21(Waf1/Cip1) as a novel mechanism of neuroprotection by glucocorticoids.* J Neurosci, 2007. **27**(17): p. 4562-71.

96. Kulik, G. and M.J. Weber, *Akt-dependent and -independent survival signaling pathways utilized by insulin-like growth factor I.* Mol Cell Biol, 1998. **18**(11): p. 6711-8.

97. Downward, J., *PI 3-kinase, Akt and cell survival.* Semin Cell Dev Biol, 2004. **15**(2): p. 177-82.

98. Kandasamy, K. and R.K. Srivastava, *Role of the phosphatidylinositol 3'-kinase/PTEN/Akt kinase pathway in tumor necrosis factor-related apoptosis-inducing ligand-induced*

apoptosis in non-small cell lung cancer cells. Cancer Res, 2002. **62**(17): p. 4929-37.

99. Steptoe, A., et al., *Cardiovascular risk and responsivity to mental stress: the influence of age, gender and risk factors.* J Cardiovasc Risk, 1996. **3**(1): p. 83-93.

100. Rozanski, A., J.A. Blumenthal, and J. Kaplan, *Impact of psychological factors on the pathogenesis of cardiovascular disease and implications for therapy.* Circulation, 1999. **99**(16): p. 2192-217.

101. Siegrist, J., et al., *Depressive symptoms and psychosocial stress at work among older employees in three continents.* Global Health. **8**(1): p. 27.

102. Djordjevic, J., G. Cvijic, and V. Davidovic, *Different activation of ACTH and corticosterone release in response to various stressors in rats.* Physiol Res, 2003. **52**(1): p. 67-72.

103. Danciger, M., et al., *A QTL on distal chromosome 3 that influences the severity of light-induced damage to mouse photoreceptors.* Mamm Genome, 2000. **11**(6): p. 422-7.

104. Noell, W.K., et al., *Retinal damage by light in rats.* Invest Ophthalmol, 1966. **5**(5): p. 450-73.

105. Li, Y., C.L. Schlamp, and R.W. Nickells, *Experimental induction of retinal ganglion cell death in adult mice.* Invest Ophthalmol Vis Sci, 1999. **40**(5): p. 1004-8.

106. Siliprandi, R., et al., *N-methyl-D-aspartate-induced neurotoxicity in the adult rat retina.* Vis Neurosci, 1992. **8**(6): p. 567-73.

107. Ueki, Y., et al., *STAT3 activation in photoreceptors by leukemia inhibitory factor is associated with protection from light damage.* J Neurochem, 2008. **105**(3): p. 784-96.

108. Chomczynski, P. and N. Sacchi, *Single-step method of RNA isolation by acid guanidinium thiocyanate-phenol-chloroform extraction.* Anal Biochem, 1987. **162**(1): p. 156-9.

109. Livak, K.J. and T.D. Schmittgen, *Analysis of relative gene expression data using real-time quantitative PCR and the 2(-Delta Delta C(T)) Method.* Methods, 2001. **25**(4): p. 402-8.

110. Laemmli, U.K., *Cleavage of structural proteins during the assembly of the head of bacteriophage T4.* Nature, 1970. **227**(5259): p. 680-5.

111. Hicks, D. and Y. Courtois, *The growth and behaviour of rat retinal Muller cells in vitro. 1. An improved method for isolation and culture.* Exp Eye Res, 1990. **51**(2): p. 119-29.

112. Tan, E., et al., *Expression of cone-photoreceptor-specific antigens in a cell line derived from retinal tumors in transgenic mice.* Invest Ophthalmol Vis Sci, 2004. **45**(3): p. 764-8.

113. Zhang, H., et al., *Apoptosis and differentiation induced by staurosporine in granulosa tumor cells is coupled with activation of JNK and suppression of p38 MAPK.* Int J Oncol, 2005. **26**(6): p. 1575-80.

114. Friedman, S.B. and R. Ader, *Parameters Relevant to the Experimental Production of "Stress" in the Mouse.* Psychosom Med, 1965. **27**: p. 27-30.

115. Harbuz, M.S. and S.L. Lightman, *Stress and the hypothalamo-pituitary-adrenal axis: acute, chronic and immunological activation.* J Endocrinol, 1992. **134**(3): p. 327-39.

116. Ulrich-Lai, Y.M., et al., *Chronic stress induces adrenal hyperplasia and hypertrophy in a subregion-specific manner.* Am J Physiol Endocrinol Metab, 2006. **291**(5): p. E965-73.

117. Silberman, D.M., M.R. Wald, and A.M. Genaro, *Acute and chronic stress exert opposing effects on antibody responses associated with changes in stress hormone regulation of T-lymphocyte reactivity.* J Neuroimmunol, 2003. **144**(1-2): p. 53-60.

118. LaVail, M.M., et al., *Genetic regulation of light damage to photoreceptors.* Invest Ophthalmol Vis Sci, 1987. **28**(7): p. 1043-8.

119. Redmond, T.M., et al., *Rpe65 is necessary for production of 11-cis-vitamin A in the retinal visual cycle.* Nat Genet, 1998. **20**(4): p. 344-51.

120. Bonfoco, E., et al., *Apoptosis and necrosis: two distinct events induced, respectively, by mild and intense insults with N-methyl-*

D-aspartate or nitric oxide/superoxide in cortical cell cultures. Proc Natl Acad Sci U S A, 1995. **92**(16): p. 7162-6.

121. Gomez-Vicente, V., M. Donovan, and T.G. Cotter, *Multiple death pathways in retina-derived 661W cells following growth factor deprivation: crosstalk between caspases and calpains.* Cell Death Differ, 2005. **12**(7): p. 796-804.

122. Bringmann, A., et al., *Muller cells in the healthy and diseased retina.* Prog Retin Eye Res, 2006. **25**(4): p. 397-424.

123. Lewis, G.P. and S.K. Fisher, *Up-regulation of glial fibrillary acidic protein in response to retinal injury: its potential role in glial remodeling and a comparison to vimentin expression.* Int Rev Cytol, 2003. **230**: p. 263-90.

124. Rattner, A. and J. Nathans, *The genomic response to retinal disease and injury: evidence for endothelin signaling from photoreceptors to glia.* J Neurosci, 2005. **25**(18): p. 4540-9.

125. Joly, S., et al., *Leukemia inhibitory factor extends the lifespan of injured photoreceptors in vivo.* J Neurosci, 2008. **28**(51): p. 13765-74.

126. Faktorovich, E.G., et al., *Basic fibroblast growth factor and local injury protect photoreceptors from light damage in the rat.* J Neurosci, 1992. **12**(9): p. 3554-67.

127. Heiduschka, P. and S. Thanos, *Cortisol promotes survival and regeneration of axotomised retinal ganglion cells and enhances effects of aurintricarboxylic acid.* Graefes Arch Clin Exp Ophthalmol, 2006. **244**(11): p. 1512-21.

128. Seitz, R., et al., *Norrin mediates neuroprotective effects on retinal ganglion cells via activation of the Wnt/beta-catenin signaling pathway and the induction of neuroprotective growth factors in Muller cells.* J Neurosci. **30**(17): p. 5998-6010.

129. Reber, S.O. and I.D. Neumann, *Defensive behavioral strategies and enhanced state anxiety during chronic subordinate colony housing are accompanied by reduced hypothalamic vasopressin, but not oxytocin, expression.* Ann N Y Acad Sci, 2008. **1148**: p. 184-95.

130. Reber, S.O., et al., *Aggravation of DSS-induced colitis after chronic subordinate colony (CSC) housing is partially mediated by adrenal mechanisms.* Stress, 2008. **11**(3): p. 225-34.

131. Reme, C.E., et al., *Apoptotic cell death in retinal degenerations.* Prog Retin Eye Res, 1998. **17**(4): p. 443-64.

132. Wenzel, A., et al., *The Rpe65 Leu450Met variation increases retinal resistance against light-induced degeneration by slowing rhodopsin regeneration.* J Neurosci, 2001. **21**(1): p. 53-8.

133. Anisman, H., et al., *Corticotropin releasing hormone receptor alterations elicited by acute and chronic unpredictable stressor challenges in stressor-susceptible and resilient strains of mice.* Behav Brain Res, 2007. **181**(2): p. 180-90.

134. Stefanski, V., G. Knopf, and S. Schulz, *Long-term colony housing in Long Evans rats: immunological, hormonal, and behavioral consequences.* J Neuroimmunol, 2001. **114**(1-2): p. 122-30.

135. Moles, A., et al., *Psychosocial stress affects energy balance in mice: modulation by social status.* Psychoneuroendocrinology, 2006. **31**(5): p. 623-33.

136. Rohleder, N., et al., *The psychosocial stress-induced increase in salivary alpha-amylase is independent of saliva flow rate.* Psychophysiology, 2006. **43**(6): p. 645-52.

137. Nakade, Y., et al., *Restraint stress stimulates colonic motility via central corticotropin-releasing factor and peripheral 5-HT3 receptors in conscious rats.* Am J Physiol Gastrointest Liver Physiol, 2007. **292**(4): p. G1037-44.

138. Gamallo, A., et al., *Stress adaptation and adrenal activity in isolated and crowded rats.* Physiol Behav, 1986. **36**(2): p. 217-21.

139. Zelena, D., et al., *Role of hypothalamic inputs in maintaining pituitary-adrenal responsiveness in repeated restraint.* Am J Physiol Endocrinol Metab, 2003. **285**(5): p. E1110-7.

140. Young, E.A. and H. Akil, *Corticotropin-releasing factor stimulation of adrenocorticotropin and beta-endorphin release: effects of acute and chronic stress.* Endocrinology, 1985. **117**(1): p. 23-30.

141. Grimee, R. and E. Wulfert, *Acute stress in rats produces a rapid and sustained increase in prostacyclin production in aortic tissue: dependence on corticosterone.* Life Sci, 1995. **57**(1): p. 69-81.

142. Ljubica, D.S.A.a.G., *ACTIVITY OF PITUITARY-ADRENAL AXIS IN RATS CHRONICALLY EXPOSED TO DIFFERENT*

STRESSORS. Acta Veterinaria (Beograd), , 2005. **Vol. 55.** (No. 2-3): p. 121-129.

143. Romero, L.M., *Seasonal changes in plasma glucocorticoid concentrations in free-living vertebrates.* Gen Comp Endocrinol, 2002. **128**(1): p. 1-24.

144. Sapolsky, R.M., L.M. Romero, and A.U. Munck, *How do glucocorticoids influence stress responses? Integrating permissive, suppressive, stimulatory, and preparative actions.* Endocr Rev, 2000. **21**(1): p. 55-89.

145. Adzic, M., et al., *Acute or chronic stress induce cell compartment-specific phosphorylation of glucocorticoid receptor and alter its transcriptional activity in Wistar rat brain.* J Endocrinol, 2009. **202**(1): p. 87-97.

146. McEwen, B.S., *Plasticity of the hippocampus: adaptation to chronic stress and allostatic load.* Ann N Y Acad Sci, 2001. **933**: p. 265-77.

147. McEwen, B.S. and A.M. Magarinos, *Stress and hippocampal plasticity: implications for the pathophysiology of affective disorders.* Hum Psychopharmacol, 2001. **16**(S1): p. S7-S19.

148. Sloviter, R.S., E. Dean, and S. Neubort, *Electron microscopic analysis of adrenalectomy-induced hippocampal granule cell degeneration in the rat: apoptosis in the adult central nervous system.* J Comp Neurol, 1993. **330**(3): p. 337-51.

149. Almeida, O.F., et al., *Subtle shifts in the ratio between pro- and antiapoptotic molecules after activation of corticosteroid receptors decide neuronal fate.* FASEB J, 2000. **14**(5): p. 779-90.

150. Hammer, S., et al., *Glucocorticoids mediate differential anti-apoptotic effects in human fibroblasts and keratinocytes via*

sphingosine-1-phosphate formation. J Cell Biochem, 2004. **91**(4): p. 840-51.

151. Cox, G., *Glucocorticoid treatment inhibits apoptosis in human neutrophils. Separation of survival and activation outcomes.* J Immunol, 1995. **154**(9): p. 4719-25.

152. Gorovits, R., et al., *Developmental changes in the expression and compartmentalization of the glucocorticoid receptor in embryonic retina.* Proc Natl Acad Sci U S A, 1994. **91**(11): p. 4786-90.

153. Tsai, M.J. and B.W. O'Malley, *Molecular mechanisms of action of steroid/thyroid receptor superfamily members.* Annu Rev Biochem, 1994. **63**: p. 451-86.

154. Bastian, L.S. and S.K. Nordeen, *Concerted stimulation of transcription by glucocorticoid receptors and basal transcription factors: limited transcriptional synergism suggests mediation by coactivators/adaptors.* Mol Endocrinol, 1991. **5**(5): p. 619-27.

155. Drouin, J., et al., *Novel glucocorticoid receptor complex with DNA element of the hormone-repressed POMC gene.* EMBO J, 1993. **12**(1): p. 145-56.

156. Wu, W., et al., *Microarray analysis reveals glucocorticoid-regulated survival genes that are associated with inhibition of apoptosis in breast epithelial cells.* Cancer Res, 2004. **64**(5): p. 1757-64.

157. Vacca, A., et al., *Glucocorticoid receptor-mediated suppression of the interleukin 2 gene expression through impairment of the cooperativity between nuclear factor of activated T cells and AP-1 enhancer elements.* J Exp Med, 1992. **175**(3): p. 637-46.

158. Karin, M., Z. Liu, and E. Zandi, *AP-1 function and regulation.* Curr Opin Cell Biol, 1997. **9**(2): p. 240-6.

159. Wenzel, A., et al., *c-fos controls the "private pathway" of light-induced apoptosis of retinal photoreceptors.* J Neurosci, 2000. **20**(1): p. 81-8.

160. Konig, H., et al., *Interference between pathway-specific transcription factors: glucocorticoids antagonize phorbol ester-*

induced AP-1 activity without altering AP-1 site occupation in vivo. EMBO J, 1992. **11**(6): p. 2241-6.

161. Ryan, K.M., et al., *Role of NF-kappaB in p53-mediated programmed cell death.* Nature, 2000. **404**(6780): p. 892-7.

162. Limbourg, F.P., et al., *Rapid nontranscriptional activation of endothelial nitric oxide synthase mediates increased cerebral blood flow and stroke protection by corticosteroids.* J Clin Invest, 2002. **110**(11): p. 1729-38.

163. Buttgereit, F., S. Krauss, and M.D. Brand, *Methylprednisolone inhibits uptake of Ca2+ and Na+ ions into concanavalin A-stimulated thymocytes.* Biochem J, 1997. **326 (Pt 2)**: p. 329-32.

164. Buttgereit, F., et al., *The effects of methylprednisolone on oxidative phosphorylation in Concanavalin-A-stimulated thymocytes. Top-down elasticity analysis and control analysis.* Eur J Biochem, 1994. **223**(2): p. 513-9.

165. Mocchetti, I., et al., *Glucocorticoids differentially increase nerve growth factor and basic fibroblast growth factor expression in the rat brain.* J Neurosci, 1996. **16**(6): p. 2141-8.

166. Barbany, G. and H. Persson, *Regulation of Neurotrophin mRNA Expression in the Rat Brain by Glucocorticoids.* Eur J Neurosci, 1992. **4**(5): p. 396-403.

167. Grosche, J., W. Hartig, and A. Reichenbach, *Expression of glial fibrillary acidic protein (GFAP), glutamine synthetase (GS), and Bcl-2 protooncogene protein by Muller (glial) cells in retinal light damage of rats.* Neurosci Lett, 1995. **185**(2): p. 119-22.

168. Bignami, A. and D. Dahl, *The radial glia of Muller in the rat retina and their response to injury. An immunofluorescence study with antibodies to the glial fibrillary acidic (GFA) protein.* Exp Eye Res, 1979. **28**(1): p. 63-9.

169. Wen, R., et al., *Injury-induced upregulation of bFGF and CNTF mRNAS in the rat retina.* J Neurosci, 1995. **15**(11): p. 7377-85.

170. Cao, W., et al., *Mechanical injury increases bFGF and CNTF mRNA expression in the mouse retina.* Exp Eye Res, 1997. **65**(2): p. 241-8.

171. Weber, A.J., C.D. Harman, and S. Viswanathan, *Effects of optic nerve injury, glaucoma, and neuroprotection on the survival, structure, and function of ganglion cells in the mammalian retina.* J Physiol, 2008. **586**(Pt 18): p. 4393-400.

172. Reiter, C.E., et al., *Characterization of insulin signaling in rat retina in vivo and ex vivo.* Am J Physiol Endocrinol Metab, 2003. **285**(4): p. E763-74.

173. Hemmings, B.A., *Akt signaling: linking membrane events to life and death decisions.* Science, 1997. **275**(5300): p. 628-30.

174. Chan, T.O., S.E. Rittenhouse, and P.N. Tsichlis, *AKT/PKB and other D3 phosphoinositide-regulated kinases: kinase activation by phosphoinositide-dependent phosphorylation.* Annu Rev Biochem, 1999. **68**: p. 965-1014.

175. Punzo, C., K. Kornacker, and C.L. Cepko, *Stimulation of the insulin/mTOR pathway delays cone death in a mouse model of retinitis pigmentosa.* Nat Neurosci, 2009. **12**(1): p. 44-52.

176. Li, G., et al., *Nonredundant role of Akt2 for neuroprotection of rod photoreceptor cells from light-induced cell death.* J Neurosci, 2007. **27**(1): p. 203-11.

177. Yao, R. and G.M. Cooper, *Requirement for phosphatidylinositol-3 kinase in the prevention of apoptosis by nerve growth factor.* Science, 1995. **267**(5206): p. 2003-6.

178. Yang, E., et al., *Bad, a heterodimeric partner for Bcl-XL and Bcl-2, displaces Bax and promotes cell death.* Cell, 1995. **80**(2): p. 285-91.

179. Datta, S.R., et al., *Akt phosphorylation of BAD couples survival signals to the cell-intrinsic death machinery.* Cell, 1997. **91**(2): p. 231-41.

180. Suzuki, A., et al., *Resistance to Fas-mediated apoptosis: activation of caspase 3 is regulated by cell cycle regulator p21WAF1 and IAP gene family ILP.* Oncogene, 1998. **17**(8): p. 931-9.

181. Cardone, M.H., et al., *Regulation of cell death protease caspase-9 by phosphorylation.* Science, 1998. **282**(5392): p. 1318-21.

182. Agarwal, A., et al., *The AKT/I kappa B kinase pathway promotes angiogenic/metastatic gene expression in colorectal cancer by activating nuclear factor-kappa B and beta-catenin.* Oncogene, 2005. **24**(6): p. 1021-31.

183. Salvesen, G.S. and C.S. Duckett, *IAP proteins: blocking the road to death's door.* Nat Rev Mol Cell Biol, 2002. **3**(6): p. 401-10.

184. Abraham, I., et al., *Glucocorticoids alter recovery processes in the rat retina.* Neuroreport, 1998. **9**(7): p. 1465-8.

185. Heim, C., U. Ehlert, and D.H. Hellhammer, *The potential role of hypocortisolism in the pathophysiology of stress-related bodily disorders.* Psychoneuroendocrinology, 2000. **25**(1): p. 1-35.

186. Raison, C.L. and A.H. Miller, *When not enough is too much: the role of insufficient glucocorticoid signaling in the pathophysiology of stress-related disorders.* Am J Psychiatry, 2003. **160**(9): p. 1554-65.

187. Naash, M.I., et al., *Simulation of human autosomal dominant retinitis pigmentosa in transgenic mice expressing a mutated murine opsin gene.* Proc Natl Acad Sci U S A, 1993. **90**(12): p. 5499-503.

188. Naash, M.L., et al., *Light-induced acceleration of photoreceptor degeneration in transgenic mice expressing mutant rhodopsin.* Invest Ophthalmol Vis Sci, 1996. **37**(5): p. 775-82.

189. Chrousos, G.P., E. Charmandari, and T. Kino, *Glucocorticoid action networks--an introduction to systems biology.* J Clin Endocrinol Metab, 2004. **89**(2): p. 563-4.

190. Lamberts, S.W., *The glucocorticoid insensitivity syndrome.* Horm Res, 1996. **45 Suppl 1**: p. 2-4.

5.12. Lists of Figures

5.13. Lists of Tables

5.14. Abbreviations

± SD	Standard deviation
ACTH	Adrenocorticotrophic hormone
AMD	Age-related macular degeneration
ANS	Autonomic nervous system
AP-1	Activator protein 1
ATP	Adenosine triphospate
ATP	Adenosine triphosphate
AVP	Arginine vasopresin
BCA	Biocinchocinate
B-LPH	Beta-lipotrophic hormone
bp	Base pair(s)
cDNA	Complementary DNA
cGMP	Cyclic guanine monophosphate
CN	Cranial nerve
CORT	Corticosterone
CRF	Corticotrophin releasing factor
CRH	Corticotrophin releasing hormone
CSC	Chronic subordinate colony
CSC L	Subordinately housed illuminated
CSC NL	Subordinately housed un illuminated
CT	CT
CT	Cycle threshold
DAPI	4', 6'- diamidino-2-phenylindole
DMEM	Dulbecco/Vogt modified eagle’s minimal essential medium
DMSO	Di methyl sulphoside
DNA	Deoxyribonucliec acid
dsDNA	Double stranded DNA
dUTP	Deoxyribosyl uridine tri phosphate
End-2	Endothelin 2

ER	Endoplasmic reticulum
Fcs	Fetal calf serum
FGF	Fibroblast growth factor
Fig	Figure
fw	Forward
G	Grams
GC	Glucocorticoids
GFP	Green fluorescent protein
GMP	Guanine monophospahate
GR	Glucocorticoid receptor
GR	Glucocorticoid receptor
GRE	Glucocorticoid response elements
GRE	Glucocorticoid response element
HPA	Hypothalamus-pituitary-adrenal
hr	Hour
IAP	Inhibitors of apoptosis protein
IL	Interleukin
MM	Master mix
MR	Mineralocortocid receptor
NO	Nitric oxide
NSB	Non specific binding
PBS	Phosphate buffered saline
PCR	polymerase chain reaction
PFA	Paraformaldehyde
POMC	Propiomelanocortin precursor protein
PVN	para ventricular nucleus
rev	Reverse
RGC	Retino ganglia cells
RIA	Radio immuno assay
RP	Retinitis pigmentosa

RPE	Retinal pigment epithelium
rpm	rounds per minute
RT	Room temperature/reverse transcriptase
rTdT	Recombinant terminal deoxy ribosyl transferase
SDS	Sodium dodecyl sulphate
Sg	SYBR-Green I
SNS	Sympathetic nervous system
SSC	Saline-sodium citrate
Δ	Delta

5.15. Aknowlegdement

My sincere thanks go to my supervisor Prof Dr Ernst Tamm and my first mentor Prof Dr Inga D Neumann who arranged and gave me the opportunity to carry out such interdisciplinary and challenging project in their Laboratories. I am equally grateful to Prof Dr Olaf strauss who joined them as my second mentor to give interesting ideas for the project.

My profound gratitude to PD Dr Andreas Ohlmann and PD Dr Stefan Reber who were there to give this thesis a very intense and thorough supervision. I benefited a lot from their academic might and technical knowhow. Their positive comments and criticisms have been a guiding cue. I equally cannot find any words sufficient enough to thank them for the late nights and early mornings. This thesis wouldn't have gotten this far without their enormous dedication, attention and patience.

I owe a lot of appreciation to Elke stauber, Margit Schimmel, Angelika Park, Silvia Babl and Corrina Unger for technical assistance. Furthermore, I like to extend my gratitude to all members of the institute of Human Anatomy and Embryology, Lehrstuhl Prof Tamm, as well as those of Department of Behavioural and Moleculecular Neuroendocrinology, Lehrstuhl Prof Neumann, for their collaboration and support. Special thanks to my friends Kewir Dufe and Rodrigue Maloumby who have made life easy and interesting on campus. I am equally grateful to my elder brothers Mota Chris who found time to read the manuscript and Dr Sabi Titus who has been a mentor not only in academics but life in general.

To all friends and family whom am not able to mention because of space limitation, I say THANK YOU.

5.16. Declaration/Erklärung

I hereby declare that this thesis is my own work and was completed independently. I did not use any resources and auxiliary other than those listed

Hiermit erkäre ich, dass diese arbeit selbstandig angefertigt habe ausser den imliteraturverzeichnis angegeben quellen habe ich keine weiteren hilfsmittel verwendet

Regensburg, Octobeber 2012

Forkwa Kieran Tembei